Feasibility of Intensity Modulated High Dose Rate Ocular Brachytherapy Using Middle Energy Isotopes Coupled with a Partially Shielded Applicator

By

Justine Dupere

A dissertation

submitted to the faculty of the

Worcester Polytechnic Institute

in partial fulfillment of the requirements for the

Degree of Doctor of Philosophy in

Medical and Health Physics

April 2021

David C. Medich, Ph.D, Associate Professor, Department of Physics WPI

Primary Advisor and Committee Member

John J. Munro III, Ph.D., Managing Director, Montrose Technology, Inc.

Advisor and Committee Member

Snehalata V. Kadam, Ph.D., Assistant Teaching Professor, Department of Physics, WPI

Committee Member

Germano S. Iannacchione, Ph.D., Professor, Department of Physics, WPI

Committee Member

Abstract

The purpose of this dissertation is to investigate a new approach of using middle-energy high dose rate brachytherapy sources, Yb-169 and Se-75, coupled with a gold shielded ring applicator to treat ocular melanoma. The feasibility of this approach is computationally tested using MCNP6 and validated against an I-125 COMS plaque, which is currently the standard treatment modality.

The proposed ring source consists of an assembly of discrete sources delivered into an applicator with a conical collimated opening that is tangent to the outside of the source tube. Using MCNP6, the dosimetric output of a ring of Yb-169 and Se-75 sources was simulated within the collimator at various conical diameters and angles to demonstrate the dosimetric distribution for various prescription dose depths and target sizes.

Using various angles of collimation, the prescription dose was delivered to a target apex of 3.5-8.0 mm depths into the eye covering target sizes ranging from 10.0-15.5 mm in diameter. This proposed device reduced the maximum absorbed dose to critical structures relative to I-125 by 5.2% to the posterior lens, 9.3% to the iris, 13.8% to the optic nerve, and 1.3% to the sclera, when using Yb-169. The percent difference in dose to the critical structures within the eye was about 30% higher when using Se-75 compared to Yb-169 however it is still within acceptable limits.

Greater conformal dose distributions were achieved from the conical opening and gold shielding on the applicator. This design also permits the use of a remote afterloader, either manual or automated, which eliminates dose to the surgeon's hands. While Yb-169 is the optimal isotope for this treatment, the longer half-life of Se-75 (120 days) may make this treatment option more practical.

Acknowledgements

First, I would like to thank my dissertation advisor, Professor David C Medich, for all of his assistance throughout the entire PhD program. He was always willing to offer his support and help me with anything I needed.

I would also like to thank John J Munro III, Managing Director of Montrose Technology Inc, for all of the projects he brought to me at WPI. He allowed me to be involved in his work and he taught me a lot about MCNP and brachytherapy. His help was invaluable with this work.

The graduate students of the radiation lab at WPI, who provided me with support throughout my Ph.D. career. Especially Nicholas Borges who trained me in the lab and taught me how to handle the brachytherapy sources and Gafchromic film. He was always willing to offer his help whenever I needed it. Also, Shaun Marshall who wrote the Matlab program used to analyze the Gafchromic film.

Lastly, I would like to thank my family for helping me get to where I am today. I could not have done this without them.

Table of Contents

List of Figures

16. GUI interface of the Matlab program used to analyze Gafchromic film, which gives the maximum and average grayscale values of the film.
17. Demonstrates the anisotropy analysis of the Matlab program.
18. A) SketchUp model of the film holder B) centerpiece of the film holder containing a catheter wrapped in gold foil and a dummy source pushed to the middle distance of the catheter C) assembled film holder in the water tank and D) afterloader device connected to a shielded box container, which holds the source, located near the water tank.
19. Dose distribution, calculated in MCNP6, of a 16 mm COMS plaque containing I-125 on the XZ plane. The dose rate is measured in Gy/hr and the prescription dose is delivered to a 5 mm depth into the eye.
20. DVH curve in log scale of a 16 mm COMS plaque containing I-125 that delivers a dose rate of 0.71 Gy/hr to a 5 mm depth in the eye, calculated in MCNP6.
21. Isodose contours of dose to ocular structures of I-125 from Lesperance et al. The solid line is representative of the full eye model.
22. Dose volume histogram of the dose to the tumor and lens region for I-125 from Lesperance et al. The solid line is representative of the full eye model.
23. Isodose curves of a 12 mm applicator containing Yb-169. The prescription dose of 3 Gy/min was delivered to 3.5-6.0 mm depths in the eye.
24. Isodose curves of a 14 mm applicator containing Yb-169. The prescription dose of 3 Gy/min was delivered to 3.5-6.5 mm depths in the eye.
25. Isodose curves of a 16 mm applicator containing Yb-169. The prescription dose of 3 Gy/min was delivered to 4.0-7.5 mm depths in the eye.

26. Isodose curves of an 18 mm applicator containing Yb-169. The prescription dose of 3 Gy/min was delivered to 4.0-8.0 mm depths in the eye.
27. A) and C) represent DVH curves for the 12 mm applicator that delivers 3 Gy/min to a 5 mm depth in the eye. B) and D) represent DVH curves for the 16 mm applicator that delivers 3 Gy/min to a 7 mm depth in the eye. A) and B) in log scale display the dose rates to the tumor compared to the critical structures. C) and D) are the dose rates in Gy/min vs volume of ocular structures of interest.
28. A) The lateral dose rate at a distance of 5 mm behind a 12 mm applicator that delivers the prescription dose to a depth of 5 mm in the eye. B) is the lateral dose rate at a distance of 5 mm behind a 16 mm applicator that delivers the prescription dose to a depth of 7 mm in the eye.
29. Isodose curves of a 12 mm applicator containing Se-75. The prescription dose of 3 Gy/min was delivered to 3.5-6.0 mm depths in the eye.
30. Isodose curves of a 14 mm applicator containing Se-75. The prescription dose of 3 Gy/min was delivered to 3.5-6.5 mm depths in the eye.
31. Isodose curves of a 16 mm applicator containing Se-75. The prescription dose of 3 Gy/min was delivered to 4.0-7.5 mm depths in the eye.
32. Isodose curves of an 18 mm applicator containing Se-75. The prescription dose of 3 Gy/min was delivered to 4.0-8.0 mm depths in the eye.
33. A) and C) are DVH curves of a 12 mm applicator with a target apex at a 5 mm depth in the eye. B) and D) are of a 16 mm applicator with a target apex at a 7 mm depth in the eye. Both applicators deliver a dose rate of 3 Gy/min. A) and B) are in log scale and

1 Introduction

1.1 Purpose

The purpose of this project is to investigate how Yb-169 and Se-75, middle-energy High Dose Rate (HDR) brachytherapy sources, coupled with a very thin gold shielded collimator, can be used to treat ocular melanoma. To achieve this, I will incorporate static intensity modulation by collimating a set of middle-energy brachytherapy sources at an angle to best conform to the shape of an ocular tumor. The goal of this work is to produce a more conformal dose distributions than what is currently achieved using the conventional Low Dose Rate (LDR) brachytherapy sources.

1.2 Literature Review

1.2.1 COMS Plaque

Modern eye plaques use an array of discrete low energy photon sources such as I-125, Pd-103, and Cs-131, or uniform planar beta plaques containing Ru-106 and Sr-90 to deliver their treatment prescribed absorbed dose[1] with I-125 plaque brachytherapy currently the most popular method for treating ocular melanomas.[2] Called a Collaborative Ocular Melanoma Study (COMS) plaque, these eye plaques contain an average of 1.3 GBq of I-125 with a mean dose rate of 2 mGy/min, which is used as a LDR source.[3] I-125 has a half-life of 59.4 days and a specific activity of 1.73E4 Ci/g. The I-125 decays by electron capture to Te-125 and emits 35 keV gamma rays (7% abundance). Some of the excess energy may be converted to x-rays through bremsstrahlung production, which is radiation produced from the deceleration of an electron deflected in the electric field of an atomic nucleus. The electron loses its kinetic energy, which is converted into x-rays. I-125 has a 113% abundance of 27 keV x-rays. About 0.02 mm of lead is

required to reach its half value layer. Currently, I-125 brachytherapy seeds are placed in a COMS standard plaque that is temporarily sewn onto the eye.

The COMS standard plaque design consists of a gold backing with a silastic seed carrier insert available from 10-22 mm diameters in 2 mm increments.[2] Plaque sizes are designed to include a 2 mm margin around the tumor. The silastic insert has grooves to hold a fixed number of radioactive sources in place and to provide a relatively cylindrically symmetric dose distribution. A standard 14 mm COMS plaque is shown in Figure 1. The plaque gets sutured onto the outside of the sclera overlying the tumor and is left in place for 5-7 days until the prescription dose is delivered. Dose prescriptions typically range from 70-100 Gy to the tumor apex, with a mean dose of 85 Gy.[1] A second surgery is later performed to remove the plaque after the dose has been delivered.

Figure 1: Standard 14 mm COMS plaque[4]

1.2.2 Limitations

Due to the fixed geometry of the plaques, it can be difficult to limit the dose to non-target locations within the eye. The increased dose in these non-target areas increases the chance of post radiation exposure complications including vision loss, retinopathy, cataracts, and dry eyes.[5,6] This procedure is also costly because it requires two minor surgeries, patient hospitalization during the dose delivery period (although sometimes this may be an outpatient

procedure), and because these brachytherapy sources are only used once.[7] Lastly, a typical COMS eye plaque containing on average, 1.3 GBq of I-125 has been shown to result in a hand dose of approximately 2-6 mSv to the surgeon per treatment.[3,8]

1.3 Overcoming Limitations

Intensity modulation has been used for many years in the field of radiation therapy to optimize dose to the target and protect critical structures.[9,10] Therefore, an alternative approach for treating choroidal melanoma is presented to overcome the limitations of LDR brachytherapy by using an afterloaded array of middle-energy HDR sources, Yb-169 and Se-75, in conjunction with a gold-shielded applicator to modulate the dosimetric output of these sources. An afterloader is a device that mechanically delivers the radioactive sources precisely to the treatment site. It also allows for the medical personnel to leave the room during delivery of the treatment, which reduces their exposure.

Therefore, an array that would be compatible with an afterloader device was designed for this study. Using this method, the surgeon also can suture and unsuture an empty applicator onto the eye, thereby eliminating the hand dose to the surgeon. As only one source stopping position is necessary, source stepping is not required. Thus, the remote afterloading could be manual or automatic. As a result of using an array of HDR sources with this technique, treatment times will be approximately 10-20 minutes per patient rather than 5-7 days, which means that the patient will not require hospitalization. Lastly, the source array can be reused for about one half-life, corresponding to 32 days for Yb-169 and 120 days for Se-75.

Yb-169 is selected for this application because it emits ionizing photons in the range of 50-308 keV, with a median energy of 58 keV and an average energy of 93 keV. Most of these

photons therefore are below the k-absorption edge for gold, resulting in very efficient shielding and intensity modulation as presented in Figure 2. For example, an applicator containing a backing of only 1.2 mm thick gold is calculated to reduce absorbed dose by 90% while a backing of 2 mm will reduce the dose by 96%. The effective shielding is largely due to the 43.7% yield of 63.1 keV photons. Because of the low energies of the Yb-169 photons and effectiveness of lead shielding (only 1 cm required), the operator can be near the patient during treatment.

Se-75 is also a promising HDR brachytherapy source as studies have indicated.[11] This is because Se-75 is a middle energy source with a gamma energy range of 66-401 keV and an average energy of 217 keV. In addition, with a tenth value layer of about 3 mm of gold, a Se-75 brachytherapy source can be shielded locally.

Ir-192 was not considered for this study because it has an average energy of 380 keV. The amount of shielding required for this source would not be acceptable to fit within the geometrical limitations of the eye plaque as the resulting higher dose would be delivered to critical structures. Therefore, only Yb-169 and Se-75 were considered. Se-75 has a higher average photon energy than Yb-169 (E_{avg}= 93 keV) however Selenium's photon energy still is much lower than Ir-192 (E_{avg}= 380 keV). While the abundant 60 keV photons emitted by Yb-169 may offer better shielding and tissue-scatter advantages for HDR ocular brachytherapy, it is more complicated and expensive to manufacture due to the low natural abundance of its progenitor, Yb-168.[12] As a result of the difficulties attributed with using Yb-169, the use of Se-75 as an intensity modulated ocular brachytherapy source may be a more practical approach.

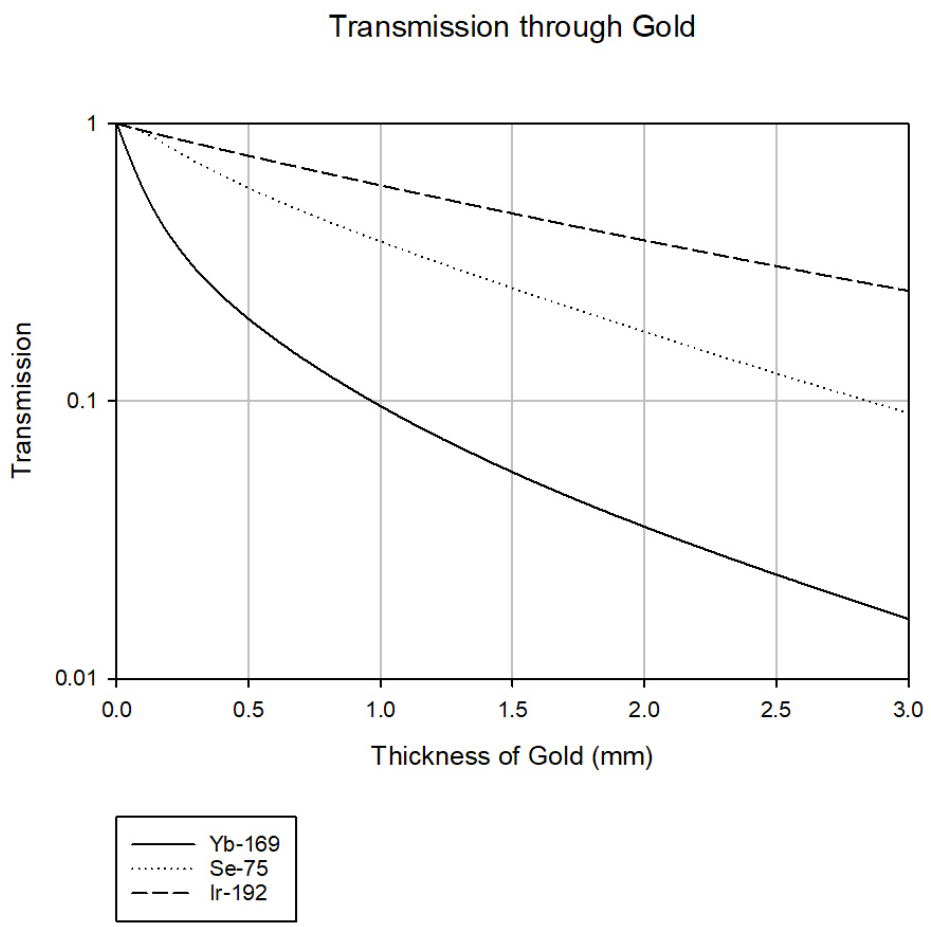

Figure 2: Transmission of several isotopes through various thicknesses of gold. The tenth value layer of Yb-169 is about 1 mm of gold and the tenth value layer of Se-75 is just under 3 mm of gold. The gold shielding is inefficient for the high photon energies of Ir-192.

1.4 Hypothesis

Coupling a circular array of middle-energy HDR sources within an applicator containing a shielded collimator is a feasible method for treating ocular melanoma and will reduce dose to non-target locations, eliminate hand dose to the surgeon, and reduce the treatment time.

1.5 Goals

The goal is to computationally test the source array and applicator design using a heterogeneous eye model in MCNP6, calculate its dose distribution, and compare it to a standard I-125 COMS plaque. The MCNP6 calculation method was first verified by simulating a COMS plaque to compare with Lesperance et al who simulated the same plaque in BrachyDose.[13] An eye model accounting for the ocular geometry and compositions was used for all of the calculations, as described in the Lesperance report.[13] After verifying my computational method, I modified the eye model with the shielded applicator and ran simulations of it with Yb-169 and Se-75 for various applicator sizes and collimator angles. Then, I compared these measurements with the I-125 plaque. Finally, I experimentally tested the ability to shield Yb-169 using gold foil and Gafchromic EBT3 film.

2 Background

2.1 Anatomy of the Eye

A depiction of the human eye is presented in Figure 3. The outermost layer of the eye is the fibrous layer, which consists of the cornea and sclera. The cornea is a dome-shaped surface on the front of the eye. It helps to focus light into the eye. The sclera is the visible white part of the eye and attaches to the extraocular muscles, which allows for the eye to move.

The vascular layer, also called the uvea, is underneath the fibrous layer and consists of the choroid, ciliary body, and iris. The choroid is mostly made up of blood vessels that nourishes the outer layer of the retina. The ciliary body is comprised of the ciliary muscle and ciliary processes. It controls the shape of the lens, which allows the lens to focus on objects and focus the light passing through. The ciliary body also contributes to the shape of the aqueous humor. The aqueous humor is contained in the anterior chamber, between the cornea and iris, and posterior chamber, between the lens and iris. It provides nutrients to the surrounding structures. The iris is the colored portion of the eye and controls the size of the pupil, which allows light to pass to the lens.

The inner layer of the eye is formed by the retina, which detects light. The outer layer of the retina attaches to the choroid, which absorbs light to prevent scatter within the eyeball. The inner layer of the retina consists of photoreceptors, which detects the light. The central part of the retina is the macula. It is highly pigmented and yellowish in color. It contains a depression called the fovea, which has a high concentration of light detecting cells. This is the area that fixates when looking directly at an object. At the back of the eye is the optic nerve. It transfers visual information from the retina to the brain by electrical impulses. The optic disc is the area of the

optic nerve that enters the retina. It has no light detecting cells corresponding with our natural blind spot. The vitreous humor is a gelatinous material that fills the space in the eye between the lens and retina and helps the eyeball keep its spherical shape.[14]

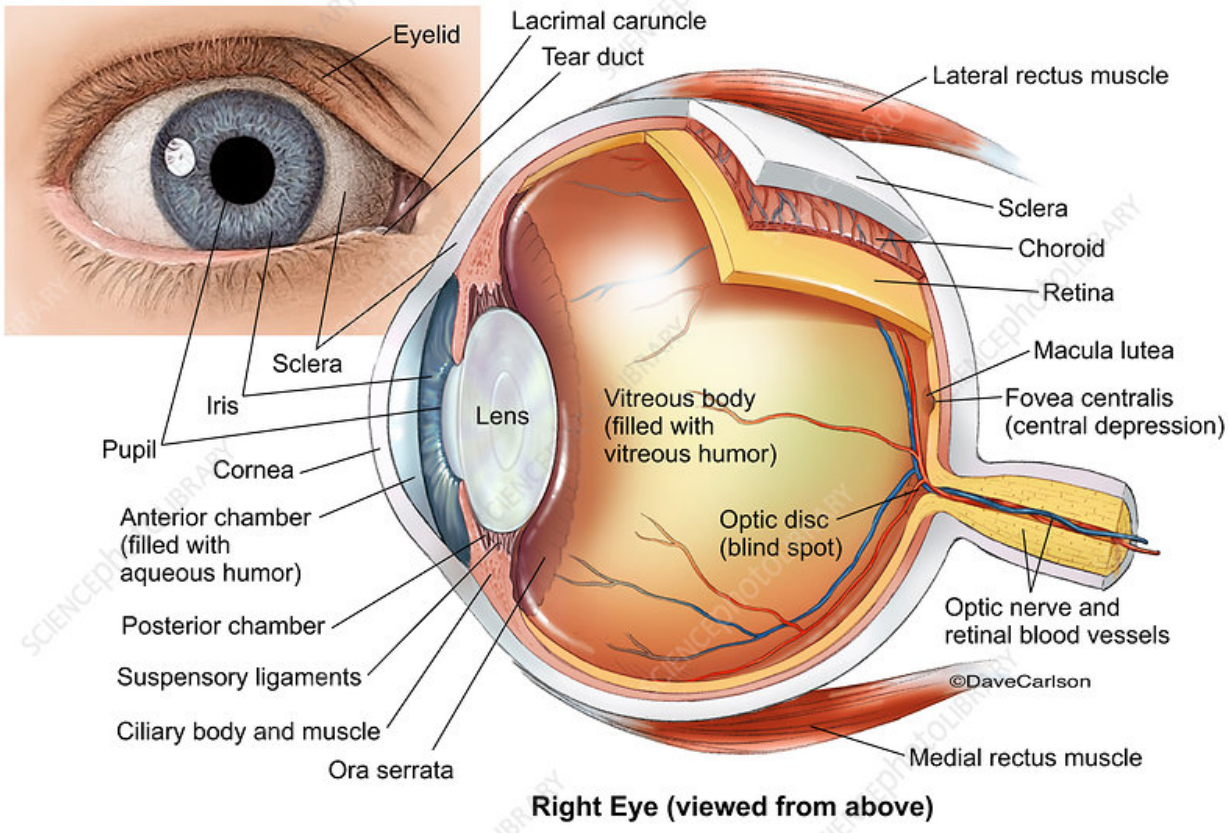

Figure 3: Image of a right eye with important structures labelled.[15]

2.2 Types of Tumors

With respect to ocular tumors, uveal melanoma is the most common intraocular tumor in adults, accounting for 83% of cases.[16] About 90% of the tumors are located in the choroid, 6% in the ciliary body, and 4% in the iris.[17] The risk of uveal melanoma increases with age. The incidence rate peaks at ages 70-75 years.[18] The median age of diagnosis for uveal melanoma in the United States and Europe is 59-62 years.[19] There is also a higher incidence in males compared to females. In 2019, there were an estimated 3,360 new intraocular cancer cases with 370 deaths in the United States.[20] Of these cases, 1,860 were male and 1,500 were female.[20] One study showed that this difference was due to significantly higher rates in men aged 65 years and older. No significant difference was found between the genders younger than 65 years.[21]

Race is also a factor. Uveal melanoma is primarily found in Caucasian populations. A study of 8,100 patients with uveal melanoma reported 98% Caucasian, 1% Hispanic, <1% Asian, and <1% African American.[22] Fair skin, light eye color, and the inability to tan are also statistically significant factors.[23] The lighter coloring means there is less melanin in the choroid and retina. As a result, there is less protection from ultraviolet light, which increases the risk of developing uveal melanoma.

About half of the patients with uveal melanoma develop metastases 10 years after diagnosis, which are usually fatal after 6-12 months.[24] The most common site of metastases includes the liver (91%), lung (28%), and bone (18%), however this is all dependent on the location and size of the tumor.[25] The different types of tumors are shown in Figure 4.

Iris melanoma comprises 3-5% of uveal melanomas.[26] It is not very common but is usually diagnosed 10-20 years earlier than other uveal melanomas due to iris color changes and pupil distortion.[26] 90% of iris melanomas are circumscribed and 10% are diffuse.[27] Iris

melanoma can be diagnosed by a clinical exam using slit lamp biomicroscopy. A biopsy may also be used to confirm diagnosis and has minimal complications.[28] If the melanoma is less than 3 mm in basal diameter in an asymptomatic patient, it may be monitored for growth. If there is growth, then a portion of the iris may be removed. If the growth has extended to other areas of the eye, such as the ciliary body, then a portion of the iris and ciliary body may be removed.[26] Plaque radiotherapy and proton beam radiotherapy are also treatment options, especially for non-resectable tumors.[29] Enucleation is used for large tumors, diffuse iris melanoma, and recurrent tumors.[29] Iris melanoma has a five to ten times lower mortality rate than other uveal melanomas.[30] Iris melanomas generally have a smaller tumor size, less biologic activity, and present at a younger age, which may be the reason for the better prognosis.[30] In a study of over 300 patients, metastases occurred in 4% of the patients and 2% of these died due to the metastases during a 53 month follow-up.[26]

Ciliary body melanoma occurs in approximately 5-8% of uveal melanomas.[31] It is generally diagnosed late because the lesion is hidden behind the iris and the patient is usually asymptomatic until the lesion is large. The mean size of the tumor when diagnosed is 11.7 mm in basal diameter and 6.6 mm thick.[17] 30% of patients are asymptomatic and 38% have blurred vision.[32] Less than 10% of the time patients experience photopsia, floaters, visual field loss, visible tumor, pain, and metamorphopsia.[32] Ciliary body melanomas cannot be visualized directly and so they are very difficult to diagnose. Oftentimes, it is not detected until it invades the iris or choroid. Gonioscopy can be used to check the anterior chamber angle, which is between the cornea and iris and contains the trabecular meshwork.[33] High-frequency ultrasound biomicroscopy is another diagnostic tool used to detect small ciliary body melanomas.[33]

Treatment includes plaque radiotherapy, proton beam radiotherapy, and enucleation for large tumors with poor vision.[26] The 10-year mortality rate is 30-50% due to metastases.[34]

Choroidal melanoma is the most common type of ocular melanoma, accounting for 85-90% of all uveal melanomas.[35] The symptoms are the same as ciliary body melanomas and the mean basal diameter of the tumor is 11.3 mm and the tumor thickness is 5.5 mm.[17] About 75% of choroidal melanomas are dome-shaped, 19% have a mushroom shape due to the rupture of Bruch's membrane, the innermost layer of the choroid, and 6% are diffuse.[17] A majority of the cases are associated with pigmented lesions and retinal detachment.[17] A fundus evaluation with indirect ophthalmoscopy is generally used to diagnose choroidal melanoma.[36] For small choroidal melanomas, enhanced depth imaging optical coherence tomography is a useful tool.[36] The most common treatment options, similar to ciliary melanomas, are plaque radiotherapy, proton beam radiotherapy, and enucleation for large tumors with poor vision.[26] The five-year relative survival rate for patients with small choroidal melanoma is 84%, medium choroidal melanoma is 68%, and large choroidal melanoma is 47%.[37]

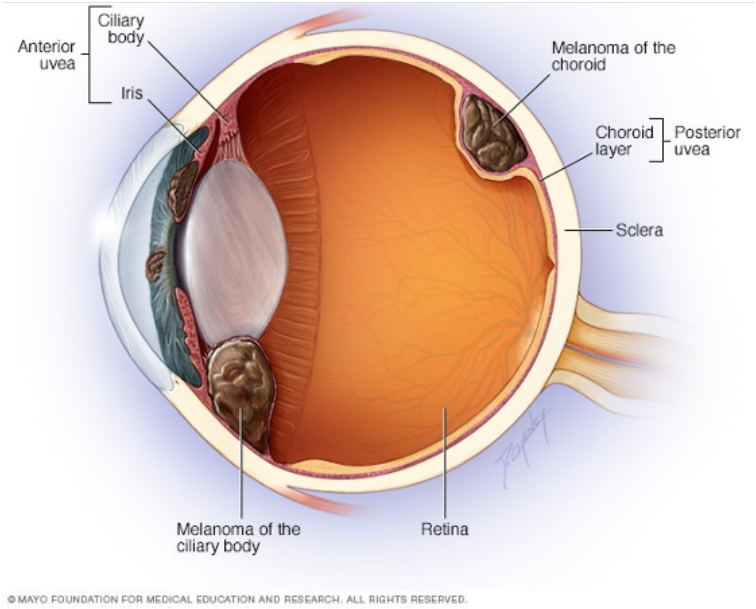

Figure 4: Types of ocular melanomas[38]

2.3 Radiation Therapy

Cancer is the second leading cause of death in the United States, with an estimated 1.76 million new cases diagnosed and over 600,000 deaths occurring in 2019.[20] Currently, approximately half of all cancer patients are treated using radiation therapy.[39] This treatment method involves using ionizing radiation to irradiate the cancer while minimizing exposure to healthy tissue. Ionizing radiation damages the DNA of cancerous cells by causing double-strand breaks, which reduces the cell's ability to function properly or replicate and can induce apoptosis or cell death.[40] Radiation is most harmful to cells undergoing mitosis. Since cancer cells divide faster than normal cells, they are more radiosensitive.[41] The purpose of radiation therapy is to deliver a high enough dose to obtain tumor control without overexposing the surrounding healthy tissue. Radiation therapy is commonly delivered to the patient using external beam radiation or radiation sources internally, known as brachytherapy.

2.3.1 External Beam Radiation Therapy

In External Beam Radiation Therapy (EBRT), a linear accelerator is used to direct ionizing radiation from outside the patient's body into their tumor. The most commonly used form of EBRT for treating ocular melanoma is proton therapy, as seen in Figure 5, due to the high local tumor control that can be achieved using this method.[42] Five-year survival rates of about 80% have been reported for ocular melanoma patients treated with proton therapy.[42] Gamma Knife is another method that may be used by precisely employing about 200 small beams of gamma rays to target the tumor and can provide a five-year survival rate of about 82%.[43] Although the survival rates of EBRT are promising, the entry point of the radiation can cause complications such as dry eye, neovascular glaucoma, and cataracts.[5]

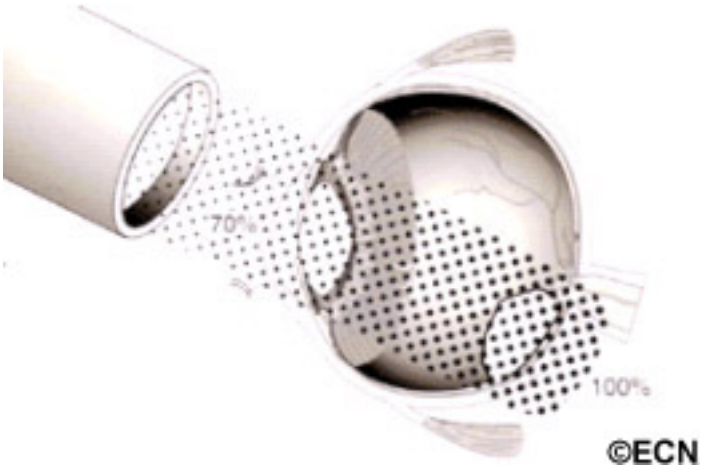

Figure 5: Proton beam therapy for the treatment of ocular melanoma[44]

2.3.2 Brachytherapy

Brachytherapy is a form of cancer treatment where small, radioactive sources are placed inside of the patient, in or near the tumor therefore, the radiation bypasses the skin. As a result, high amounts of radiation can be delivered to the tumor while minimizing dose to the skin and critical structures. Brachytherapy was started shortly following Wilhelm Roentgen's discovery of x-rays in 1895. In 1896, Henri Becquerel discovered radioactivity by observing the emission of radiation from uranium. In 1898, Marie and Pierre Curie discovered the radioactive elements polonium and radium from uranium ore. Shortly later in 1901, Alexandre Danlos and Paul Bloch used some of the radium from the Curie's to treat a patient with a malignant tumor in Paris, thus beginning the field of brachytherapy.

A Curie is defined as the unit of activity of the nuclear decay rate of 1 g of Radium-226. Radium has a very low specific activity due to its long half-life of 1.6 years and would take about a week to deliver a dose that would be effective for treatment. Therefore, its daughter product, radon, was used instead. Radon has a much shorter half-life of 3.8 days, which results in

a higher specific activity. Radon was later encased in gold in order to reduce the harmful beta particles that were produced while allowing the therapeutic gamma rays to pass through.

In 1919, Ernest Rutherford discovered artificial radioactivity. Then in 1934, Irene Curie and Frederick Joliot discovered artificial radionuclides, which transformed the field of brachytherapy. Radionuclides were synthesized, such as Cobalt-60, Gold-198, Tantalum-182, and Cesium-137, which replaced Radium-226. Then in 1958, Iridium-192 replaced these sources and is currently the most used HDR radioactive source in brachytherapy. HDR sources are attached to metal wires. A hollow needle or catheter is surgically implanted in the patient to guide the wire, containing the radioactive source, using an afterloader. An afterloader is a mechanical device used to move the wire into the catheter in order to reduce exposure to the surgeon and staff. In 1957, Strontium-90 was first used in combination with an eye applicator to treat ocular melanoma. In the 1980s, LDR seeds such as I-125, Pd-103, and Cs-131, were implanted in patients to treat tumors.[45,46]

Brachytherapy sources can either be permanently implanted in the body or temporarily implanted. LDR brachytherapy uses permanent, loose sources as they are lower energy and decay quickly. Common LDR sources are I-125, Pd-103, and Cs-131. These sources have energy emissions less than 50 keV and dose rates of 0.4-2.0 Gy/hr.[47] The treatment time for these sources is usually on the order of days. Temporary implants, such as eye plaques, are placed over the tumor and sutured onto the patient. They are removed once the prescription dose has been delivered. Permanent implants, such as prostate seeds, are left within the patient as the LDR sources will decay to a safe level within a matter of weeks or months. HDR sources are generally attached to wires and inserted using a manual or remote afterloader device. Common HDR sources are Ir-192, Co-60, and Cs-137. These sources have energy emissions greater than 300

keV and dose rates of more than 12 Gy/hr.[47] These treatments usually take 10-20 minutes. The full dose can be delivered in a single treatment or fractionated into multiple treatments.

2.3.2.1 COMS Trials

In the early 1900s, the primary treatment for choroidal melanoma was enucleation. Enucleation is the removal of the eye and is the preferred treatment for large tumors, recurrent tumors, or if the tumor has caused vision loss. In the 1970s, Zimmerman observed a peak in mortality two to three year following enucleation and hypothesized that enucleation contributed to metastases by disseminating the tumor cells.[48] Shortly after, Manschot stressed that radiotherapy was not a good alternative due to the frequent presence of cancer cells in irradiated eyes.[49] Co-60 eye plaques were being used at the time and about 50% of the patients died within five years of treatment due to metastases.[50] However due to differences between the patients with each study, a clear treatment method was difficult to support as tumor size greatly impacts mortality. In the late 1900s, a study reported a mortality of 16% for small tumors, 32% for medium tumors, and 53% for large tumors.[51]

In 1985, the Collaborative Ocular Melanoma Study (COMS), funded by the National Eye Institute, was created to perform a randomized clinical trial to compare radiation to enucleation. This was the largest ocular oncology study ever done including more than 2,000 total patients. Patients with large choroidal melanomas (more than 10 mm in apical height and 16 mm in basal diameter) were treated with either enucleation alone or enucleation followed by 20 Gy of external beam radiation. 1,003 patients were used for this study. The five-year all-cause mortality was 43% and 38% respectively for each treatment. It was concluded that there was no statistically significant difference between the treatments therefore invalidating Zimmerman's

hypothesis. As a result, it was concluded that enucleation does not accelerate death from metastases.[52,53,54]

Patients with medium choroidal melanomas (2.5-10 mm in apical height and no more than 16 mm in basal diameter) were treated with enucleation or brachytherapy using I-125. 1,317 patients participated in this study with an all-cause mortality of 43% in the brachytherapy patients and 41% in the enucleation patients. These results are not significantly different thus proving that brachytherapy is as safe as enucleation.[55,56]

Patients with small choroidal melanomas (1.5-2.4 mm in apical height and 5-16 mm in basal diameter) were followed clinically. 204 patients with small melanomas were observed. The five-year Kaplan-Meier estimates of tumor growth were 31%. The five-year all-cause mortality was 6%.[57]

As a result of this study, the use of LDR brachytherapy for the treatment of ocular melanomas greatly increased and is now the most popular method used today.[2]

Due to the popularization of this technique, protocols have been created to standardize the practice.

2.3.2.2 Eye Brachytherapy Protocols

2.3.2.2.1 AAPM TG-43

The American Association of Physicists in Medicine (AAPM) first developed the Task Group No. 43 (TG-43) Report in 1995 to standardize brachytherapy dose calculations. In 2004 this protocol was updated in TG-43U1 to account for advances in the field. The protocol defines the formalism for both a two-dimensional cylindrically symmetric line source and a one-dimensional point source. The air-kerma strength, dose rate constant, geometry function, radial

dose function, and anisotropy function are the parameters defined in TG-43 to characterize a radioactive source.[58]

The two-dimensional dose-rate equation is given as:

$$(1)\ \dot{D}(r,\theta) = S_k \Lambda \frac{G_L(r,\theta)}{G_L(r_0,\theta_0)} g_L(r) F(r,\theta)$$

Where r is the distance (in cm) from the center of the source to a point of interest, P(r, θ). r_0 is the reference distance (1 cm), θ is the polar angle from the center of the source along the longitudinal axis to a point of interest, and θ_0 is the reference angle (90°) on the transverse plane.

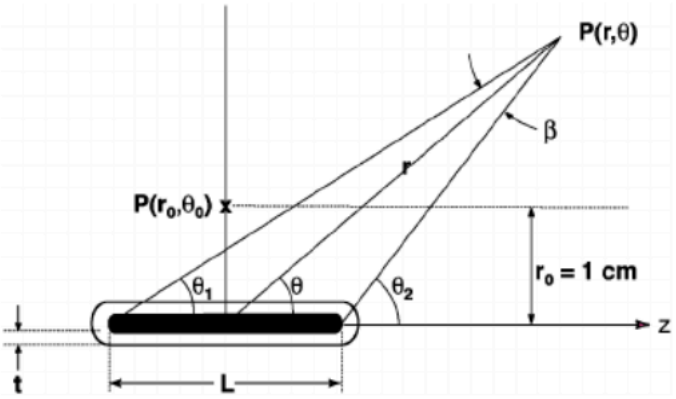

Figure 6: Coordinate system defined in the TG-43 report for brachytherapy dosimetry calculations.[44]

S_k is the air-kerma strength in μGy m^2 h^{-1} or U which is defined by $S_k = \dot{K}_\delta(d)d^2$. $\dot{K}_\delta(d)$ is the air-kerma rate in a vacuum, δ is the energy cutoff (5 keV), and d is the distance from the center

of the source to the point where the air-kerma rate is specified on the transverse plane of the source.

Λ is the dose-rate constant in water, which is defined as the ratio of the dose rate at the reference point $P(r_0,\theta_0)$ and the air-kerma strength, $\Lambda = \frac{\dot{D}(r_0,\theta_0)}{S_k}$.

The geometry function, $G_x(r,\theta)$ with units of cm^{-2}, interpolates between dose-rate data at defined points to give an inverse square law correction for the influence of the radionuclides physical distribution on the dose distribution. The approximations are given as:

$$(2)\ G_P(r,\theta) = r^{-2} \text{ for a point-source and}$$

$$(3)\ G_L(r,\theta) = \begin{cases} \frac{\beta}{Lr\sin\theta}\ if\ \theta \neq 0^\circ \\ (r^2 - L^2/4)^{-1}\ if\ \theta = 0^\circ \end{cases} \text{ for a line-source.}$$

Brachytherapy sources are seeds with a non-zero length and so the line-source approximation is more accurate. The subscript 'P' is used for point-source and 'L' is used for line-source. β is the subtended angle (in radians) of the point of interest, $P(r, \theta)$, to each end of the radioactive portion of the source. The total length of the active source is L (in cm). If there are multiple radioactive components then the effective length, L_{eff}, is used instead: $L_{eff} = \Delta S*N$, where N is the number of pellets and ΔS is the center-to-center spacing.

The radial dose function, $g_x(r)$, describes the dose rate from the source to a distance r relative to the reference distance r_0. It accounts for the dose fall-off on the transverse plane caused by photon scatter and attenuation. At the reference distance, this value is equal to 1.

$$(4)\ g_x(r) = \frac{\dot{D}(r,\theta_0)}{\dot{D}(r_0,\theta_0)}\frac{G_x(r_0,\theta_0)}{G_x(r,\theta_0)}$$

A fifth-order polynomial fit may be used to evaluate $g_x(r)$ by:

$$(5)\ g_x(r) = a_0 + a_1 r + a_2 r^2 + a_3 r^3 + a_4 r^4 + a_5 r^5.$$

Higher order regression equations can more precisely represent all of the parameters and better fit the data therefore, the fifth-order polynomial is used over lower orders.

The 2D anisotropy function, $F(r,\theta)$, describes the variation in dose as a function of the polar angle relative to the transverse plane. A point-source in theory would have a perfectly spherical spread of dose. The anisotropy function accounts for this deviation of dose around the source. It takes the ratio of the dose rate at radius r and angle θ around the source to the dose rate at r_0, which is 1 cm, and θ_0, which is 90°:

$$(6)\ F(r,\theta) = \frac{\dot{D}(r,\theta)}{\dot{D}(r,\theta_0)}\frac{G_L(r,\theta_0)}{G_L(r,\theta)}$$

The true 2D dose distribution may be approximated by a 1D isotropic point-source. The 1D anisotropy function, $\phi_{an}(r)$, is described as:

$$(7)\ \phi_{an}(r) = \frac{\int_0^{\pi}\dot{D}(r,\theta)sin(\theta)d\theta}{2\dot{D}(r,\theta_0)}.$$

The TG-43 protocol describes the currently accepted dose-calculation formalisms for characterizing a brachytherapy source. A limitation of this report, however, is that all of these calculations are performed in a homogeneous water medium. The report acknowledges that accounting for the heterogeneity effects would be more accurate however there is currently no FDA approved software to do this.[58]

2.3.2.2.2 AAPM TG-129

Most dose distributions are measured in water as specified by TG-43.[58] Advances in Monte Carlo simulations include the ability to reproduce complex geometries and account for heterogeneous materials. The gold-alloy backing and the silastic insert of the eye plaque can be modeled and perturbation effects from these materials measured using Monte Carlo simulations. Also, COMS was the only standardized clinical trial for choroidal melanoma and only included I-125 plaques.[56] Modern plaques currently utilize low energy photon seeds including I-125, Pd-103, and Cs-131, or solid beta plaques such as Ru-106 and Sr-90. The simulated materials, choice of radionuclide, and prescribed dose all affect the tumor control.[59,60] As a result, the Task Group-129 report by the AAPM and ABS was formed to review the current literature and make updated recommendations for eye-plaque dosimetry.[2]

COMS plaques are composed of a gold-alloy backing and silastic insert to hold LDR sources in place. There are grooves in the insert so the seeds may be placed in the exact same position each time. The silastic insert is also 1 mm thick between the seeds and the eye surface to reduce hot spots in the sclera. The radius of curvature is 12.3 mm for the silastic insert and 15.05 mm for the gold-alloy backing. The plaques range from 10-22 mm in diameter in 2 mm increments to cover different sized tumors, shown in Figure 7. The angle ϕ, in Figure 7, is the

angle between the $+x_p$ axis and the projection on the x-y plane where the line passes through the center of the seed. The angle ϕ is used to define the orientation and location of each seed in the COMS plaques. The origin is defined at the inner sclera of the eye, 1 mm from the outer sclera with the z_p axis pointing into the eye. The nominal physical length of the seed is 4.5 mm. The seed center and end coordinates (in mm) are defined for each COMS plaque 10-22 mm in diameter using the origin $x_p=0$, $y_p=0$, and $z_p=0$.

A

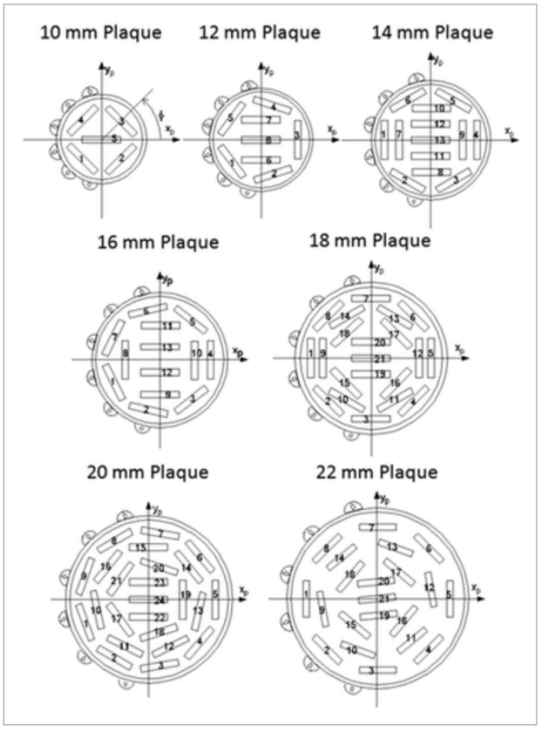

B

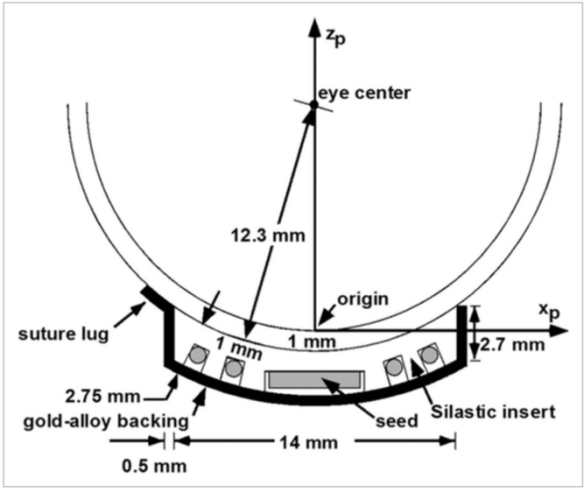

Figure 7: A) Seed diagrams of 10-22 mm COMS plaques. B) Side view of a 14 mm COMS plaque on an eye.[2]

The original COMS protocol used the 1D formalism from TG-43 because the approximation is almost identical to the central-axis dose results. The sources on the transverse

plane were aligned with the central axis of the plaque. However, off the central axis, there were dose differences greater than 5% between the 1D and 2D formalisms. Therefore, the recommendation from the AAPM and ABS is to only use the 2D formalism for eye plaque dosimetry along with the line-source geometry function.

Many studies have been performed, which demonstrated the differences in dose distribution of high-z materials compared to homogeneous water.[59-62] The AAPM and ABS now recommend performing dose calculations for both homogeneous water using TG-43, and heterogeneous materials.[58] The most accurate way to account for the heterogeneities would be with a Monte Carlo based treatment planning system however none are FDA approved. Until software is approved, a TG-43 hybrid technique or conventional TG-43 method may be used.[63,64] However, dose to the prescription point should at least be heterogeneity-corrected, but a 2D dose distribution would be preferred. The report presents the central-axis dose values for homogeneous and heterogeneous cases for each COMS plaque, normalized to 85 Gy at a depth of 5 mm into the eye.[64]

The AAPM and ABS also recommend for image-guidance, that treatment planning systems include tumor localization data. The distance from the tumor edge to the central fovea and optic disc should be calculated in order to aid in tumor measurement and determining intraocular distances. Accurate dose calculations are important for treatment planning and this report outlines updated methods that should be employed once more accurate treatment planning software is available.[2]

2.3.2.2.3 ABS Guidelines

The American Brachytherapy Society presented a set of guidelines specifically for the treatment of choroidal melanoma and retinoblastoma when using plaque brachytherapy.[65]

The tumor T is defined by its size and extent. Generally, patients with small T1 uveal melanomas (<2.5 mm height and <10 mm basal diameter) are observed for growth. Medium-sized T2 (2.5-10 mm height and <16 mm basal diameter) and large-sized T3 and T4 uveal melanomas (>10 mm height or >16 mm basal diameter) require treatment unless they have already metastasized. Patients may be candidates for plaque brachytherapy if they have been diagnosed with malignant uveal melanoma. Small melanomas may be treated if there is growth. Tumors with extraocular extension, basal diameters that exceed the limits of brachytherapy, blind painful eyes, and patients with no light perception vision are excluded from plaque brachytherapy.

The dose prescription currently used is based off of COMS, which is 85 Gy to tumors with an apical height ≥5 mm. However, it uses the TG-43 formalism (homogeneous medium) using a point-source approximation and no anisotropy correction. The ABS recommends a prescription dose of 85 Gy to the tumor apex for I-125. This isodose line should encompass the whole tumor and pass through the prescription point. The dose rate recommended by COMS is 0.43-1.05 Gy/h to the prescription point. However, dose rates less than 0.60 Gy/h have shown lower control rates. The ABS recommends a dose rate of 0.60-1.05 Gy/h for I-125 when delivering the total dose over 5-7 days. The dose may be modified if heterogeneous materials, anisotropy correction, and line-source approximations are considered.

Complications from eye plaque brachytherapy can be caused by radiation and patient-specific factors. Dry eye, iris neovascularization, secondary glaucoma, and cataracts are complications associated with the late anterior segment. The acute posterior segment or intraocular complications from the radiation include secondary retinal detachment and hemorrhage. The late posterior segment complication most commonly reported is radiation retinopathy. Strabismus, scleral atrophy, cystoid macular edema, and optic neuropathy are less common complications. These side effects may result in vision loss and decreased quality of life.

The ABS has presented their current guidelines for patient selection and treatment and they conclude that brachytherapy remains an effective way to treat uveal melanoma.[65]

2.3.3 Absorbed Dose Calculations

The absorbed dose (D) can be calculated from a radioactive source, assuming charged particle equilibrium, by the equation:

$$(8)\ D = \frac{\mu_{en}}{\rho} * N * E$$

where $\frac{\mu_{en}}{\rho}$ is the mass-energy absorption coefficient in cm^2/g. This is a measure of the fraction of the beam that is deposited to the medium per unit distance over the medium density. N is the photon fluence, a measure of the total number of photons which enter an area, in photons/cm^2 and E is the energy per photon in MeV. The photon fluence and energy per photon can also be combined into one quantity known as the photon energy fluence. The SI unit for absorbed dose is a gray (Gy), which is equal to 1 J/kg.

Equivalent dose (H) is a measure of the biological damage to tissue as a result of radiation exposure:

(9) $H = D * W_r$

where D is the absorbed dose in Gy and W_r is a radiation weighting factor. Each type of radiation has a different biological effect and so W_r takes this into account. X-rays and gamma rays have a W_r of 1 whereas alpha particles, which have a heavy, charged nucleus, have a W_r of 20. The units for equivalent dose are in sieverts (Sv) because this is a derived quantity, which provides a measure of the potential harm from the radiation. A gray on the other hand is a measurable quantity.

The effective dose (E_T) converts all doses into an equivalent whole-body dose:

(10) $E_T = \sum(H * W_T)$

where H is the equivalent dose in Sv and W_T is a tissue weighting factor because each type of tissue has a different sensitivity to radiation. Therefore, the dose to each tissue and organ can be summed together to calculate the dose for the whole-body. This effective dose quantity is also derived therefore the units are in Sv.

The biological effective dose (BED) is a measure of the true biological dose delivered by a particular combination of dose per fraction and total dose to a particular tissue:

(11) $\mathrm{BED} = D\left[1 + \frac{d}{\alpha/\beta}\right]$

where D is the total dose in Gy and d is the dose per fraction (Gy). The sensitivity of a specific cell type to radiation is described by α/β in Gy. This quantity can be found experimentally by testing the cell lines. The BED is an important quantity in radiation therapy because it can be used to compare different fractionation schemes or determine how one treatment type could be equivalent to another.

3 Methods

3.1 Computational Validation

I used the MCNP6 radiation simulations program (from the Los Alamos National Laboratories, Los Alamos NM) to simulate the transport of radiation and its transfer and deposition of energy into matter created by the proposed middle-energy treatment system in a model human eye. MCNP6 has the ability to transport many particles over an extended energy range with an updated library package, MCPLIB04 to give excellent low photon transport and dosimetry data.[66] Prior to simulating the proposed device, I validated my Monte Carlo model by simulating the eye plaque used by Lesperance with my results compared against those published by Lesperance.[13]

In this study, Lesperance simulated a 16 mm COMS plaque with multiple sources, including I-125, in BrachyDose using an eye model including various compositions and geometries.[13] They investigated the dose to these ocular structures when accounting for heterogeneities. BrachyDose is a Monte Carlo code. It is a software that utilizes a tracklength estimator to calculate collision kerma in voxels. This is especially useful for approximating dose from low energy photon sources, like I-125. The range of the electrons is smaller than the voxel size so it is assumed that all of the electrons deposit their energy locally. The photon transport cut-off was 1 keV and included Compton and Rayleigh scattering. Yegin's multigeometry package can be used with BrachyDose so that the eye plaque can be simulated with the eye model.

3.1.1 Eye Model

Current dose calculation methods approximate the eye as a pseudo-infinite homogeneous water phantom. Knowing the oversimplicity of this model, Lesperance et al. developed a human

eye model that accounted for the ocular geometry, composition, and density of each structure.[2,13] He also modeled the tissues surrounding the eye in reference to the ICRP computational phantom.[13,67,68] Because Lesperance's model is more realistic, I also used this model for my Monte Carlo study rather than the more generic AAPM model.

The Lesperance eye model is representative of an adult right eye centered at the origin, as presented in Figure 8. The positive x-axis is pointed in the anterior direction, the positive z-axis is pointed in the lateral direction, and the y-axis is pointed in the superior direction. The dimensions and compositions of the ocular structures used include the sclera, cornea, iris, lens, optic nerve, vitreous humor, aqueous humor, and tumor.

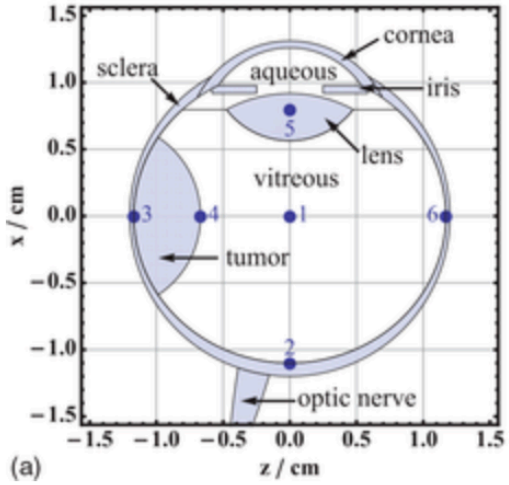

Figure 8: Coordinate system used for a computational model of a right eye.[13]

A voxelized eye model was created by using bounding surfaces to define each ocular structure, which was based on average values. The outer surface of the sclera is defined as a 24 mm diameter sphere and the inside surface as an ellipsoid. The ellipsoid is 1 mm thick at the posterior poles and 0.3 mm thick on the medial and lateral sides of the eye. The outer surface of the cornea is defined as a 7.8 mm sphere, which intersects with the outer sclera forming an 11.7 mm diameter circle. The inner cornea is a 6.5 mm sphere, which creates a 0.52 mm thick cornea

on the x-axis. The iris is formed by two 5 and 11.7 mm diameter cylinders and two planes. A thickness of 0.6 mm is created in the x-direction. The anterior surface intersects with the inner sclera and cornea. The anterior surface of the lens is defined as a 10 mm radius sphere and the posterior surface is a 6 mm sphere. On the yz plane, the intersection of these spheres forms the lens with a 9.5 mm diameter across the center. The region between the inner cornea and anterior lens is the aqueous humor. The remaining region between the inner sclera and posterior lens is the vitreous humor. The optic nerve is defined by three cylinders measuring a total length of 1.1 cm that increases in diameter at the optic disk to 1.5 mm, at the midsclera to 2.5 mm, and at the outer sclera to 3.5 mm. Not all of the optic nerve was modeled as dose to these points are very low. The optic disk, which intersects with the inner sclera, is not modeled either because it is located at y = -1 mm and z = -3 mm. The tumor is defined as a 12 mm diameter sphere in the y-direction from where it intersects with the inner sclera and with its apex 5 mm inward from the inner edge of the sclera. This medium-sized tumor is representative of a very common dome-shaped choroidal melanoma. It is located on the medial side of the right eye and centered on the z-axis. The elemental compositions by mass fraction and the densities used in this study are given in Table 1.

Table 1: Elemental compositions of various eye structures[13]

Eye Structure	Elemental mass fraction									
	H	C	N	O	Na	P	S	Cl	K	Density (g/cm^3)
Cornea	0.1016	0.1199	0.0364	0.7411	-	-	0.0009	-	-	1.050
Sclera	0.0970	0.1696	0.0499	0.6831	-	-	0.0003	-	-	1.050
Vitreous	0.1109	-	-	0.8804	0.0038	-	-	0.0045	0.0003	1.0071
Aqueous	0.1110	0.0010	-	0.8810	0.0030	-	-	0.0040	-	1.0035
Lens	0.0960	0.1950	0.0570	0.6460	0.0010	0.0010	0.0030	0.0010	-	1.070
Optic nerve	0.1060	0.1940	0.0250	0.6610	0.0020	0.0040	0.0020	0.0030	0.0030	1.040
Iris	0.1020	0.1430	0.0340	0.7100	0.0010	0.0020	0.0030	0.0010	0.0040	1.050
Tumor	0.0940	0.2120	0.0560	0.6150	0.0025	0.0051	0.0064	0.0039	0.0051	1.040

The eye model was created using voxels each having a volume of 0.5 mm^3. If the center of the voxel is within a bounding surface of a structure, it is assigned the composition of that structure.

Lesperance used the ICRP female reference computational phantom to model the media around the eye. The female phantom has a higher resolution than the male phantom, which is why it was chosen. The voxelized eye model was superimposed on the eye region of the ICRP model so that the resultant model contained the eye with defined ocular structures and tissue surrounding the eye.[67,68] Lesperance also used a 12 mm radius eye as opposed to the TG-129 report which used a 12.3 mm radius.[2,13] They also defined the sclera as an ellipsoid 1 mm thick at the posterior poles of the eye and in the plane separating the anterior and posterior halves as 0.3 mm thick.[13] The tumor modeled is located in this thinner section of the sclera, which is more prone to hot spots. TG-129 used a sphere 1 mm thick for the sclera.[2] These measurements also were used for this study. I also added the eye's choroid, which I modeled as an ellipsoid with the same thicknesses as the sclera.[69] The Monte Carlo model used for this study is presented in Figure 9.

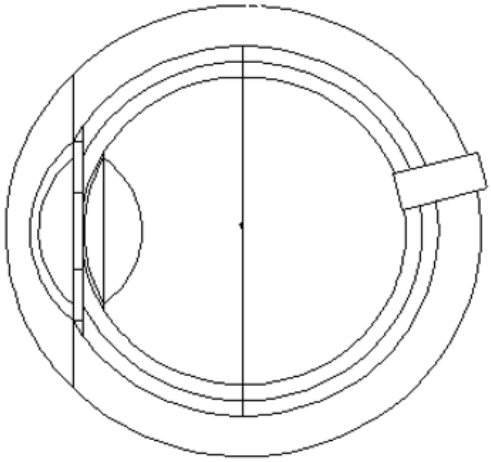

Figure 9: XY view of the eye model

3.1.1.1 MCNP Geometry Surfaces

The outer surface of the sclera is defined by a sphere with radius 1.20 cm

SO 1.20

The inner surface of the sclera is defined by an ellipsoid centered on the origin with semi-principal axes a (x-axis) = 1.10 cm, b (y-axis) = 1.10 cm, and c (z-axis) = 1.17 cm.

SQ 1.00 1.00 0.8839 0.00 0.00 0.00 -1.21 0.00 0.00 0.00

The inner surface of the choroid is defined by an ellipsoid centered on the origin with semi-principal axes a (x-axis) = 1.00 cm, b (y-axis) = 1.00 cm, and c (z-axis) = 1.14 cm.

SQ 1.00 1.00 0.7695 0.00 0.00 0.00 -1.00 0.00 0.00 0.00

The outer cornea is bounded by a sphere with radius 0.78 cm and its intersection with the outer sclera forms a circle of diameter 1.17 cm. The center of the sphere is at x = -0.5318 cm.

SX -0.5318 0.78

The inner cornea is bounded by a sphere with a radius of 0.65 cm and is positioned so the corneal thickness is 0.052 cm on the x-axis. The center of the sphere is at x = -0.6098 cm.

SX -0.6098 0.65

The iris is bounded by two cylinders with diameters 0.5 and 1.17 cm and two planes so that its thickness in the x-direction is 0.06 cm and its anterior surface is at the intersection of the outer sclera and cornea.

CX 0.585

CX 0.250

PX -1.0477

PX -0.9877

The lens is defined by two spheres with a radius of 1.0 cm for the anterior surface and 0.6 cm for the posterior surface. Their intersection creates a diameter of 0.95 cm at the widest point of the lens in the yz plane. The anterior face of the lens is 0.01 cm from the posterior face of the iris.

SX 0.0223 1.00

SX -1.2243 0.60

PX -0.8577

The optic nerve is defined as a right circular cylinder with a diameter of 2.5 mm. It begins just inside the inner surface of the choroid (radius 9.8 mm) and continues 3.2 mm outside the outer surface of the sclera. The optic nerve is in the xy plane and rotated 15° from the x-axis using the *TR card.

RCC 0.98 0.00 0.00 0.54 0.00 0.00 0.125

*TR1 0 0 0 15 75 90 105 15 90 90 90 0

A medium-sized tumor is modeled in the region of the choroid as a segment of a sphere to emulate a dome-shaped choroidal uveal melanoma. The tumor has a diameter of ~12 mm in

the y-direction at its intersection with the inner sclera and its apex is 5 mm inward from the outer edge of the sclera. The tumor is chosen to lie on the medial side of the right eye and centered on the z-axis.

SZ 1.4435 0.7435

3.1.1.2 Tallies

Various tallies were used to characterize the dose distribution within the eye. The mass energy-absorption coefficients for each ocular structure were calculated by taking the sum of each of their elemental mass fractions (Table 1) times the mass energy-absorption coefficients for that element, obtained from NIST, for energies 0.001-1.5 MeV. For the bone, calculations were not necessary as values were already given by NIST for cortical bone. The planar dose from photons in the planes located behind the gold shield used flux modifiers based on the composition of water, which is also given by NIST.

Depth Dose

A cylindrical mesh tally was used to determine the depth dose along the z-axis of the eye in 0.5 mm increments. This *FMESH214 tally was coupled with a flux modifier (DE/DF card) comprised of μ_{en}/ρ values for the composition of the vitreous humor, which comprises most of the tissue along this path.

Planar Distribution

A rectangular mesh tally was used to determine the dose distribution throughout the eye along the x-z plane in 0.5 mm increments. This *FMESH224 tally was coupled with a flux

modifier (DE/DF card) comprised of μ_{en}/ρ values for the composition of the vitreous humor, which comprises most of the tissue along this path. A cell-by-cell analysis was performed to determine which cells are within the eye:

$$x^2 + z^2 \leq (1.2)^2$$

The cells outside of this volume were rejected.

Scleral Absorbed Dose

A cylindrical mesh tally was used to determine the dose distribution at a depth to 1 mm in the x-z plane of the eye in 1° increments. This *FMESH234 tally was coupled with a flux modifier (DE/DF card) comprised of μ_{en}/ρ values for the composition of the sclera.
An F6 tally was used to determine the average dose to the sclera. Due to the geometric complexity of this structure, the 'vol=' command was used in the code to specify the volume of each cell in the sclera. Then the weighted average was calculated.

Tumor Absorbed Dose

A rectangular mesh tally was used to determine the dose distribution within the tumor in 0.5 mm increments. The mesh has a range from:

$$-0.525 \leq x \leq 0.525$$
$$-0.525 \leq y \leq 0.525$$
$$0.675 \leq z \leq 1.225$$

This *FMESH244 tally was coupled with a flux modifier (DE/DF card) comprised of μ_{en}/ρ values for the composition of the tumor. A cell-by-cell analysis was performed to determine which cells lie within the tumor:

$$x^2 + y^2 + 0.8839(z)^2 \leq (1.1)^2$$

and a rejection of cells outside of this volume:

$$x^2 + y^2 + (z - 1.4435)^2 \leq (0.7435)^2.$$

The average dose to the tumor was also calculated using an F246 tally.

Lens Absorbed Dose

A rectangular mesh tally was used to determine the dose distribution within the lens in 0.5 mm increments. The mesh has a range from:

$-1.025 \leq x \leq 0.625$
$-0.475 \leq y \leq 0.475$
$0.475 \leq z \leq 0.475$

This *FMESH254 tally was coupled with a flux modifier (DE/DF card) comprised of μ_{en}/ρ values for the composition of the lens. A cell-by-cell analysis was performed to determine which cells lie within the lens:

$$(x - 0.0223)^2 + y^2 + x^2 \leq (1.0)^2$$

and a rejection of cells outside of this volume:

$$(x + 1.2243)^2 + y^2 + x^2 \leq (0.60)^2.$$

The average dose to the anterior lens was also calculated using an F256 tally and the average dose to the lens using an F266 tally.

Cornea Absorbed Dose

A rectangular mesh tally was used to determine the dose distribution within the cornea in 0.5 mm increments. The mesh has a range from:

$-1.325 \leq x \leq -1.025$
$-0.625 \leq y \leq 0.625$
$-0.625 \leq z \leq 0.625$

This *FMESH274 tally was coupled with a flux modifier (DE/DF card) comprised of μ_{en}/ρ values for the composition of the cornea. A cell-by-cell analysis was performed to determine which cells lie within the cornea:

$$(x + 0.5318)^2 + y^2 + z^2 \leq (0.78)^2$$

and a rejection of cells outside of this volume:

$$(x + 0.6098)^2 + y^2 + z^2 \geq (0.65)^2.$$

The average dose to the cornea was also calculated using an F276 tally.

Iris Absorbed Dose

A rectangular mesh tally was used to determine the dose distribution within the iris in 0.5 mm increments. The mesh has a range from:

$-1.025 \leq x \leq -0.975$
$-0.625 \leq y \leq 0.625$
$-0.625 \leq z \leq 0.625$

This *FMESH284 tally was coupled with a flux modifier (DE/DF card) comprised of μ_{en}/ρ values for the composition of the iris. A cell-by-cell analysis was performed to determine which cells lie within the iris:

$$y^2 + z^2 \leq (0.585)^2$$

and a rejection of cells outside of this volume:

$$y^2 + z^2 \geq (0.25)^2.$$

The average dose to the iris was also calculated using an F286 tally.

Optic Absorbed Dose

A rectangular mesh tally was used to determine the dose distribution within the optic nerve in 0.5 mm increments. Even though the optic nerve is rotated 15° from the x-axis, the source is located at the top of the eye and symmetry permits the dose to be calculated as if the optic nerve were located along the x-axis. The mesh has a range from:

$$0.975 \leq x \leq 1.525$$
$$-0.125 \leq y \leq 0.125$$
$$-0.125 \leq z \leq 0.125$$

This *FMESH294 tally was coupled with a flux modifier (DE/DF card) comprised of μ_{en}/ρ values for the composition of the optic nerve. A cell-by-cell analysis was performed to determine which cells lie within the optic nerve:

$$y^2 + z^2 \leq (0.125)^2$$

and a rejection of cells outside of this volume:

$$y^2 + z^2 \geq (0.25)^2.$$

The average dose to the optic nerve was also calculated using an F296 tally.

3.1.2 COMS Plaque

Lesperance et al modeled a standard 16 mm I-125 COMS plaque with their eye model in BrachyDose, therefore I modeled this same plaque with their eye model in MCNP6. The 16 mm COMS plaque contains thirteen sources positioned according to their seed coordinates from the TG129 report.[2] However these coordinates are in reference to an origin defined at the inner sclera from the TG-129 eye model, which defines the sclera as a 1 mm thick sphere. Lesperance's eye model used an ellipsoid for the sclera, which is only 0.3 mm thick near the plaque, therefore the seed coordinates were adjusted accordingly. Table 2 gives the seed coordinates in millimeters of the 16 mm plaque as specified by the TG-129 report. The seeds were rotated according to their angle from the table.

Table 2: Seed center coordinates of a 16 mm COMS plaque from TG-129[2]

		Seed center coordinates			
	Seed #	x	y	z	Angle ϕ (°)
16 mm plaque	1	-5.68	-2.73	-0.87	206
	2	-1.40	-6.14	-0.87	257
	3	3.93	-4.93	-0.87	309
	4	6.30	0.00	-0.87	0
	5	3.93	4.93	-0.87	51
	6	-1.40	6.14	-0.87	103
	7	-5.68	2.73	-0.87	154
	8	-4.50	0.00	-1.64	180
	9	0.00	-4.50	-1.64	270
	10	4.50	0.00	-1.64	0
	11	0.00	4.50	-1.64	90
	12	0.00	-1.80	-2.28	270
	13	0.00	1.80	-2.28	90

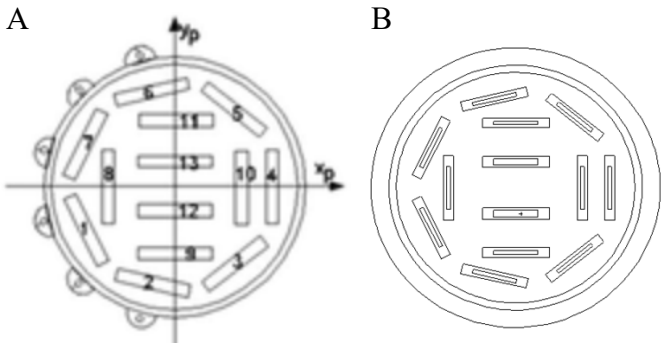

Figure 10: A) An image from the TG-129 report[2] of the 16 mm COMS plaque and B) is an image of the seeds in the XY plane from my MCNP6 model.

The I-125 seeds were modeled from the Oncura model 6711, which is a standard I-125 seed commonly used for ocular brachytherapy. The radioactive portion of the seed contains a 2.5:1 ratio of AgI:AgBr with a density of 6.2 g/cm^3. This is coated 1.75 μm thick over the entire surface of a silver rod. The rod measures 2.80 mm long with a 0.25 mm radius. It is encapsulated in a titanium tube 3.75 mm long with 0.070 mm thick walls, a 0.80 mm outer diameter, and 0.375 mm thick hemi-spherical end welds. The total seed length is 4.55 mm and the active length is 2.80 mm.[70]

The seeds were placed in a silicone-polymer silastic insert.[70] The silastic insert has a 1 mm thick spacing between the outer surface of the sclera and the sources.[2] The plaque was placed along the surface of the outer sclera and centered on the z axis of the central tumor. A 0.5 mm gold alloy backing covered the outer surface of the plaque.

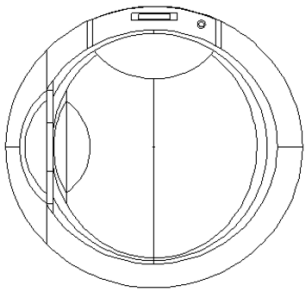

Figure 11: XZ view of the eye model with the plaque from MCNP6.

The dose rate constant for this source reported in TG-43 is 0.965 cGy h^{-1} U^{-1}. The radial dose function and anisotropy values are given in Table 3 and Table 4 respectively.[58]

Table 3: Consensus radial dose function values from TG-43 for the OncoSeed 6711.[58]

r (cm)	Line-source	Point-source
0.10	1.055	0.696
0.15	1.078	0.853
0.25	1.082	0.982
0.50	1.071	1.048
0.75	1.042	1.036
1.00	1.000	1.000
1.50	0.908	0.912
2.00	0.814	0.819
3.00	0.632	0.636
4.00	0.496	0.499
5.00	0.364	0.367
6.00	0.270	0.272
7.00	0.199	0.200
8.00	0.148	0.149
9.00	0.109	0.110
10.00	0.0803	0.0809

Table 4: Consensus anisotropy function values from TG-43 for the OncoSeed 6711.[58]

Polar angle	r (cm)					
θ (degrees)	0.5	1	2	3	4	5
0	0.333	0.370	0.442	0.488	0.520	0.550
5	0.400	0.429	0.497	0.535	0.561	0.587
10	0.519	0.537	0.580	0.609	0.630	0.645
20	0.716	0.705	0.727	0.743	0.752	0.760
30	0.846	0.834	0.842	0.846	0.848	0.852
40	0.926	0.925	0.926	0.926	0.928	0.928
50	0.972	0.972	0.970	0.969	0.969	0.969
60	0.991	0.991	0.987	0.987	0.987	0.987
70	0.996	0.996	0.996	0.995	0.995	0.995
80	1.000	1.000	1.000	0.999	0.999	0.999
$\phi_{an}(r)$	0.973	0.944	0.941	0.942	0.943	0.944

A dose of 85 Gy over 5-7 days to the apex of the tumor is the standard prescription dose for LDR eye plaque brachytherapy using I-125.[42] In this case, I assumed that depth to be 5 mm and normalized the results to 85 Gy over 5 days (0.71 Gy/hr). MCNP6 simulations were performed using the described eye model and plaque to calculate the dose distribution in the eye. An fmesh4 photon tally was used for each ocular structure with its unique mass energy absorption coefficients for the flux modifier. The I-125 gamma energies and abundances were obtained from the Brookhaven National Laboratory (BNL) National Nuclear Data Center (NNDC) database.[72] The simulations accounted for bremsstrahlung production and coherent scattering. The maximum, minimum, and average dose to the critical structures were reported as well as isodose curve of the dose distributions. These measurements were then compared to Lesperance's results.[13]

Dose volume histogram (DVH) are presented in the results as well. DVH curves are histograms that relate the radiation dose to the tissue volume of interest. They are commonly used in radiation therapy planning to evaluate different plans and compare the dose to critical structures. DVH curves present 2D information from a 3D dose distribution. I calculated the

DVH curves in this study by first creating a number of bins for each structure. The dose rates were then sorted into the bins by using Excel's frequency function. This calculates how often the values occur within the range of each bin and gives an array of these results. Then the frequency of each bin was divided by the total number of values in the array. Finally, the summation of the fraction of the frequency of each bin was subtracted from 1. Therefore, the array starts at 1 and ends at 0. At 1, 100% of the volume of the structure is receiving 0 dose. At 0, no volume of the structure is receiving a dose. Therefore, the DVH curves show the range of dose that is absorbed in a structure based on its volume.

3.2 The Proposed HDR Applicator Monte Carlo Design

3.2.1 Ring Source and Plaque Design

Once the COMS Monte Carlo code is validated against the COMS published data, the code will be modified to simulate my proposed middle energy HDR ocular treatment system. The proposed ocular plaque for HDR brachytherapy, presented in Figure 12, consists of an assembly of discrete sources that are delivered simultaneously into the shielded applicator which forms the sources into a circular ring. These sources will be delivered using a remote afterloader, which may be manual or automatic, with only a single stopping position therefore no source stepping is required.

The active element in the Yb-169 sources consist of Ytterbium Oxide (Yb_2O_3) enriched to 20% in Yb-168 and pressed to a density of 6 mg/mm^3 (sintering not required) with an active diameter of 0.39 mm and active length of 1.75 mm. The mass of Ytterbium Oxide for each pellet is 0.72 mg. These pellets are enclosed in titanium with a capsule outside diameter of 0.55 mm and 0.08 mm wall for a total length of 2.25 mm. The same measurements were employed for the Se-75 pellets, which contain an active element of Iron Selenide encapsulated in titanium. The array of sources is contained inside a 1.00 mm diameter stainless steel source sheath and a 1.25 mm diameter stainless steel source tube. Air fills the spacing between the sources and source sheath. The source sheath is a spring-like structure, which is flexible enough to curve around the inside of the applicator (US Patent 10,576,299), and the source tube is used to guide the array into a toroidal shape.[73] A polyether ether ketone (PEEK) insert, composed of carbon, hydrogen, and oxygen, makes up the inside of the plaque and is backed by 1.3 mm thick gold.

The shielded applicator here was modeled as a 12 mm annular ring plaque with a radius of curvature of 6.2 mm and circumference of 39 mm. Sixteen individual pellets were designed to fit within this channel to cover the circumference of the ring.

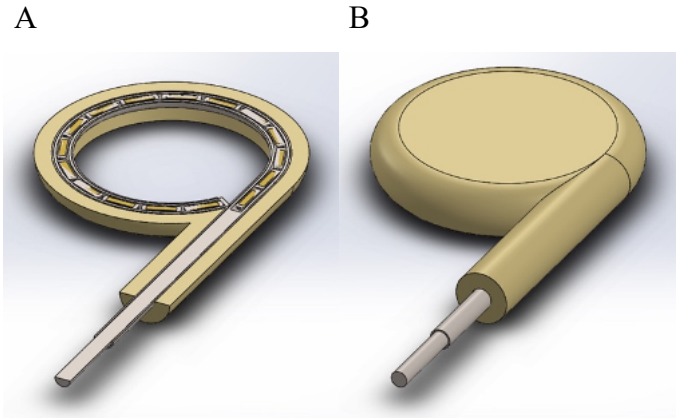

Figure 12: A 12 mm applicator with sixteen individual sources contained in a source array, which can curve to very small diameters.

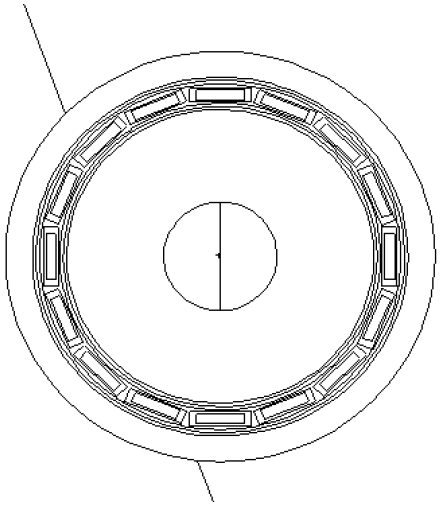

Figure 13: XY view of the source array contained in a 12 mm ring applicator.

The standard dose prescription for LDR ocular brachytherapy is 85 Gy to the apex of the tumor within a period of 5 to 7 days. For this prescription dose, I calculated the Biologically Effective Dose (BED) using the relationship of Gagne et al:[74]

$$\mathrm{BED} = \left(\frac{R_0(1-e^{-\lambda T})}{\lambda}\right) \times \left\{1 + \frac{2R_0\lambda}{(\mu-\lambda)(\frac{\alpha}{\beta})(1-e^{-\lambda T})} \times \left[\frac{1}{2\lambda}\left(1-e^{-\lambda T}\right) - \frac{1}{(\mu+\lambda)}(1-e^{-(\mu+\lambda)T})\right]\right\}$$

For the standard prescription, the initial dose rate R_0 of I-125 is 0.71 Gy/h (85 Gy per 5 days), the decay constant λ is 4.85E-4 hours, the treatment time T is 5 days, the repair constant of sublethal damage μ is 0.46 h^{-1}, and the mean α/β tumor value is 11.5 Gy. This results in a BED of 103.67 Gy.

My approach is to use HDR brachytherapy with a treatment time of ~10 minutes. Therefore, using this same relationship of Gagne et al, a decay constant of 9.02E-4 h, and treatment time for Yb-169 of 10 minutes (all other factors constant), this BED results in a dose of 30 Gy (or 3 Gy/min). Se-75, with a decay constant of 2.41E-4 h, also results in a dose of 30 Gy. Therefore, this HDR dosimetric criteria is biologically equivalent to an LDR of 85 Gy over 5 days.

The plaque was designed to collimate Yb-169 and Se-75 photons to maximize dose to the tumor and minimize dose to healthy tissues. Gold shielding is positioned around the outside of the ring source to collimate and align the beam to the outer edge of the target using static intensity modulation. This is different from the COMS plaques because gold is not angled around the sources to control the depth of the dose. Different plaque gold inserts for the ring applicator (diameter and angle openings) are selected to accommodate delivery of the prescription dose to different targets (base diameter and apex height). Therefore, different applicators are selected depending on the patient in order to control the amount of modulation. As with COMS plaques, the plaque size is selected to include a margin of 2 mm around the tumor. The target in this study is defined as the tumor plus margin.

Using a specified target depth and applicator diameter, the desired collimator angle and apex were calculated. These measurements (in mm) are presented in Table 5. The collimator

angle is defined by the location of the conical apex (relative to the center of the eye; 0 mm). Positive values are distances above the center of the eye and negative values are below the center of the eye. The collimation begins at a position tangent to the outside of the source tube and is conical in shape, as seen in Figures 14 and 15. In this way, the same source array can be used to treat a variety of tumor sizes. The source array can also be used for different diameter applicators. Any unused sources are located at the straight lead-in to the collimator and shielded with 2 mm of gold.

In Table 5, the applicator diameter and target depth were chosen. The target is defined by a sphere and the outer surface of the sclera is defined by an ellipsoid. This point of intersection defines the target edge, which gives the target diameter. The collimator apex is defined by a cone, which is just large enough to encompass the target. Therefore, the surface of the cone is tangent to the point of intersection between the target and sclera. By solving the three equations, the collimator apex was found and then through geometry, the collimator angle was calculated.

Table 5: Ring applicator measurements (in mm)

Applicator Diameter	Collimator Apex	Collimator Angle (°)	Target Diameter	Target Depth
12	5.3	44.6	10.0	3.5
	3.7	38.5	10.4	4.0
	1.8	32.7	10.8	4.5
	-0.7	27.2	11.1	5.0
	-4.0	22.1	11.4	5.5
	-8.7	17.4	11.6	6.0
14	6.1	53.6	11.0	3.5
	4.8	47.6	11.4	4.0
	3.4	41.9	11.7	4.5
	1.6	36.5	12.0	5.0
	-0.5	31.4	12.3	5.5
	-3.1	26.5	12.5	6.0
	-6.5	22.0	12.9	6.5
16	5.6	56.4	12.3	4.0
	4.4	50.9	12.7	4.5
	3.1	45.6	13.0	5.0
	1.5	40.5	13.3	5.5
	-0.3	35.6	13.6	6.0
	-2.4	31.0	13.8	6.5
	-5.1	26.6	14.1	7.0
	-8.5	22.5	14.3	7.5
18	6.2	65.1	13.3	4.0
	5.2	59.8	13.6	4.5
	4.1	54.6	14.0	5.0
	2.8	49.6	14.3	5.5
	1.5	44.8	14.5	6.0
	-0.1	40.1	14.8	6.5
	-1.9	35.7	15.0	7.0
	-4.1	31.5	15.2	7.5
	-6.6	27.4	15.5	8.0

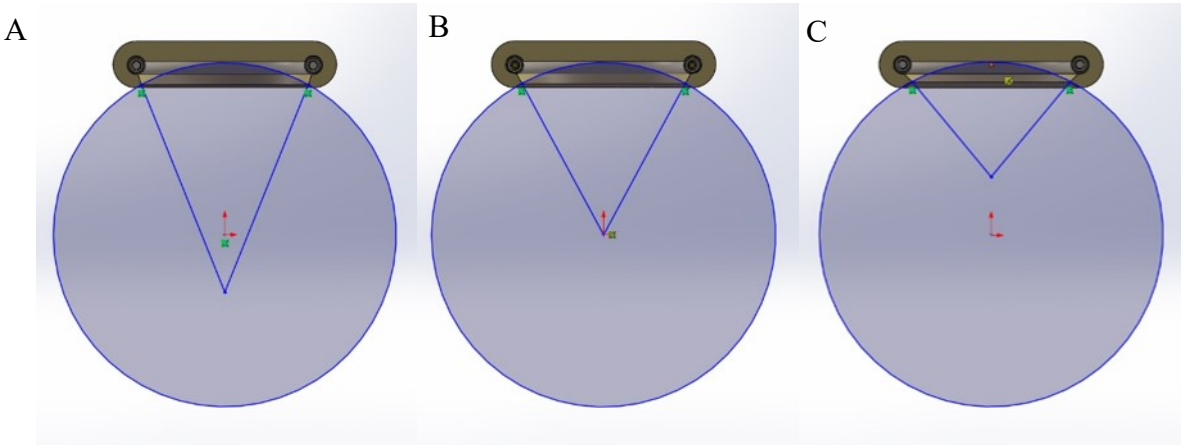

Figure 14: Demonstrates the collimator apex at various foci relative to the center of the eye. A) is the collimator apex at -4 mm, which is 4 mm below the center of the eye. B) is at 0 mm and C) is at 4 mm.

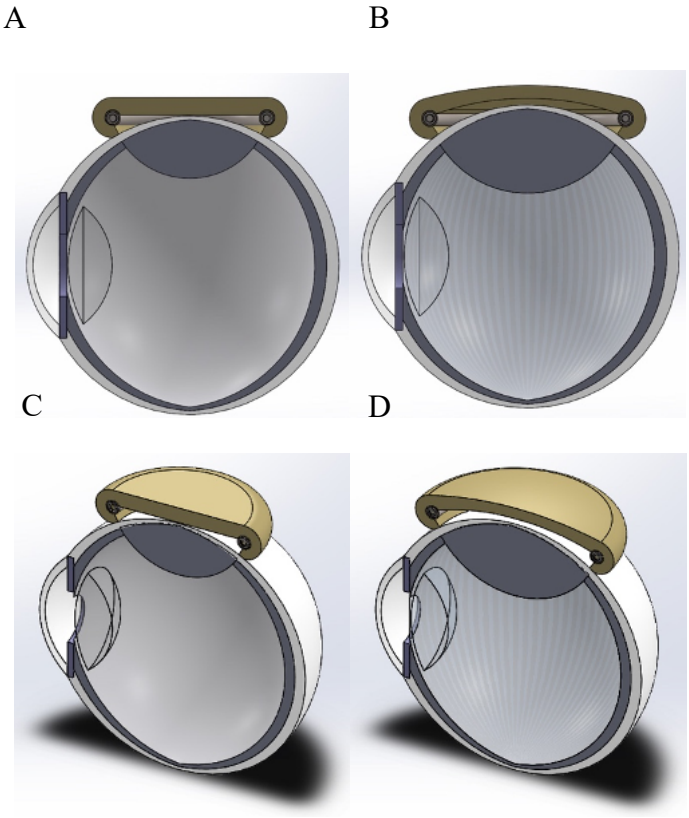

Figure 15: A) and C) are of a 12 mm applicator. B) and D) are of a 16 mm applicator.

3.2.2 MCNP Simulations

MCNP6 was used to model applicators 12-18 mm in diameter containing various collimator angles to deliver the prescription dose of 30 Gy to a range of depths in the eye with a resolution of 0.5 mm^3. The fmesh4 photon tally (average cell flux tally) was used for each structure and accounted for Bremsstrahlung production and coherent scattering with photon transport cutoffs set to 1 keV. The Yb-169 and Se-75 gamma energies and abundances were obtained from BNL.[72]

The ring source was modeled in a toroidal shape and placed in a PEEK insert. The outside edge of the source tube was aligned with the edge of the target by adjusting the angle of the collimator to control the depth of the prescription dose for different sized targets. The specifications were modeled as described in the ring source and plaque design section.

A disadvantage of middle energy brachytherapy sources, especially those with energies around 60 keV, is that they tend to deposit higher absorbed dose to bone relative to low energy sources. Therefore, the orbital bone was included in the eye model to verify if the dose to bone is within acceptable limits. The orbital cavity was approximated as a 40 mm diameter spherical shell composed of muscle. The orbital bone was modeled as a 50 mm diameter sphere, 5 mm thick, and composed of cortical bone.[75] The orbital bone wall began just below the center of the lateral side of the eye and extended about 165 degrees around to the medial side of the eye. The remainder of the sphere was modeled as air and the area outside of this surface as water.

The orbital bone is defined as a sphere enclosed by two surfaces, 2.0 mm and 2.5 mm in diameter. Outside of this sphere is infinite water and inside is the orbital cavity composed of muscle. As part of the orbital is exposed to air and the other part to the orbital cavity, the orbital wall was used to create this separation using a plane.

SO 2.00

SO 2.50

P 0.96 -0.35 0 -0.35

A rectangular mesh tally was used to determine the dose distributions within the bone in 0.5 mm increments. The mesh has a range from:

$-2.5 \leq x \leq 2.5$
$-2.5 \leq y \leq 2.5$
$-2.5 \leq z \leq 2.5$

This *FMESH314 tally was coupled with a flux modifier (DE/DF card) comprised of μ_{en}/ρ values for the composition of the bone. A cell-by-cell analysis was performed to determine which cells lie within the bone:

$$x^2 + y^2 + z^2 \leq 2.5^2$$

and a rejection of cells outside of this volume:

$$x^2 + y^2 + z^2 \geq 2^2$$

$$0.8x^2 - 0.25y^2 \geq 0.25^2$$

The average dose to the bone was also calculated using an F316 tally.

Various isodose curves are presented for applicators 12-18 mm in diameter and a range of collimator angles and target sizes. A dose volume histogram was made for selected applicators. As the dose rate is higher with HDR sources, the lateral dose rate 5 mm from the surface of the eye, behind the applicator, was measured. In addition, a comparison of the percent dose rate to ocular structures from the Yb-169 and Se-75 ring applicator is made to the I-125 COMS plaque for a plaque 16 mm in diameter that delivers the prescription dose to a 5 mm depth in the eye.

3.3 Experimental validation

The next step of this study is to experimentally verify the intensity modulation of middle-energy HDR brachytherapy sources with gold shielding by using Gafchromic EBT3 film. Radiochromic film is a type of dosimeter that is used to measure the absorbed dose of ionizing radiation.[76] The film contains crystalline diacetylenes that undergo polymerization when exposed to radiation.

Gafchromic EBT3 film by Ashland Specialty Ingredients, is a specific type of radiochromic film that is well suited for high-energy photons and performs best in the dose range from 0.2-10 Gy.[76] There is a minimal response difference with energies from 100 keV into the MeV range. It is comprised of an active layer, 28 μm thick, between two matte-surface polyester substrates, each 125 μm thick. The atomic composition of the active layer is H (56.8%), C (27.6%), O (13.3%), Al (1.6%), and Li (0.6%) with an effective atomic number of 7.26, near tissue equivalent. It contains a yellow marker dye to decrease UV and visible light sensitivity and to enable non-uniform correction by using multi-channel dosimetry with an RGB film scanner. It has a high spatial resolution of about 25μm. Due to the symmetric structure of the film, either side can face the light source of the scanner. It also features an anti-Newton ring coating to prevent the formation of Newton's Rings, an interference pattern, in the images. The coating maintains a gap between the film surface and glass window of the scanner, which is larger than the wavelength of visible light. The film also develops in real time and does not need any post exposure treatment.

The active component in the film reacts with radiation to form a blue colored polymer. Its absorption maxima is 633 nm. A 48-bit flatbed color scanner is recommended to be used with this film. This would measure the red, green, and blue color components of light at 16-bits per

channel. Specific scanner models include the EPSON Expression 10000 XL and 11000XL Photo scanners. The calibration curve is recommended to be fit to a function of the form:

$$d_x(D) = a + b/(D - c)$$

Where $d_x(D)$ is the optical density of the film at dose D in scanner channel x, and a, b, and c, are the equation parameters that are to be fitted.

3.3.1 Film Calibration

Experimental validation measurements were obtained using Gafchromic film (Ashland Advanced Materials, Bridgewater NJ). When not in use, the Gafchromic film was stored in a black envelope inside a box to prevent any exposure to light. When handling the film, the edges were held to avoid excess fingerprints and smudges. A guillotine cutter was used to cut the film into appropriate sizes. The film was held down close to the knife and the knife was quickly brought down to achieve clean-cut edges and to avoid splitting the film. After cutting, the film was marked to indicate orientation so that the film would be consistently placed on the scanner. An Epson 10000XL scanner was used because the larger format reduces the lateral response artifact. The scanner was kept on so the electronics would always be warm. All image correction features were turned off on the scanner software window. No color correction was used. Professional mode allowed for all the necessary features for scanning to be selected. The scans were in transparency mode rather than reflection and in landscape orientation. The film type was positive film and the image type was 48-bit color. The resolution was 72 dpi. The light source was warmed up before scanning so that a stable color temperature would be used. This required performing 3-5 “Preview” scans if the scanner was not used within the last hour. A cardboard template was placed on the scanner to position the films at a reproducible location.

EBT3 film is very tissue equivalent over the Compton range of photon energies produced by middle and low energy brachytherapy sources. While the average photon energy of Yb-169 is 93 keV it predominantly produces 63 and 197 keV photons and smaller contributions from 301 kev photons. Therefore, as the film is placed deeper in the water, the spectrum hardens getting to the point where its 301 keV photons start dominating the energy profile. Therefore, Cs-137 is used in place of an orthovoltage source to calibrate the films because there's greater confidence in the isotope's output over time and because the energy response curve is flat in this range.

To calibrate the film, it was first cut and scanned. The film then was exposed to the Cs-137 source with exposures of 0-100 cGy in 25 cGy increments and 100-600 cGy in 50 cGy increments, as the film's response of optical density change to dose is linear up to 600 cGy. This was performed at Massachusetts General Hospital. Then the exposed film was scanned. The film darkens with exposure, which correlates to a lower grayscale value. The grayscale values of the unexposed and exposed film were used to calculate the net optical density where 16 is the true black value for the Epson 10000 XL scanner used for the scans:

$$\text{Net OD} = \log_{10} \frac{\text{average grayscale unexposed} - 16}{\text{average grayscale exposed} - 16}$$

The net optical density vs dose is graphed and fitted with a quadratic least squares regression to create an equation to use the net optical density to determine an unknown dose.

A program was written in Matlab to analyze the RGB channels of the Gafchromic film to obtain the grayscale values with its interface presented in Figure 16.[77] Isotropic and anisotropic sources can be characterized by relating the grayscale contrast from the scanned film to the irradiation dose. It is able to automatically scan the film and find the global minimum value

(highest optical density) and an average value over the region of interest. The scan can be filtered using a customized mean or gaussian blur to remove any spikes in the data in order to determine the true global image vertex. For an isotropy analysis, the angular and radial grayscale function is plotted for a user defined radius and tolerance in 0.1 mm increments. An automatically calculated “critical angle” along the steepest descent is used to determine the radial grayscale function however the vertex location and critical angle may be overridden if needed. For an anisotropy analysis Figure 17, a linear grayscale function is constructed along the vertical of the scan image. Each local minimum value by row is plotted with a marker on the image and a plot of the axis vs intensity is generated. The resolution, blur type, and color channel can all be selected. In this study, a resolution of 72 dpi was used as well as a gaussian blur. The red channel was selected because it is more radiosensitive. Then, the program was used to obtain the unexposed and exposed average values of the film in order to calculate the net optical density. Using the net optical density and polynomial fit function (from the calibrated films) the dose was calculated. In this way, the dose rate of an irradiated film was determined using a known exposure time.

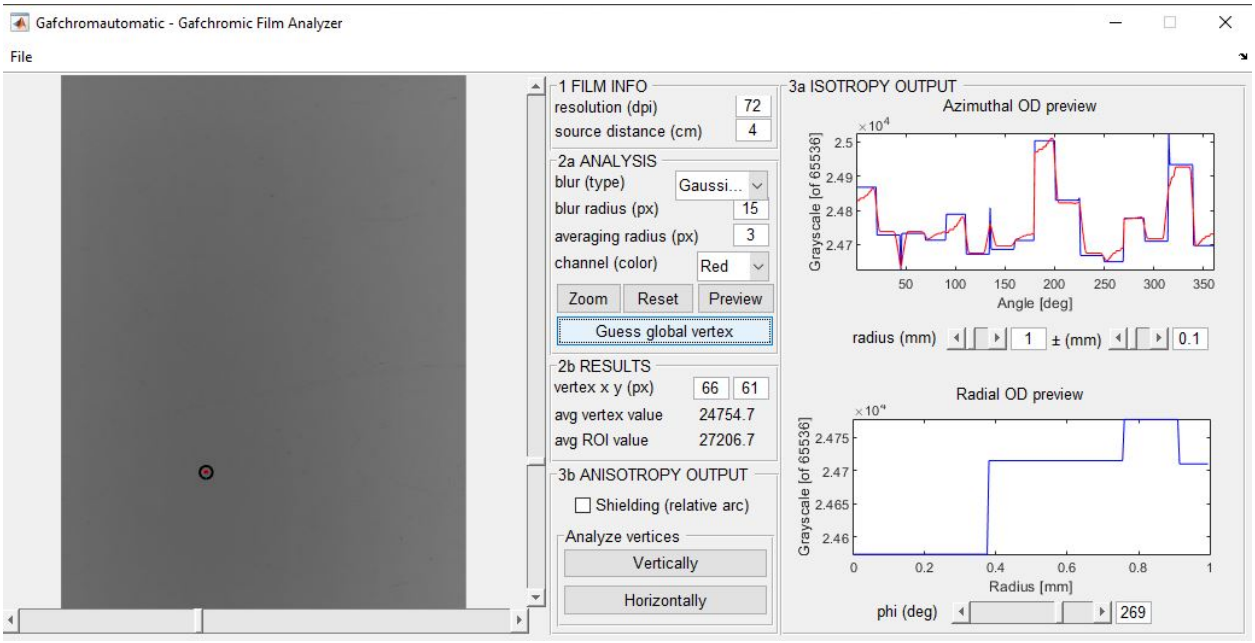

Figure 16: GUI interface of the Matlab program used to analyze Gafchromic film, which gives the maximum and average grayscale values of the film.

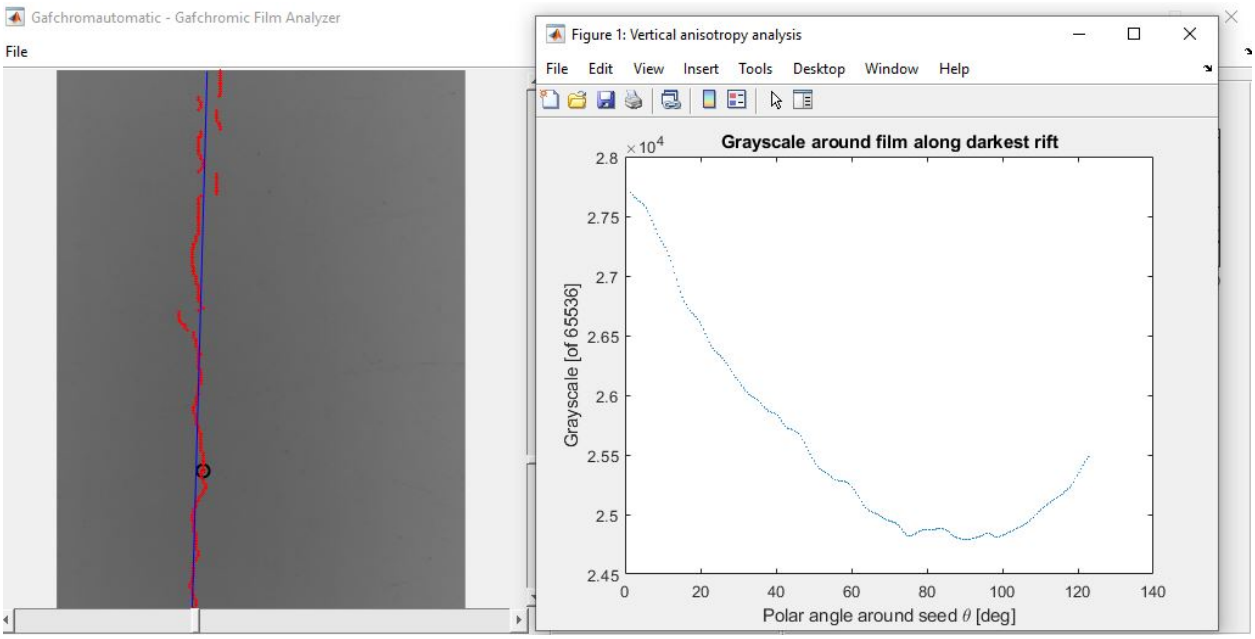

Figure 17: Demonstrates the anisotropy analysis of the Matlab program.

3.3.2 Measurements

A film holder device was 3D printed using ABS plastic in order to irradiate the film at set distances from the source. This setup is shown in Figure 18. It was comprised of two circular base plates with half circles 1-10 cm from the center and two half circle walls for the film to be placed in between. A center piece was made to hold the two base plates together, through which a catheter was strung. Once the film holder device was assembled it was submerged in a tank of water measuring over 30 cm on each side to account for scatter. A weight was attached to this device to keep the film holder at an appropriate depth in the water. A string was pulled through the base plates and tied to the edge of the tank to prevent movement. A custom-built afterloader device was used, which was programmed by an Arduino board. The dwell time of the source and distance to the film holder was specified using this program so that measurements could be repeatedly acquired while keeping these factors constant.

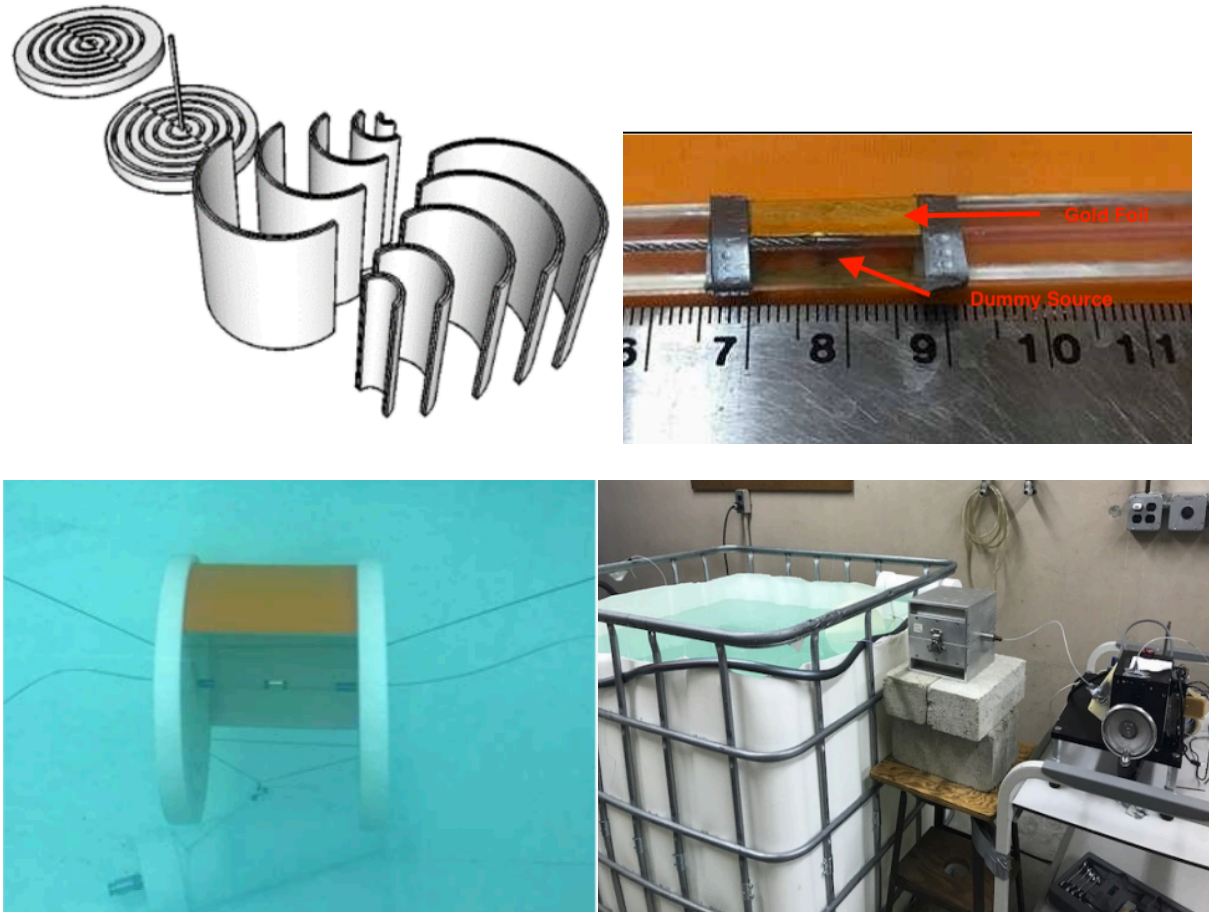

Figure 18: A) SketchUp model of the film holder B) centerpiece of the film holder containing a catheter wrapped in gold foil and a dummy source pushed to the middle distance of the catheter C) assembled film holder in the water tank and D) afterloader device connected to a shielded box container, which holds the source, located near the water tank.

In this experiment, 0.1 mm thick gold was wrapped 270° around a catheter, which was inserted into the base plates of the film holder. The source was pushed through this catheter using the afterloader device to reach the center of the gold foil. The absorbed dose to the film was measured at 1-3 cm from the source in the water tank. Data was collected with 90° of the unshielded catheter facing the film. It was then repeated with the catheter rotated 180° so the side completely covered with gold was facing the film. The films were irradiated for a set time to receive a dose of 200 cGy. Next, the gold foil was replaced with a new piece, 0.3 mm thick and was wrapped 270° around the catheter. The absorbed dose was measured 1 cm from the source with the 90° of unshielded catheter facing the film and then with the completely shielded side of the catheter facing the film.

4 Results

4.1 Computational Validation

4.1.1 COMS Plaque

The dose to various structures in the eye was calculated for a 16 mm diameter COMS plaque simulated in MCNP6 using 1E8 particle histories. Figures 19 and 20 present these results. Figures 21 and 22 correspond to the BrachyDose results with a comparison of the MCNP6 results to BrachyDose in Table 6. Table 6 shows the maximum, average, and minimum dose to ocular structures. D is the dose in Gy and D (%) is the percent dose. MCNP6 corresponds to the results simulated in my study and BrachyDose corresponds to the results simulated by Lesperance et al. All of the results are based on an eye model accounting for the ocular structures and compositions. For each study, the dose is normalized to 85 Gy and to give the 100% prescription dose to the tumor apex of a 12 mm diameter tumor. Lesperance et al. did not report values for the cornea and iris.

Figures 19 and 20, of a 16 mm I-125 COMS plaque, deliver a dose rate of 0.71 Gy/hr to the tumor apex at a 5 mm depth in the eye, calculated in MCNP6. Figure 19 shows the distribution of the dose rates in the eye using an isodose curve. Figure 20 relates the dose rates to the volume of each structure of interest in a DVH curve. The maximum percent dose was 17.6% to the cornea, 25.8% to the posterior lens, 23.7% to the iris, 16.3% to the optic nerve, 148.1% to the vitreous, 255.4% to the sclera, and 369.0% to the tumor. The absorbed dose to each structure was 14.95 Gy, 21.96 Gy, 20.17 Gy, 13.88 Gy, 125.88 Gy, 217.11 Gy, and 313.65 Gy respectively. These values are also presented in Table 6.

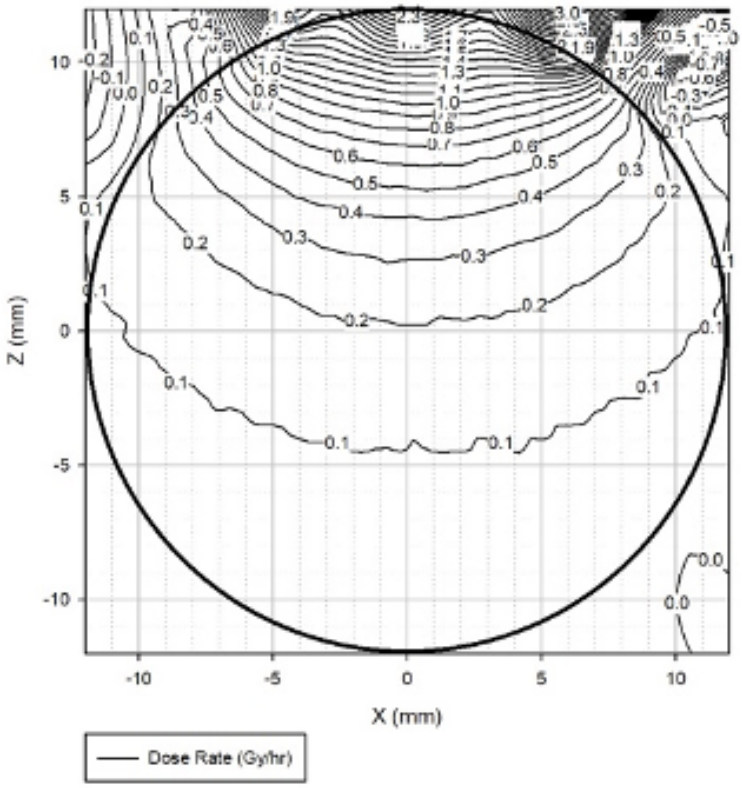

Figure 19: Dose distribution, calculated in MCNP6, of a 16 mm COMS plaque containing I-125 on the XZ plane. The dose rate is measured in Gy/hr and the prescription dose is delivered to a 5 mm depth into the eye.

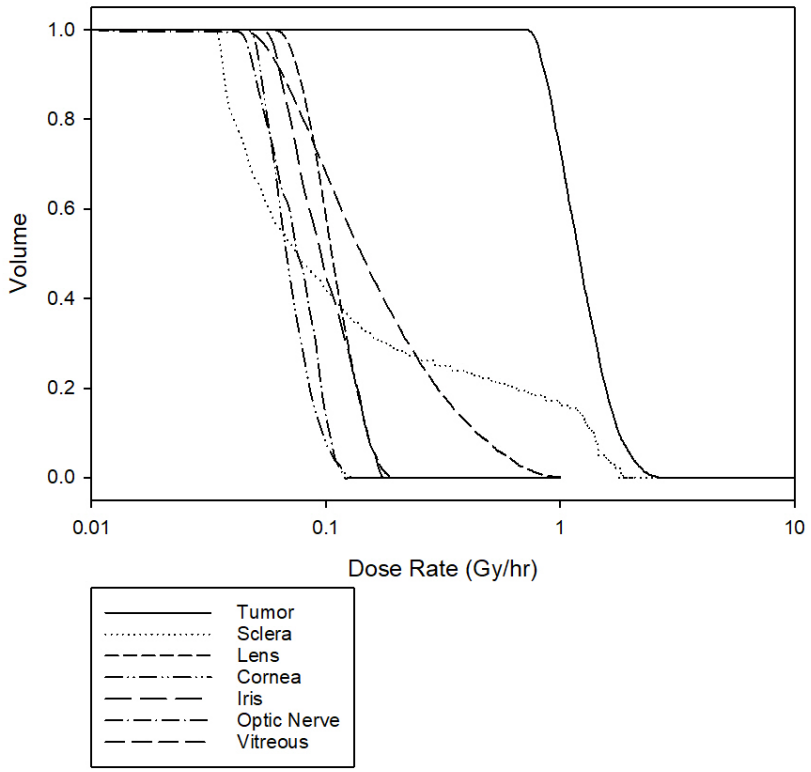

Figure 20: DVH curve in log scale of a 16 mm COMS plaque containing I-125 that delivers a dose rate of 0.71 Gy/hr to a 5 mm depth in the eye, calculated in MCNP6.

Figures 21 and 22, of a 16 mm I-125 COMS plaque, deliver a dose rate of 0.71 Gy/hr to the tumor apex at a 5 mm depth in the eye, calculated in BrachyDose by Lesperance et al. Figure 21 shows the distribution of the dose rates in the eye using an isodose curve. Figure 22 relates the dose to the volume of each structure in a DVH curve. The maximum percent dose was 32.5% to the posterior lens, 20.5% to the optic nerve, 188.0% to the vitreous, 285.1% to the sclera, and 313.2% to the tumor. The absorbed dose to each structure was 27.63 Gy, 17.40 Gy, 159.77 Gy, 242.34 Gy, and 266.18 Gy respectively. These values are also presented in Table 6.

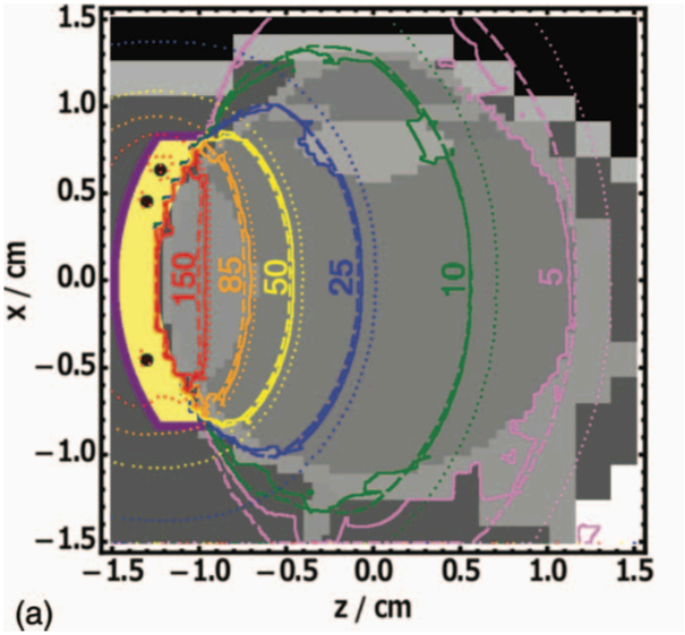

Figure 21: Isodose contours of dose to ocular structures of I-125 from Lesperance et al. The solid line is representative of the full eye model.[13]

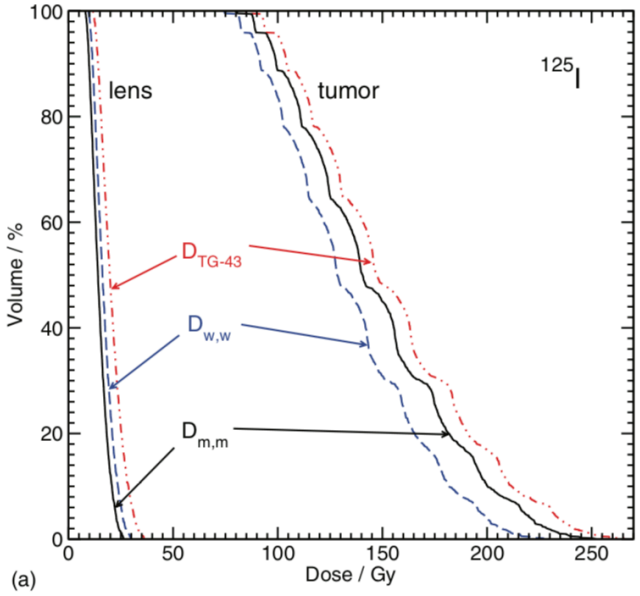

Figure 22: Dose volume histogram of the dose to the tumor and lens region for I-125 from Lesperance et al. The solid line is representative of the full eye model.[13]

Table 6: Dose to ocular structures from a 16 mm I-125 COMS plaque[13]

		MCNP6		BrachyDose	
Simulation	Geometry	D	D (%)	D	D (%)
Cornea	Max	14.95	17.6%	-	-
	Avg	8.37	9.9%	-	-
	Min	5.38	6.3%	-	-
Posterior	Max	21.96	25.8%	27.63	32.5%
Lens	Avg	12.88	15.2%	15.50	18.2%
	Min	7.23	8.5%	8.44	9.9%
	Center	12.43	14.6%	14.45	17.0%
Iris	Max	20.17	23.7%	-	-
	Avg	11.91	14.0%	-	-
	Min	6.30	7.4%	-	-
Optic Nerve	Max	13.88	16.3%	17.40	20.5%
	Avg	8.93	10.5%	8.33	9.8%
	Min	5.08	6.0%	1.58	1.9%
	Optic disk	10.69	12.6%	14.87	17.5%
Vitreous	Max	125.88	148.1%	159.77	188.0%
	Avg	23.82	28.0%	24.47	28.8%
	Min	5.32	6.3%	5.06	6.0%
	Center of eye	21.02	24.7%	22.67	26.7%
Sclera	Max	217.11	255.4%	242.34	285.1%
	Avg	20.15	23.7%	25.63	30.2%
	Min	3.88	4.6%	3.90	4.6%
	Near side	216.76	255.0%	210.18	247.3%
	Far side	4.18	4.9%	4.11	4.8%
	Fovea	9.13	10.7%	10.23	12.0%
Tumor	Max	313.65	369.0%	266.18	313.2%
	Avg	148.71	175.0%	155.66	183.1%
	Min	85.00	100.0%	84.68	99.6%
	Apex	85.00	100.0%	85.00	100.0%

4.2 HDR Applicator

4.2.1 Yb-169

A range of collimators were used to deliver the prescription dose to various depths within the eye in order to treat different sized targets. Applicators ranging from 12-18 mm in diameter were used. Isodose curves of these simulations are presented in Figures 23-26 for the 12-18 mm diameter applicators respectively that delivers the prescription dose to a target depth of 3.5-8 mm in the eye. Their corresponding dose rates to ocular structures of interest are presented in Tables 7-10, which gives the maximum, minimum, and average dose rates in Gy/min to ocular structures normalized to a tumor minimum dose rate of 3 Gy/min (D). D (%) is the normalized percent dose rate, which delivers 100% of the prescription dose to the tumor. Several dose volume histograms are shown for different diameter applicators that deliver the prescription dose to varying depths in the eye, shown in Figure 27. An example of the lateral distribution of the absorbed dose rate behind the applicator is also shown, in Figure 28.

Figure 23A is an isodose curve of Yb-169 used with a 12 mm diameter applicator with a collimator apex at 5.3 mm, collimator angle at 44.6°, target diameter at 10.0 mm, and target depth at 3.5 mm. The maximum percent dose was 11.3% to cornea, 14.0% to the posterior lens, 12.5% to the iris, 8.4% to the optic nerve, 9.2% to the bone, 206.8% to the sclera, and 216.6% to the tumor. The absorbed dose to each structure was 0.34 Gy, 0.42 Gy, 0.38 Gy, 0.25 Gy, 0.28 Gy, 6.21 Gy, and 6.50 Gy respectively.

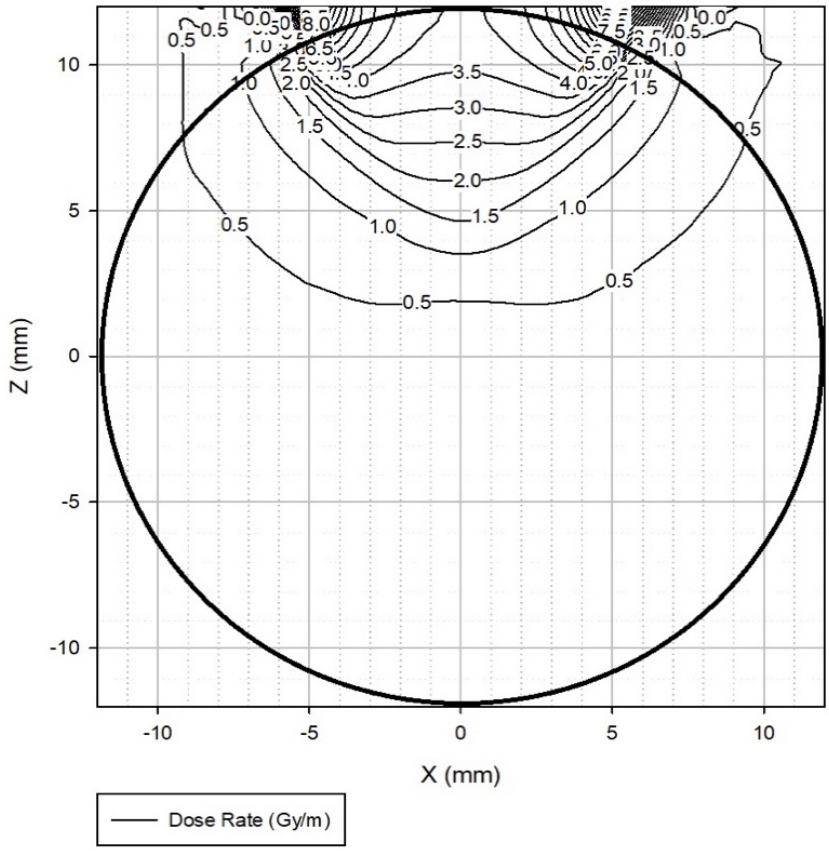

Figure 23A: Isodose curve of a 12 mm applicator containing Yb-169. The prescription dose of 3 Gy/min was delivered to a 3.5 mm depth in the eye.

Figure 23B is an isodose curve of Yb-169 used with a 12 mm diameter applicator with a collimator apex at 3.7 mm, collimator angle at 38.5°, target diameter at 10.4 mm, and target depth at 4.0 mm. The maximum percent dose was 12.8% to cornea, 16.8% to the posterior lens, 14.4% to the iris, 10.0% to the optic nerve, 10.3% to the bone, 226.2% to the sclera, and 234.1% to the tumor. The absorbed dose to each structure was 0.38 Gy, 0.50 Gy, 0.43 Gy, 0.30 Gy, 0.31 Gy, 6.78 Gy, and 7.02 Gy respectively.

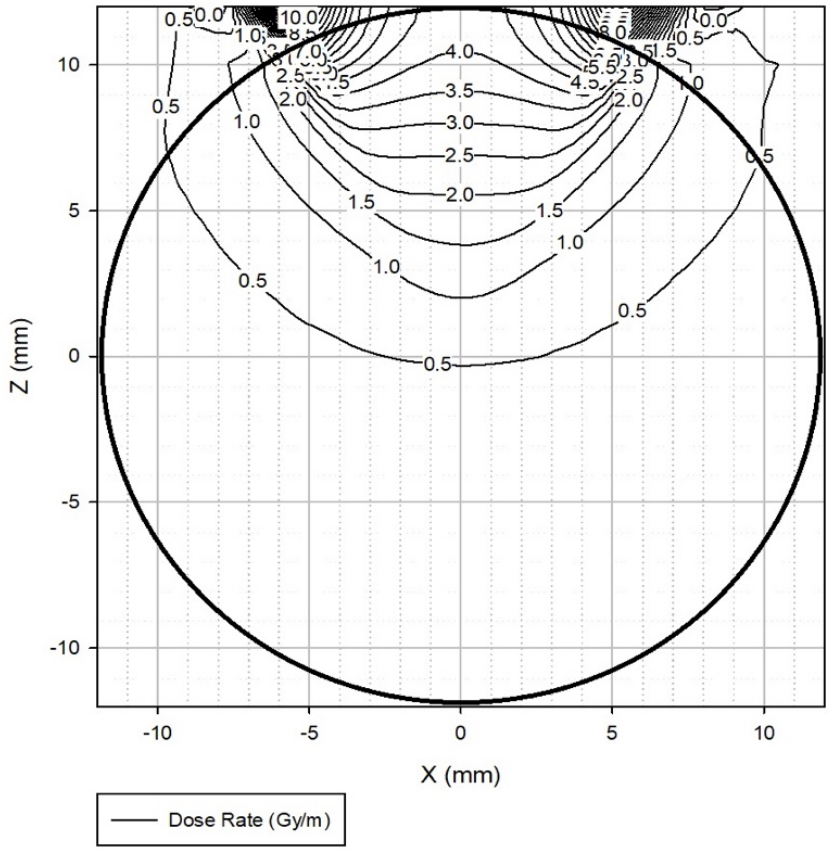

Figure 23B: Isodose curve of a 12 mm applicator containing Yb-169. The prescription dose of 3 Gy/min was delivered to a 4.0 mm depth in the eye.

Figure 23C is an isodose curve of Yb-169 used with a 12 mm diameter applicator with a collimator apex at 1.8 mm, collimator angle at 32.7°, target diameter at 10.8 mm, and target depth at 4.5 mm. The maximum percent dose was 14.6% to cornea, 19.6% to the posterior lens, 16.3% to the iris, 11.6% to the optic nerve, 11.4% to the bone, 244.8% to the sclera, and 253.6% to the tumor. The absorbed dose to each structure was 0.44 Gy, 0.59 Gy, 0.49 Gy, 0.35 Gy, 0.34 Gy, 7.34 Gy, and 7.61 Gy respectively.

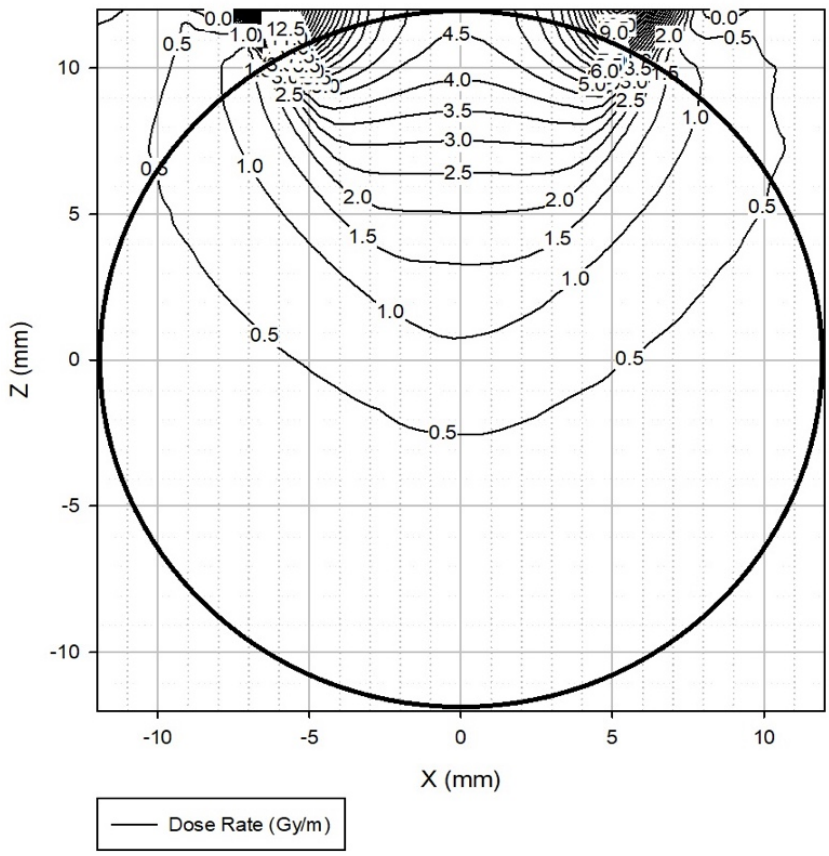

Figure 23C: Isodose curve of a 12 mm applicator containing Yb-169. The prescription dose of 3 Gy/min was delivered to a 4.5 mm depth in the eye.

Figure 23D is an isodose curve of Yb-169 used with a 12 mm diameter applicator with a collimator apex at -0.7 mm, collimator angle at 27.2°, target diameter at 11.1 mm, and target depth at 5.0 mm. The maximum percent dose was 16.4% to cornea, 23.0% to the posterior lens, 18.4% to the iris, 13.3% to the optic nerve, 12.6% to the bone, 264.9% to the sclera, and 274.6% to the tumor. The absorbed dose to each structure was 0.49 Gy, 0.69 Gy, 0.55 Gy, 0.4.0 Gy, 0.38 Gy, 7.95 Gy, and 8.24 Gy respectively.

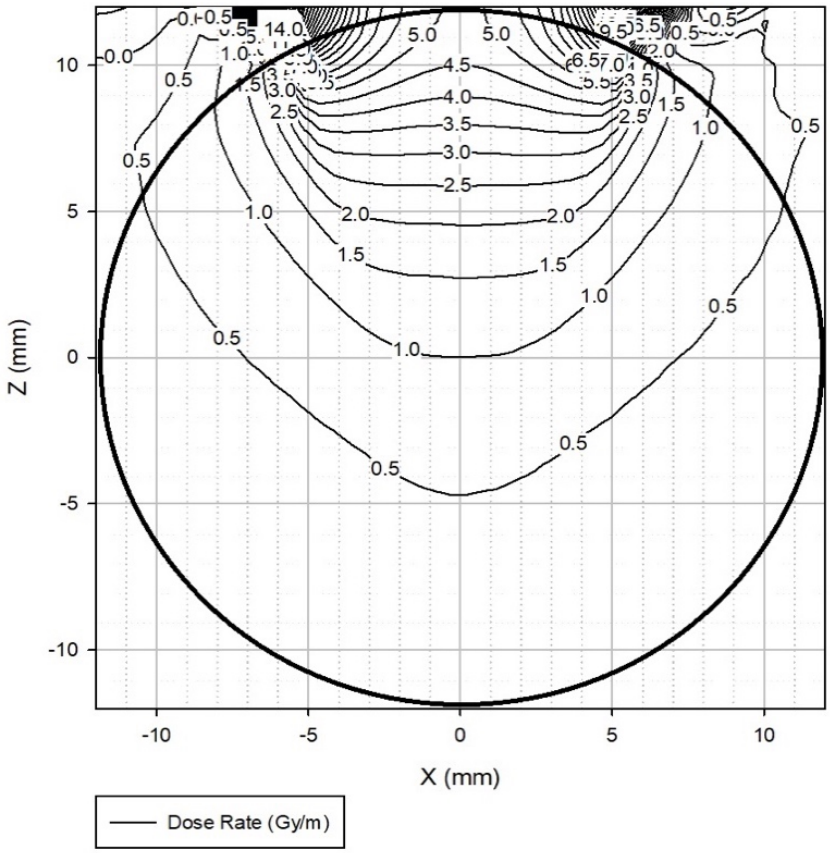

Figure 23D: Isodose curve of a 12 mm applicator containing Yb-169. The prescription dose of 3 Gy/min was delivered to a 5.0 mm depth in the eye.

Figure 23E is an isodose curve of Yb-169 used with a 12 mm diameter applicator with a collimator apex at -4.0 mm, collimator angle at 22.1°, target diameter at 11.4 mm, and target depth at 5.5 mm. The maximum percent dose was 18.3% to cornea, 26.7% to the posterior lens, 20.6% to the iris, 15.2% to the optic nerve, 14.0% to the bone, 286.0% to the sclera, and 296.4% to the tumor. The absorbed dose to each structure was 0.55 Gy, 0.80 Gy, 0.62 Gy, 0.46 Gy, 0.42 Gy, 8.59 Gy, and 8.89 Gy respectively.

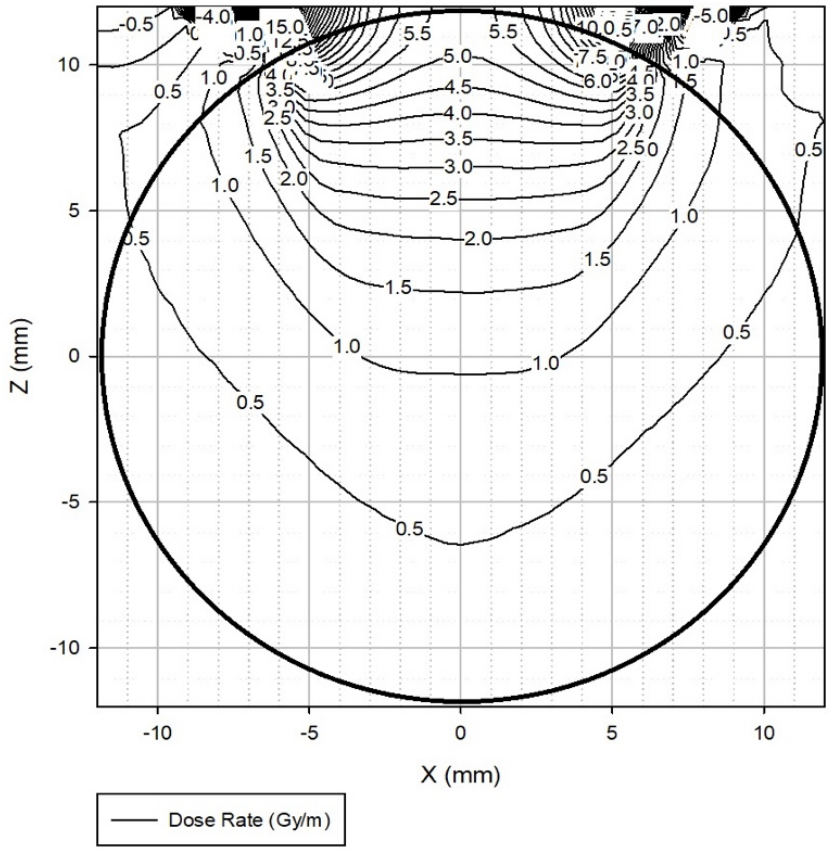

Figure 23E: Isodose curve of a 12 mm applicator containing Yb-169. The prescription dose of 3 Gy/min was delivered to a 5.5 mm depth in the eye.

Figure 23F is an isodose curve of Yb-169 used with a 12 mm diameter applicator with a collimator apex at -8.7 mm, collimator angle at 17.4°, target diameter at 11.6 mm, and target depth at 6.0 mm. The maximum percent dose was 20.3% to cornea, 30.7% to the posterior lens, 23.2% to the iris, 17.3% to the optic nerve, 15.3% to the bone, 307.9% to the sclera, and 319.0% to the tumor. The absorbed dose to each structure was 0.61 Gy, 0.92 Gy, 0.69 Gy, 0.52 Gy, 0.46 Gy, 9.24 Gy, and 9.57 Gy respectively.

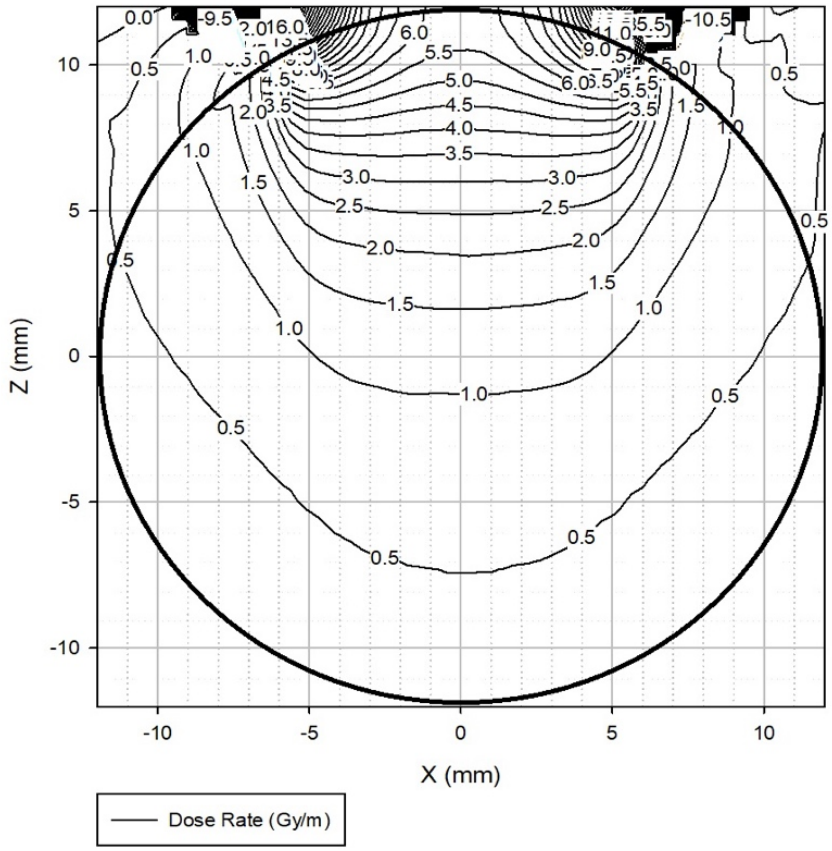

Figure 23F: Isodose curve of a 12 mm applicator containing Yb-169. The prescription dose of 3 Gy/min was delivered to a 6.0 mm depth in the eye.

Table 7: Dose rates to ocular structures from a Yb-169 12 mm applicator

Target Depth		3.5		4.0		4.5		5.0		5.5		6.0	
Simulation	Geometry	D	D (%)	D	D (%)	D	D (%)	D	D (%)	D	D (%)	D	D (%)
Cornea	Max	0.34	11.3%	0.38	12.8%	0.44	14.6%	0.49	16.4%	0.55	18.3%	0.61	20.3%
	Avg	0.18	6.1%	0.22	7.2%	0.25	8.3%	0.29	9.5%	0.32	10.8%	0.36	12.1%
	Min	0.11	3.7%	0.14	4.6%	0.17	5.5%	0.20	6.6%	0.23	7.7%	0.27	8.9%
Posterior	Max	0.42	14.0%	0.50	16.8%	0.59	19.6%	0.69	23.0%	0.80	26.7%	0.92	30.7%
Lens	Avg	0.25	8.3%	0.30	10.1%	0.36	12.1%	0.42	14.2%	0.49	16.5%	0.57	19.0%
	Min	0.13	4.4%	0.18	5.9%	0.21	7.2%	0.26	8.5%	0.30	10.0%	0.35	11.7%
Iris	Max	0.38	12.5%	0.43	14.4%	0.49	16.3%	0.55	18.4%	0.62	20.6%	0.69	23.2%
	Avg	0.22	7.2%	0.26	8.6%	0.30	10.0%	0.35	11.6%	0.40	13.2%	0.45	14.9%
	Min	0.12	3.9%	0.15	5.0%	0.18	6.1%	0.22	7.2%	0.25	8.4%	0.29	9.7%
Optic	Max	0.25	8.4%	0.30	10.0%	0.35	11.6%	0.40	13.3%	0.46	15.2%	0.52	17.3%
Nerve	Avg	0.18	6.1%	0.21	7.2%	0.25	8.3%	0.29	9.6%	0.33	10.9%	0.37	12.2%
	Min	0.14	4.5%	0.16	5.3%	0.18	6.1%	0.21	7.0%	0.24	7.9%	0.26	8.8%
Bone	Max	0.28	9.2%	0.31	10.3%	0.34	11.4%	0.38	12.6%	0.42	14.0%	0.46	15.3%
	Avg	0.13	4.2%	0.15	5.0%	0.18	5.9%	0.20	6.8%	0.23	7.8%	0.26	8.8%
	Min	0.05	1.6%	0.06	2.0%	0.08	2.6%	0.09	3.0%	0.10	3.4%	0.11	3.7%
Sclera	Max	6.21	206.8%	6.78	226.2%	7.34	244.8%	7.95	264.9%	8.59	286.0%	9.24	307.9%
	Avg	0.44	14.5%	0.51	16.9%	0.58	19.4%	0.67	22.2%	0.76	25.2%	0.86	28.6%
	Min	0.06	2.0%	0.07	2.5%	0.10	3.4%	0.17	5.6%	0.22	7.3%	0.26	8.7%
Tumor	Max	6.50	216.6%	7.02	234.1%	7.61	253.6%	8.24	274.6%	8.89	296.4%	9.57	319.0%
	Avg	4.38	146.1%	4.61	153.8%	4.91	163.5%	5.17	172.2%	5.41	180.2%	5.62	187.4%
	Min	3.00	100.0%	3.00	100.0%	3.00	100.0%	3.00	100.0%	3.00	100.0%	3.00	100.0%

Figure 24A is an isodose curve of Yb-169 used with a 14 mm diameter applicator with a collimator apex at 6.1 mm, collimator angle at 53.6°, target diameter at 11.0 mm, and target depth at 3.5 mm. The maximum percent dose was 12.5% to cornea, 14.8% to the posterior lens, 13.7% to the iris, 8.5% to the optic nerve, 10.2% to the bone, 204.5% to the sclera, and 197.4% to the tumor. The absorbed dose to each structure was 0.38 Gy, 0.44 Gy, 0.41 Gy, 0.25 Gy, 0.31 Gy, 6.14 Gy, and 5.92 Gy respectively.

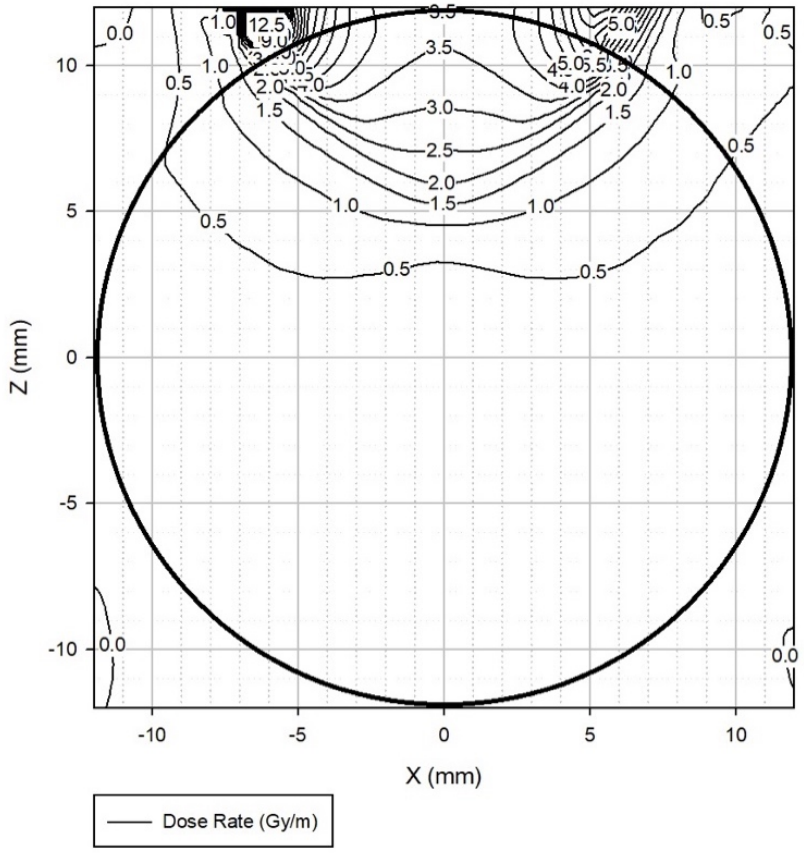

Figure 24A: Isodose curve of a 14 mm applicator containing Yb-169. The prescription dose of 3 Gy/min was delivered to a 3.5 mm depth in the eye.

Figure 24B is an isodose curve of Yb-169 used with a 14 mm diameter applicator with a collimator apex at 4.8 mm, collimator angle at 47.6°, target diameter at 11.4 mm, and target depth at 4.0 mm. The maximum percent dose was 14.0% to cornea, 17.1% to the posterior lens, 15.4% to the iris, 10.1% to the optic nerve, 11.2% to the bone, 219.1% to the sclera, and 216.3% to the tumor. The absorbed dose to each structure was 0.42 Gy, 0.51 Gy, 0.46 Gy, 0.30 Gy, 0.33 Gy, 6.57 Gy, and 6.49 Gy respectively.

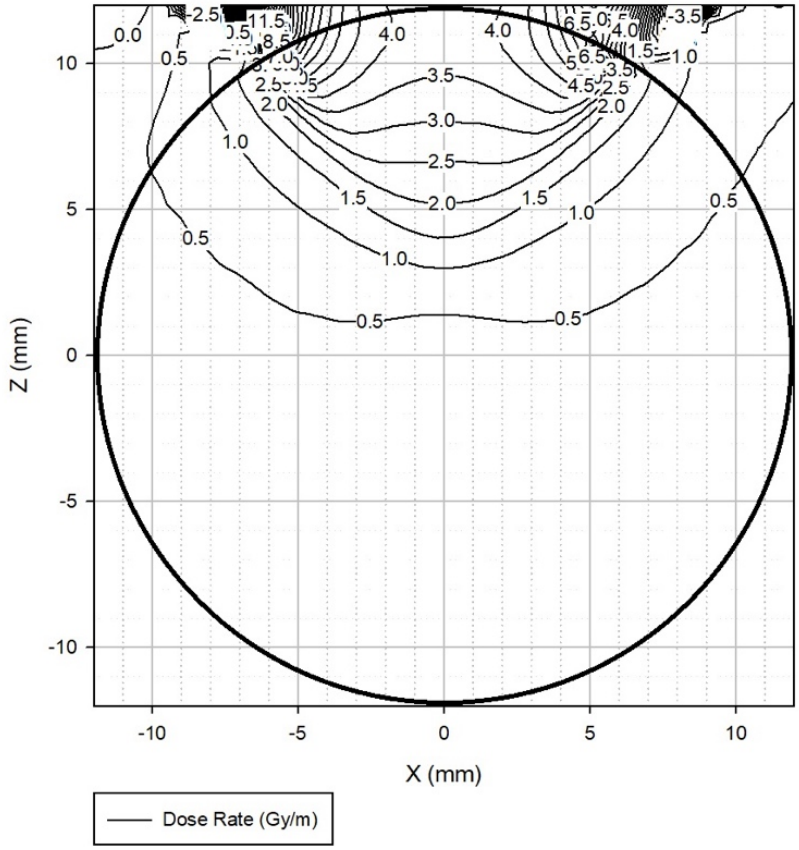

Figure 24B: Isodose curve of a 14 mm applicator containing Yb-169. The prescription dose of 3 Gy/min was delivered to a 4.0 mm depth in the eye.

Figure 24C is an isodose curve of Yb-169 used with a 14 mm diameter applicator with a collimator apex at 3.4 mm, collimator angle at 41.9°, target diameter at 11.7 mm, and target depth at 4.5 mm. The maximum percent dose was 15.7% to cornea, 20.0% to the posterior lens, 17.5% to the iris, 11.8% to the optic nerve, 12.2% to the bone, 238.2% to the sclera, and 246.6% to the tumor. The absorbed dose to each structure was 0.47 Gy, 0.60 Gy, 0.53 Gy, 0.35 Gy, 0.37 Gy, 7.15 Gy, and 7.40 Gy respectively.

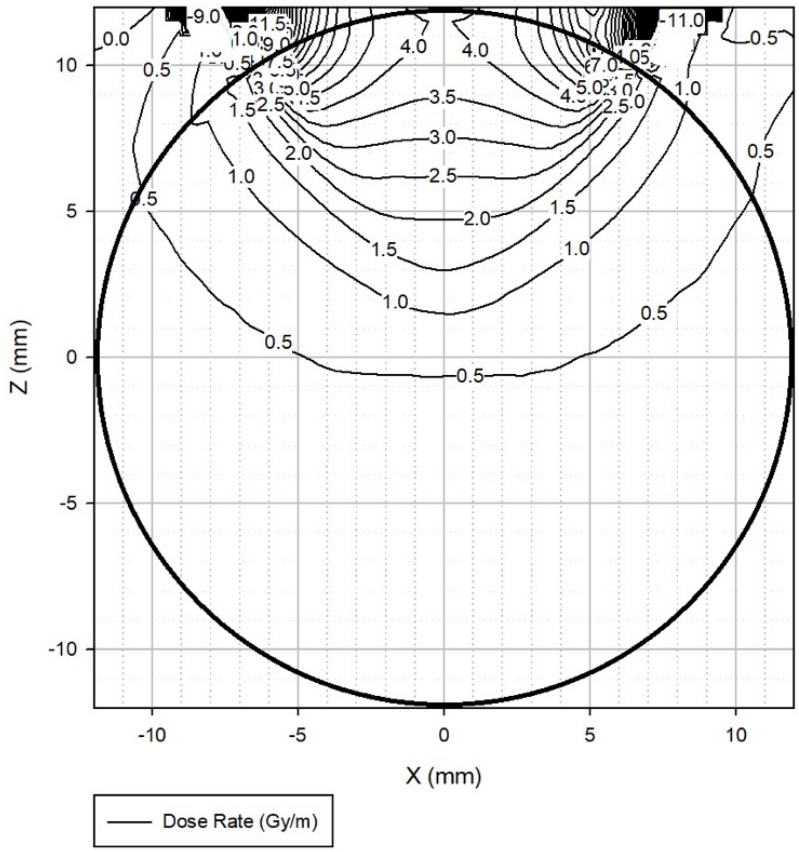

Figure 24C: Isodose curve of a 14 mm applicator containing Yb-169. The prescription dose of 3 Gy/min was delivered to a 4.5 mm depth in the eye.

Figure 24D is an isodose curve of Yb-169 used with a 14 mm diameter applicator with a collimator apex at 1.6 mm, collimator angle at 36.5°, target diameter at 12.0 mm, and target depth at 5.0 mm. The maximum percent dose was 17.7% to cornea, 23.1% to the posterior lens, 19.7% to the iris, 13.6% to the optic nerve, 13.3% to the bone, 254.8% to the sclera, and 266.4% to the tumor. The absorbed dose to each structure was 0.53 Gy, 0.69 Gy, 0.59 Gy, 0.41 Gy, 0.40 Gy, 7.64 Gy, and 7.99 Gy respectively.

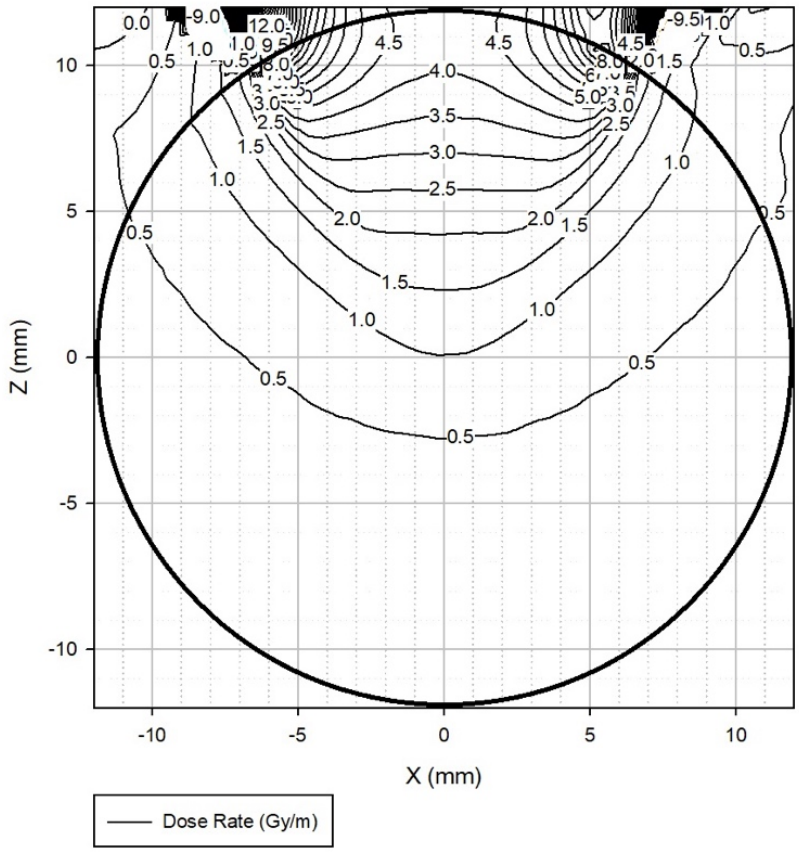

Figure 24D: Isodose curve of a 14 mm applicator containing Yb-169. The prescription dose of 3 Gy/min was delivered to a 5.0 mm depth in the eye.

Figure 24E is an isodose curve of Yb-169 used with a 14 mm diameter applicator with a collimator apex at -0.5 mm, collimator angle at 31.4°, target diameter at 12.3 mm, and target depth at 5.5 mm. The maximum percent dose was 19.7% to cornea, 26.8% to the posterior lens, 22.0% to the iris, 15.6% to the optic nerve, 14.7% to the bone, 272.3% to the sclera, and 285.1% to the tumor. The absorbed dose to each structure was 0.59 Gy, 0.80 Gy, 0.66 Gy, 0.47 Gy, 0.44 Gy, 8.17 Gy, and 8.55 Gy respectively.

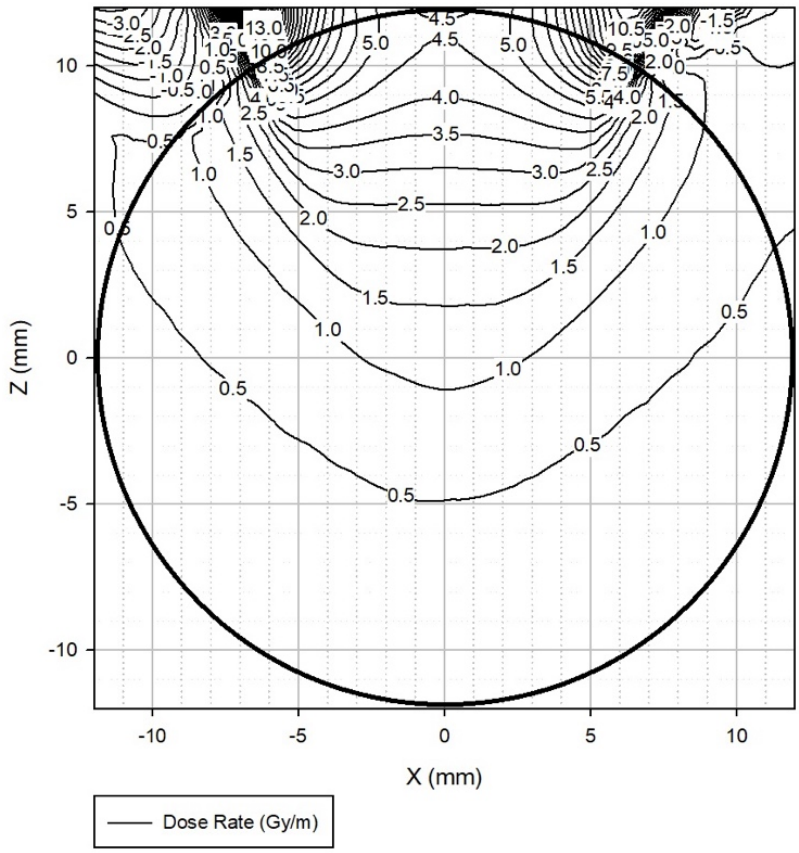

Figure 24E: Isodose curve of a 14 mm applicator containing Yb-169. The prescription dose of 3 Gy/min was delivered to a 5.5 mm depth in the eye.

Figure 24F is an isodose curve of Yb-169 used with a 14 mm diameter applicator with a collimator apex at -3.1 mm, collimator angle at 26.5°, target diameter at 12.5 mm, and target depth at 6.0 mm. The maximum percent dose was 21.6% to cornea, 30.8% to the posterior lens, 24.3% to the iris, 17.6% to the optic nerve, 16.1% to the bone, 291.6% to the sclera, and 305.6% to the tumor. The absorbed dose to each structure was 0.65 Gy, 0.92 Gy, 0.73 Gy, 0.53 Gy, 0.48 Gy, 8.75 Gy, and 9.17 Gy respectively.

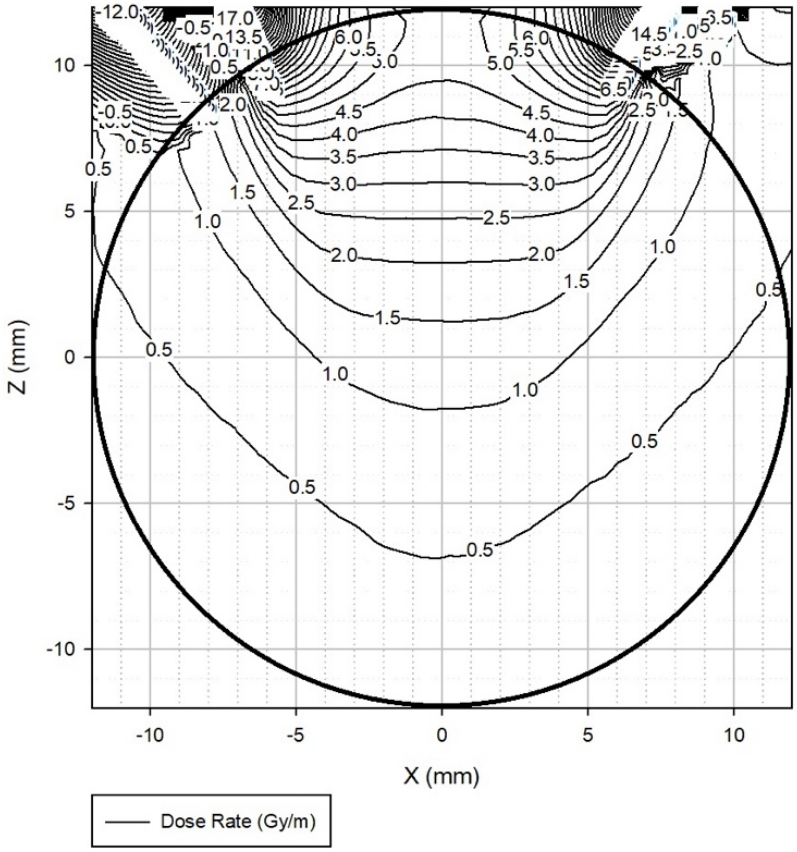

Figure 24F: Isodose curve of a 14 mm applicator containing Yb-169. The prescription dose of 3 Gy/min was delivered to a 6.0 mm depth in the eye.

Figure 24G is an isodose curve of Yb-169 used with a 14 mm diameter applicator with a collimator apex at -6.5 mm, collimator angle at 22.0°, target diameter at 12.9 mm, and target depth at 6.5 mm. The maximum percent dose was 23.9% to cornea, 35.9% to the posterior lens, 27.1% to the iris, 20.0% to the optic nerve, 17.7% to the bone, 314.1% to the sclera, and 328.8% to the tumor. The absorbed dose to each structure was 0.72 Gy, 1.08 Gy, 0.81 Gy, 0.60 Gy, 0.53 Gy, 9.42 Gy, and 9.86 Gy respectively.

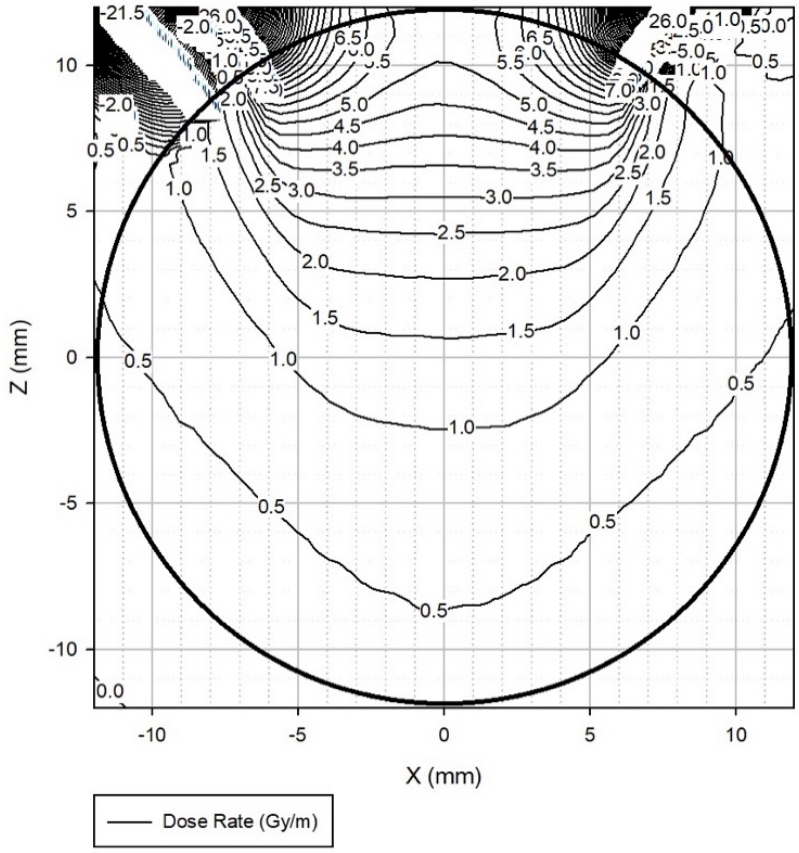

Figure 24G: Isodose curve of a 14 mm applicator containing Yb-169. The prescription dose of 3 Gy/min was delivered to a 6.5 mm depth in the eye.

Table 8: Dose rates to ocular structures from a Yb-169 14 mm applicator

Target Depth		3.5		4.0		4.5		5.0		5.5		6.0		6.5	
Simulation	Geometry	D	D (%)	D	D (%)	D	D (%)	D	D (%)	D	D (%)	D	D (%)	D	D (%)
Cornea	Max	0.38	12.5%	0.42	14.0%	0.47	15.7%	0.53	17.7%	0.59	19.7%	0.65	21.6%	0.72	23.9%
	Avg	0.19	6.3%	0.22	7.4%	0.26	8.6%	0.29	9.8%	0.33	11.1%	0.37	12.4%	0.42	14.0%
	Min	0.09	3.0%	0.13	4.3%	0.16	5.4%	0.20	6.5%	0.23	7.6%	0.26	8.7%	0.30	10.0%
Posterior	Max	0.44	14.8%	0.51	17.1%	0.60	20.0%	0.69	23.1%	0.80	26.8%	0.92	30.8%	1.08	35.9%
Lens	Avg	0.24	7.9%	0.30	10.0%	0.36	12.0%	0.42	14.1%	0.49	16.3%	0.56	18.8%	0.65	21.7%
	Min	0.10	3.4%	0.15	5.0%	0.20	6.6%	0.24	8.0%	0.29	9.6%	0.34	11.2%	0.39	13.2%
Iris	Max	0.41	13.7%	0.46	15.4%	0.53	17.5%	0.59	19.7%	0.66	22.0%	0.73	24.3%	0.81	27.1%
	Avg	0.22	7.3%	0.26	8.7%	0.31	10.2%	0.35	11.8%	0.40	13.4%	0.45	15.2%	0.51	17.2%
	Min	0.09	3.2%	0.13	4.4%	0.17	5.7%	0.21	6.9%	0.24	8.1%	0.28	9.4%	0.32	10.8%
Optic	Max	0.25	8.5%	0.30	10.1%	0.35	11.8%	0.41	13.6%	0.47	15.6%	0.53	17.6%	0.60	20.0%
Nerve	Avg	0.19	6.2%	0.22	7.4%	0.26	8.6%	0.29	9.8%	0.33	11.1%	0.37	12.5%	0.42	14.1%
	Min	0.14	4.6%	0.16	5.4%	0.19	6.2%	0.21	7.1%	0.24	7.9%	0.27	8.8%	0.30	10.1%
Bone	Max	0.31	10.2%	0.33	11.2%	0.37	12.2%	0.40	13.3%	0.44	14.7%	0.48	16.1%	0.53	17.7%
	Avg	0.12	4.2%	0.15	4.9%	0.17	5.8%	0.20	6.7%	0.23	7.7%	0.26	8.7%	0.29	9.8%
	Min	0.04	1.5%	0.05	1.8%	0.07	2.2%	0.08	2.8%	0.10	3.3%	0.11	3.7%	0.12	4.0%
Sclera	Max	6.14	204.5%	6.57	219.1%	7.15	238.2%	7.64	254.8%	8.17	272.3%	8.75	291.6%	9.42	314.1%
	Avg	0.47	15.8%	0.55	18.2%	0.62	20.8%	0.71	23.6%	0.80	26.6%	0.90	29.9%	1.00	33.5%
	Min	0.06	2.1%	0.07	2.3%	0.08	2.7%	0.10	3.5%	0.16	5.3%	0.23	7.8%	0.28	9.5%
Tumor	Max	5.92	197.4%	6.49	216.3%	7.40	246.6%	7.99	266.4%	8.55	285.1%	9.17	305.6%	9.86	328.8%
	Avg	4.19	139.8%	4.36	145.5%	4.59	152.9%	4.78	159.5%	4.99	166.4%	5.20	173.3%	5.43	181.1%
	Min	3.00	100.0%	3.00	100.0%	3.00	100.0%	3.00	100.0%	3.00	100.0%	3.00	100.0%	3.00	100.0%

Figure 25A is an isodose curve of Yb-169 used with a 16 mm diameter applicator with a collimator apex at 5.6 mm, collimator angle at 56.4°, target diameter at 12.3 mm, and target depth at 4.0 mm. The maximum percent dose was 15.8% to cornea, 18.5% to the posterior lens, 17.5% to the iris, 10.6% to the optic nerve, 11.8% to the bone, 220.4% to the sclera, and 221.1% to the tumor. The absorbed dose to each structure was 0.47 Gy, 0.55 Gy, 0.53 Gy, 0.32 Gy, 0.35 Gy, 6.61 Gy, and 6.63 Gy respectively.

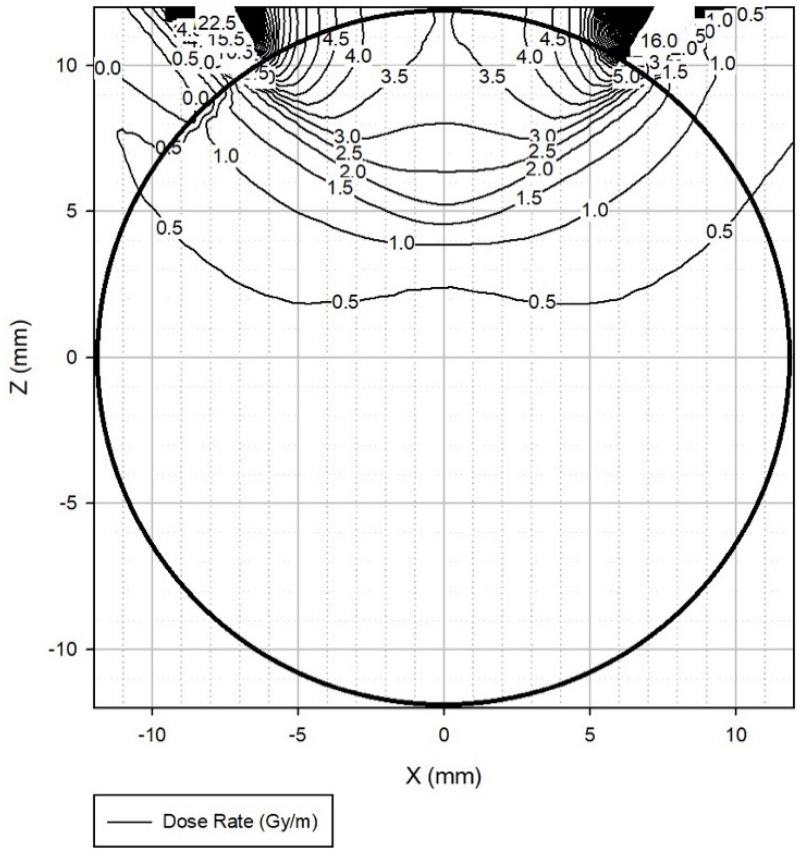

Figure 25A: Isodose curve of a 16 mm applicator containing Yb-169. The prescription dose of 3 Gy/min was delivered to a 4.0 mm depth in the eye.

Figure 25B is an isodose curve of Yb-169 used with a 16 mm diameter applicator with a collimator apex at 4.4 mm, collimator angle at 50.9°, target diameter at 12.7 mm, and target depth at 4.5 mm. The maximum percent dose was 17.5% to cornea, 21.3% to the posterior lens, 19.5% to the iris, 12.4% to the optic nerve, 12.8% to the bone, 236.1% to the sclera, and 231.6% to the tumor. The absorbed dose to each structure was 0.53 Gy, 0.64 Gy, 0.58 Gy, 0.37 Gy, 0.38 Gy, 7.08 Gy, and 6.95 Gy respectively.

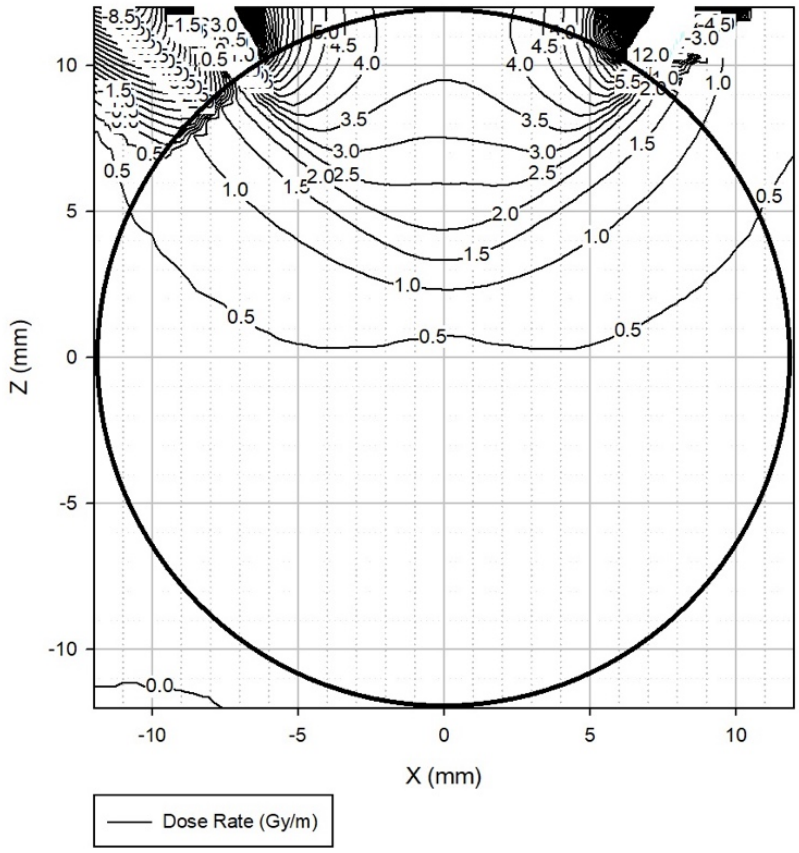

Figure 25B: Isodose curve of a 16 mm applicator containing Yb-169. The prescription dose of 3 Gy/min was delivered to a 4.5 mm depth in the eye.

Figure 25C is an isodose curve of Yb-169 used with a 16 mm diameter applicator with a collimator apex at 3.1 mm, collimator angle at 45.6°, target diameter at 13.0 mm, and target depth at 5.0 mm. The maximum percent dose was 19.3% to cornea, 24.5% to the posterior lens, 21.6% to the iris, 14.2% to the optic nerve, 13.9% to the bone, 252.2% to the sclera, and 250.3% to the tumor. The absorbed dose to each structure was 0.58 Gy, 0.74 Gy, 0.65 Gy, 0.42 Gy, 0.42 Gy, 7.56 Gy, and 7.51 Gy respectively.

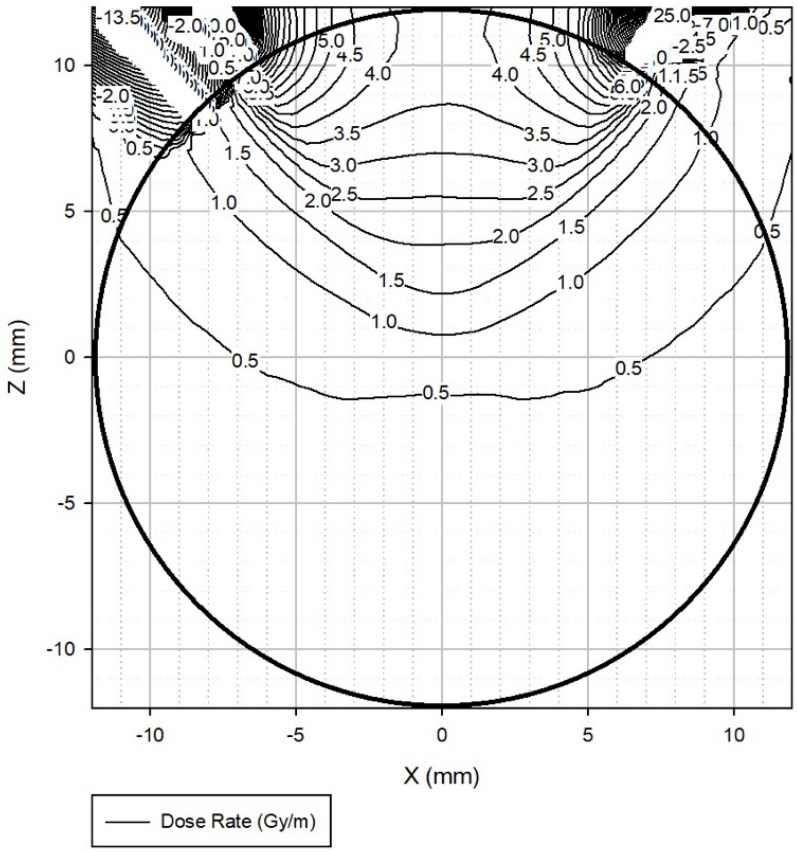

Figure 25C: Isodose curve of a 16 mm applicator containing Yb-169. The prescription dose of 3 Gy/min was delivered to a 5.0 mm depth in the eye.

Figure 25D is an isodose curve of Yb-169 used with a 16 mm diameter applicator with a collimator apex at 1.5 mm, collimator angle at 40.5°, target diameter at 13.3 mm, and target depth at 5.5 mm. The maximum percent dose was 21.3% to cornea, 27.9% to the posterior lens, 23.9% to the iris, 16.0% to the optic nerve, 15.2% to the bone, 265.7% to the sclera, and 269.9% to the tumor. The absorbed dose to each structure was 0.64 Gy, 0.84 Gy, 0.72 Gy, 0.48 Gy, 0.46 Gy, 7.97 Gy, and 8.10 Gy respectively.

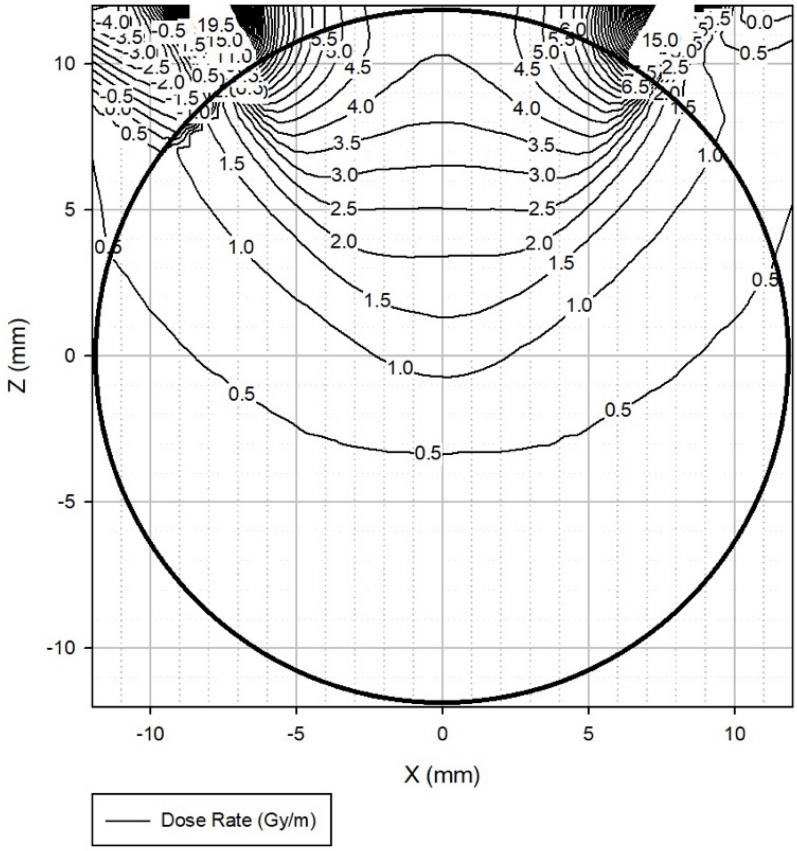

Figure 25D: Isodose curve of a 16 mm applicator containing Yb-169. The prescription dose of 3 Gy/min was delivered to a 5.5 mm depth in the eye.

Figure 25E is an isodose curve of Yb-169 used with a 16 mm diameter applicator with a collimator apex at -0.3 mm, collimator angle at 35.6°, target diameter at 13.6 mm, and target depth at 6.0 mm. The maximum percent dose was 23.6% to cornea, 32.0% to the posterior lens, 26.7% to the iris, 18.0% to the optic nerve, 16.5% to the bone, 281.5% to the sclera, and 286.5% to the tumor. The absorbed dose to each structure was 0.71 Gy, 0.96 Gy, 0.80 Gy, 0.54 Gy, 0.49 Gy, 8.45 Gy, and 8.59 Gy respectively.

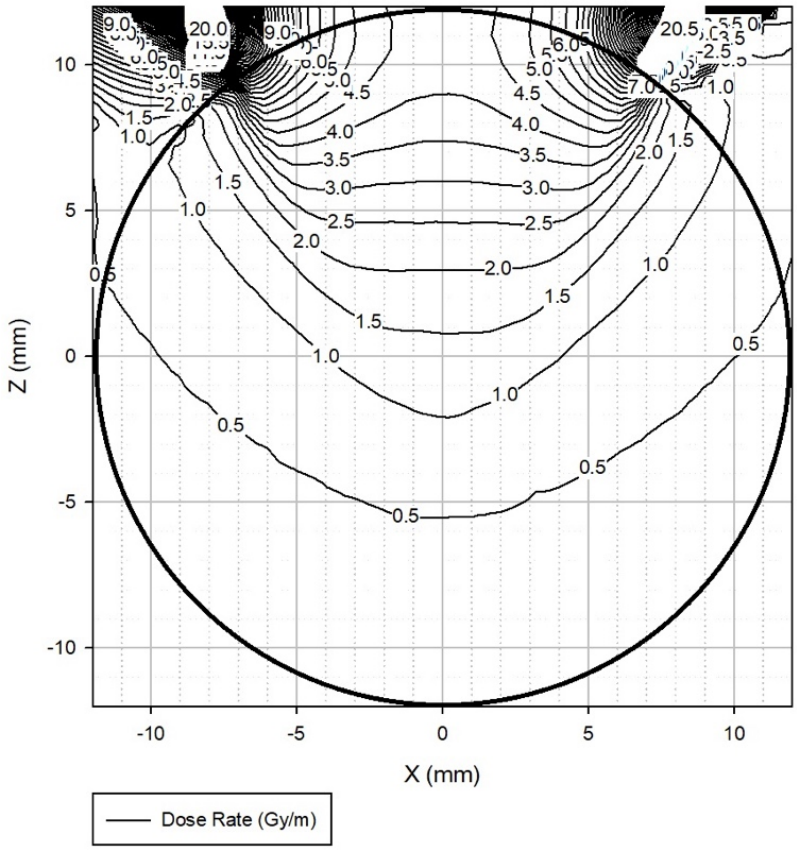

Figure 25E: Isodose curve of a 16 mm applicator containing Yb-169. The prescription dose of 3 Gy/min was delivered to a 6.0 mm depth in the eye.

Figure 25F is an isodose curve of Yb-169 used with a 16 mm diameter applicator with a collimator apex at -2.4 mm, collimator angle at 31.0°, target diameter at 13.8 mm, and target depth at 6.5 mm. The maximum percent dose was 26.1% to cornea, 37.1% to the posterior lens, 29.4% to the iris, 20.5% to the optic nerve, 17.9% to the bone, 300.6% to the sclera, and 306.3% to the tumor. The absorbed dose to each structure was 0.78 Gy, 1.11 Gy, 0.88 Gy, 0.61 Gy, 0.54 Gy, 9.02 Gy, and 9.19 Gy respectively.

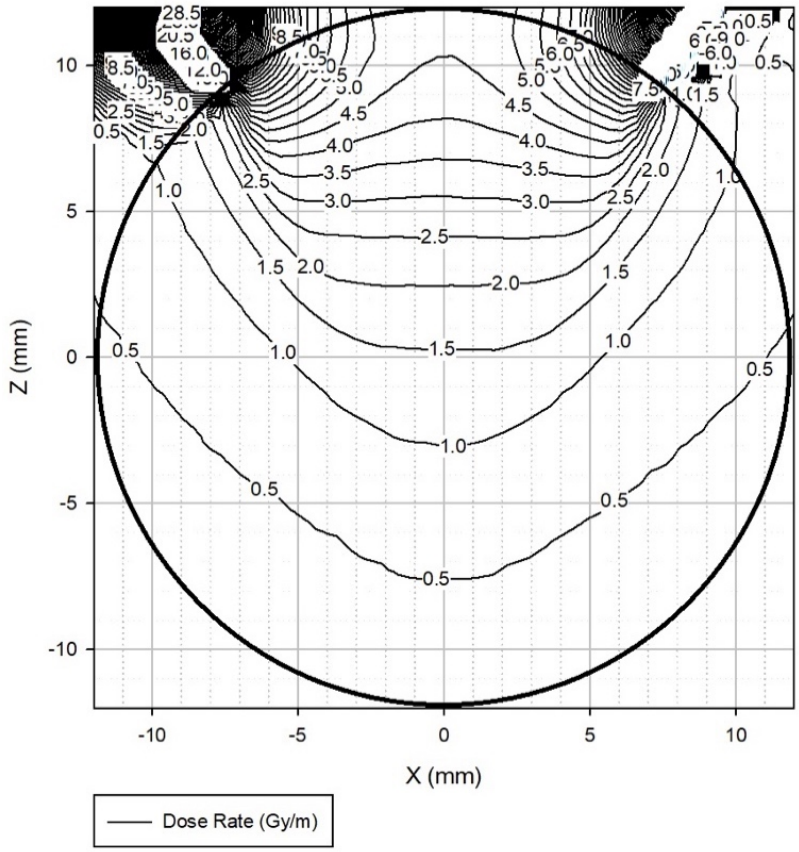

Figure 25F: Isodose curve of a 16 mm applicator containing Yb-169. The prescription dose of 3 Gy/min was delivered to a 6.5 mm depth in the eye.

Figure 25G is an isodose curve of Yb-169 used with a 16 mm diameter applicator with a collimator apex at -5.1 mm, collimator angle at 26.6°, target diameter at 14.1 mm, and target depth at 7.0 mm. The maximum percent dose was 28.5% to cornea, 42.8% to the posterior lens, 32.2% to the iris, 22.9% to the optic nerve, 19.4% to the bone, 319.6% to the sclera, and 325.5% to the tumor. The absorbed dose to each structure was 0.85 Gy, 1.28 Gy, 0.97 Gy, 0.69 Gy, 0.58 Gy, 9.59 Gy, and 9.77 Gy respectively.

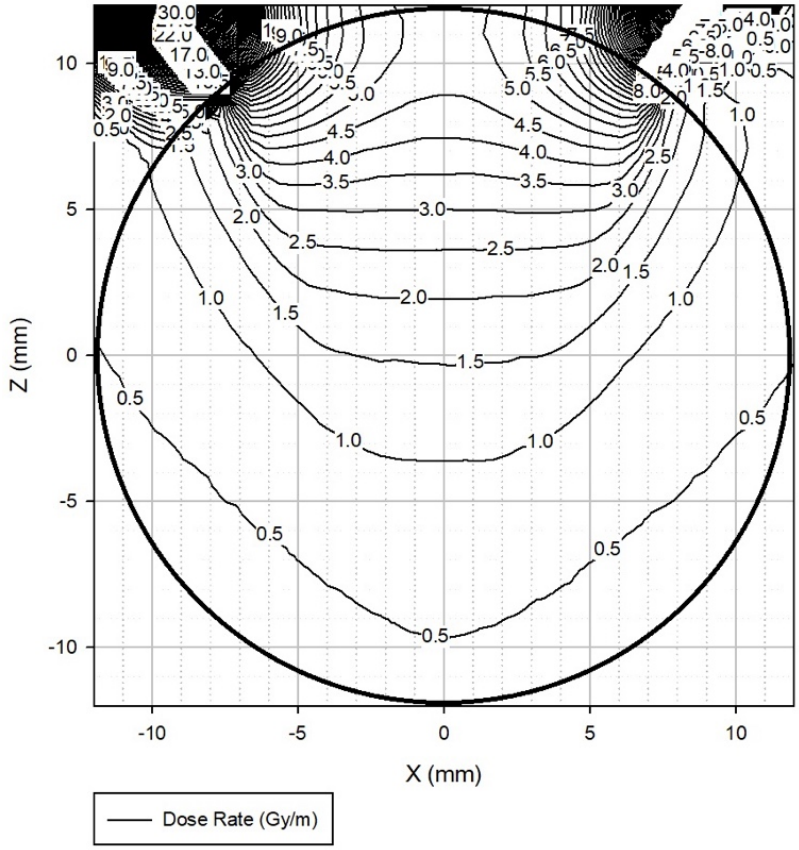

Figure 25G: Isodose curve of a 16 mm applicator containing Yb-169. The prescription dose of 3 Gy/min was delivered to a 7.0 mm depth in the eye.

Figure 25H is an isodose curve of Yb-169 used with a 16 mm diameter applicator with a collimator apex at -8.5 mm, collimator angle at 22.5°, target diameter at 14.3 mm, and target depth at 7.5 mm. The maximum percent dose was 31.3% to cornea, 49.8% to the posterior lens, 35.7% to the iris, 25.6% to the optic nerve, 21.1% to the bone, 341.8% to the sclera, and 348.3% to the tumor. The absorbed dose to each structure was 0.94 Gy, 1.50 Gy, 1.07 Gy, 0.77 Gy, 0.63 Gy, 10.25 Gy, and 10.45 Gy respectively.

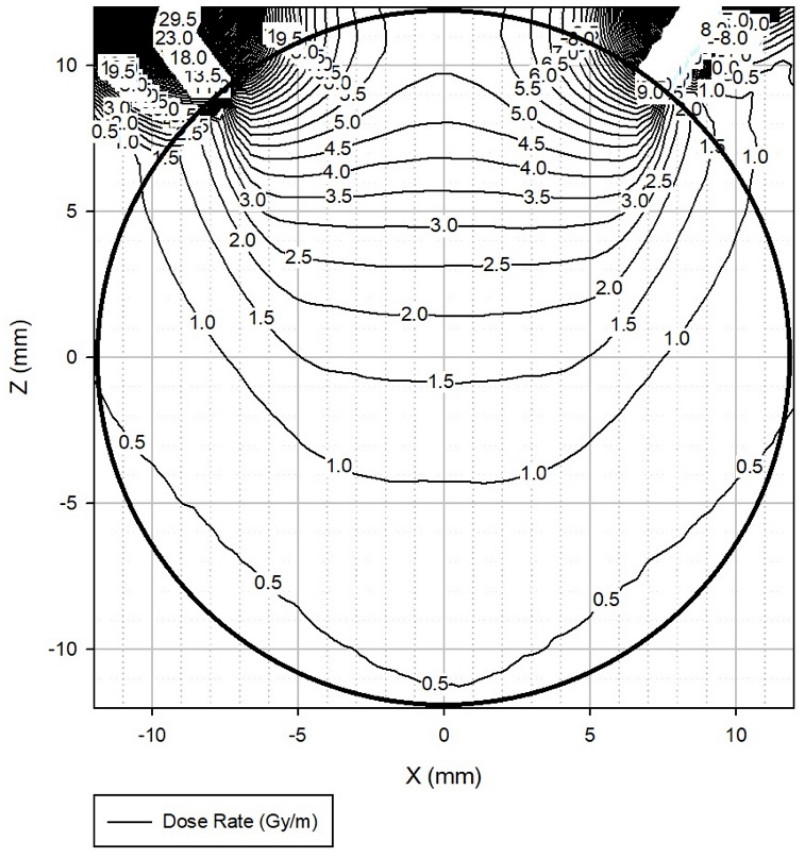

Figure 25H: Isodose curve of a 16 mm applicator containing Yb-169. The prescription dose of 3 Gy/min was delivered to a 7.5 mm depth in the eye.

Table 9: Dose rates to ocular structures from a Yb-169 16 mm applicator

Target Depth		4.0		4.5		5.0		5.5		6.0		6.5		7.0		7.5	
Simulation	Geometry	D	D (%)	D	D (%)	D	D (%)	D	D (%)	D	D (%)	D	D (%)	D	D (%)	D	D (%)
Cornea	Max	0.47	15.8%	0.53	17.5%	0.58	19.3%	0.64	21.3%	0.71	23.6%	0.78	26.1%	0.85	28.5%	0.94	31.3%
	Avg	0.23	7.7%	0.27	9.0%	0.31	10.3%	0.35	11.6%	0.39	12.9%	0.43	14.5%	0.48	16.1%	0.54	17.9%
	Min	0.11	3.6%	0.15	5.0%	0.19	6.3%	0.22	7.4%	0.26	8.6%	0.30	9.9%	0.34	11.3%	0.38	12.8%
Posterior Lens	Max	0.55	18.5%	0.64	21.3%	0.74	24.5%	0.84	27.9%	0.96	32.0%	1.11	37.1%	1.28	42.8%	1.50	49.8%
	Avg	0.29	9.8%	0.37	12.2%	0.43	14.4%	0.50	16.6%	0.57	19.1%	0.66	22.0%	0.75	25.1%	0.86	28.8%
	Min	0.13	4.4%	0.18	6.1%	0.24	7.9%	0.29	9.5%	0.33	11.1%	0.39	13.1%	0.45	15.1%	0.51	17.1%
Iris	Max	0.53	17.5%	0.58	19.5%	0.65	21.6%	0.72	23.9%	0.80	26.7%	0.88	29.4%	0.97	32.2%	1.07	35.7%
	Avg	0.27	9.0%	0.32	10.7%	0.37	12.3%	0.42	13.9%	0.47	15.7%	0.53	17.7%	0.59	19.8%	0.67	22.2%
	Min	0.11	3.8%	0.16	5.3%	0.20	6.7%	0.24	7.9%	0.28	9.3%	0.32	10.7%	0.36	12.1%	0.41	13.8%
Optic Nerve	Max	0.32	10.6%	0.37	12.4%	0.42	14.2%	0.48	16.0%	0.54	18.0%	0.61	20.5%	0.69	22.9%	0.77	25.6%
	Avg	0.23	7.6%	0.27	9.0%	0.31	10.2%	0.35	11.5%	0.39	12.9%	0.43	14.5%	0.48	16.1%	0.54	17.9%
	Min	0.17	5.7%	0.20	6.6%	0.23	7.6%	0.25	8.3%	0.28	9.3%	0.31	10.5%	0.34	11.4%	0.38	12.6%
Bone	Max	0.35	11.8%	0.38	12.8%	0.42	13.9%	0.46	15.2%	0.49	16.5%	0.54	17.9%	0.58	19.4%	0.63	21.1%
	Avg	0.15	4.9%	0.17	5.7%	0.20	6.6%	0.22	7.5%	0.25	8.5%	0.29	9.6%	0.32	10.7%	0.36	11.9%
	Min	0.05	1.8%	0.06	2.1%	0.07	2.5%	0.09	3.1%	0.11	3.7%	0.12	4.0%	0.13	4.4%	0.14	4.7%
Sclera	Max	6.61	220.4%	7.08	236.1%	7.56	252.2%	7.97	265.7%	8.45	281.5%	9.02	300.6%	9.59	319.6%	10.25	341.8%
	Avg	0.60	20.1%	0.68	22.8%	0.77	25.8%	0.87	28.8%	0.97	32.2%	1.07	35.8%	1.19	39.8%	1.32	44.1%
	Min	0.08	2.6%	0.09	2.9%	0.10	3.3%	0.12	4.0%	0.16	5.4%	0.26	8.6%	0.32	10.7%	0.38	12.5%
Tumor	Max	6.63	221.1%	6.95	231.6%	7.51	250.3%	8.10	269.9%	8.59	286.5%	9.19	306.3%	9.77	325.5%	10.45	348.3%
	Avg	4.18	139.4%	4.34	144.5%	4.49	149.5%	4.63	154.4%	4.80	160.1%	5.01	167.0%	5.18	172.7%	5.40	179.8%
	Min	3.00	100.0%	3.00	100.0%	3.00	100.0%	3.00	100.0%	3.00	100.0%	3.00	100.0%	3.00	100.0%	3.00	100.0%

Figure 26A is an isodose curve of Yb-169 used with an 18 mm diameter applicator with a collimator apex at 6.2 mm, collimator angle at 65.1°, target diameter at 13.3 mm, and target depth at 4.0 mm. The maximum percent dose was 17.7% to cornea, 19.7% to the posterior lens, 19.3% to the iris, 9.6% to the optic nerve, 12.5% to the bone, 212.5% to the sclera, and 222.8% to the tumor. The absorbed dose to each structure was 0.53 Gy, 0.59 Gy, 0.58 Gy, 0.29 Gy, 0.37 Gy, 6.37 Gy, and 6.68 Gy respectively.

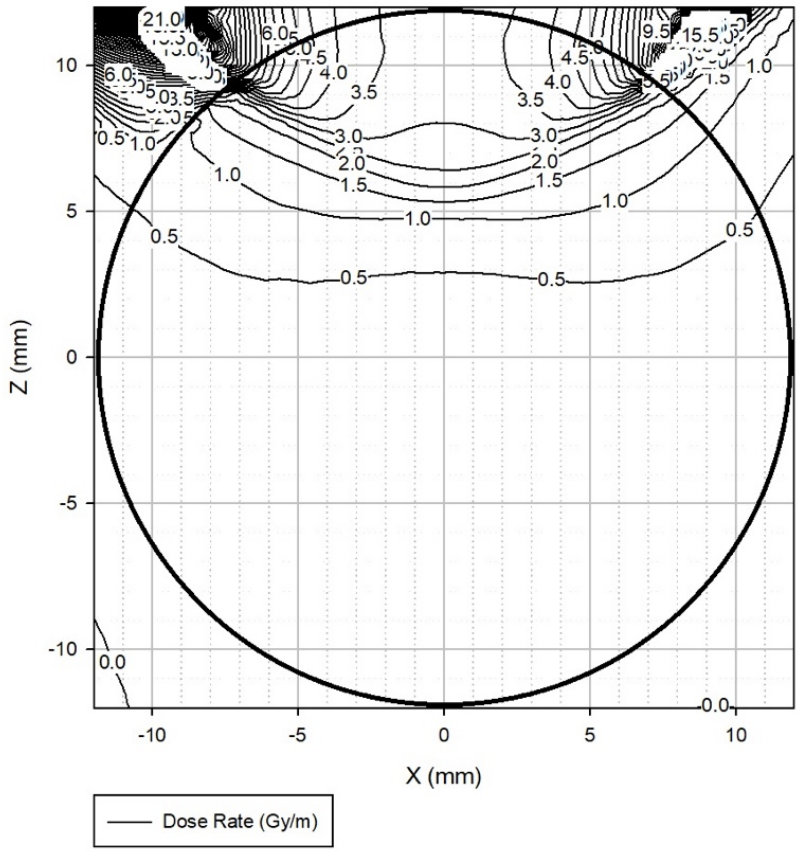

Figure 26A: Isodose curve of an 18 mm applicator containing Yb-169. The prescription dose of 3 Gy/min was delivered to a 4.0 mm depth in the eye.

Figure 26B is an isodose curve of Yb-169 used with an 18 mm diameter applicator with a collimator apex at 5.2 mm, collimator angle at 59.8°, target diameter at 13.6 mm, and target depth at 4.5 mm. The maximum percent dose was 19.7% to cornea, 22.9% to the posterior lens, 21.6% to the iris, 12.2% to the optic nerve, 13.7% to the bone, 232.7% to the sclera, and 231.0% to the tumor. The absorbed dose to each structure was 0.59 Gy, 0.69 Gy, 0.65 Gy, 0.37 Gy, 0.41 Gy, 6.98 Gy, and 6.93 Gy respectively.

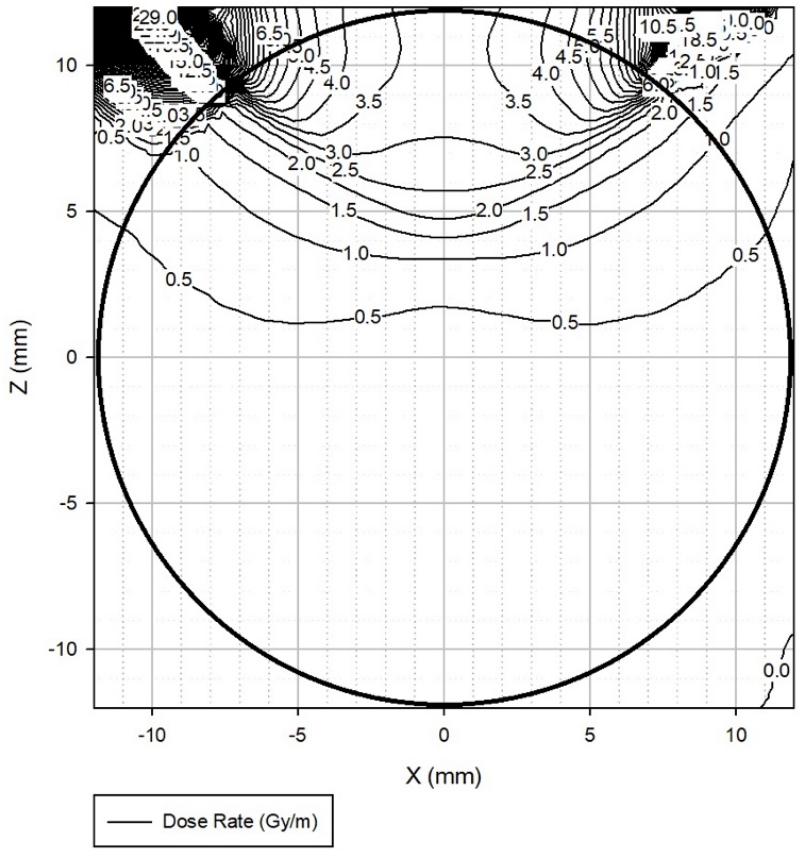

Figure 26B: Isodose curve of an 18 mm applicator containing Yb-169. The prescription dose of 3 Gy/min was delivered to a 4.5 mm depth in the eye.

Figure 26C is an isodose curve of Yb-169 used with an 18 mm diameter applicator with a collimator apex at 4.1 mm, collimator angle at 54.6°, target diameter at 14.0 mm, and target depth at 5.0 mm. The maximum percent dose was 21.8% to cornea, 26.0% to the posterior lens, 24.0% to the iris, 14.4% to the optic nerve, 14.9% to the bone, 250.9% to the sclera, and 240.3% to the tumor. The absorbed dose to each structure was 0.65 Gy, 0.78 Gy, 0.72 Gy, 0.43 Gy, 0.45 Gy, 7.53 Gy, and 7.21 Gy respectively.

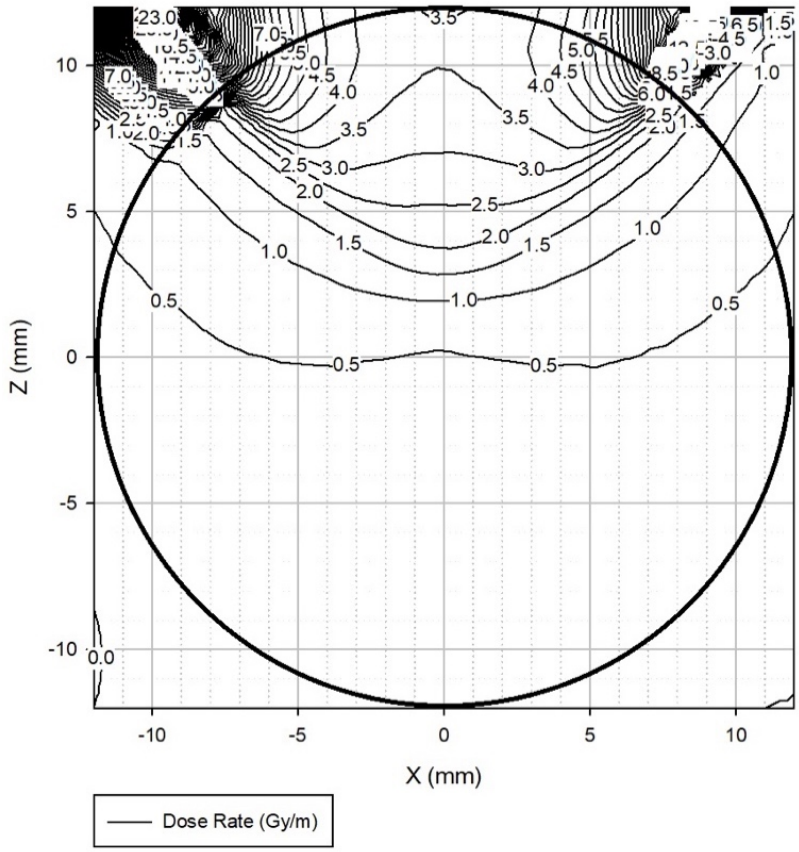

Figure 26C: Isodose curve of an 18 mm applicator containing Yb-169. The prescription dose of 3 Gy/min was delivered to a 5.0 mm depth in the eye.

Figure 26D is an isodose curve of Yb-169 used with an 18 mm diameter applicator with a collimator apex at 2.8 mm, collimator angle at 49.6°, target diameter at 14.3 mm, and target depth at 5.5 mm. The maximum percent dose was 24.0% to cornea, 29.3% to the posterior lens, 26.5% to the iris, 16.5% to the optic nerve, 16.1% to the bone, 264.9% to the sclera, and 250.9% to the tumor. The absorbed dose to each structure was 0.72 Gy, 0.88 Gy, 0.79 Gy, 0.49 Gy, 0.48 Gy, 7.95 Gy, and 7.53 Gy respectively.

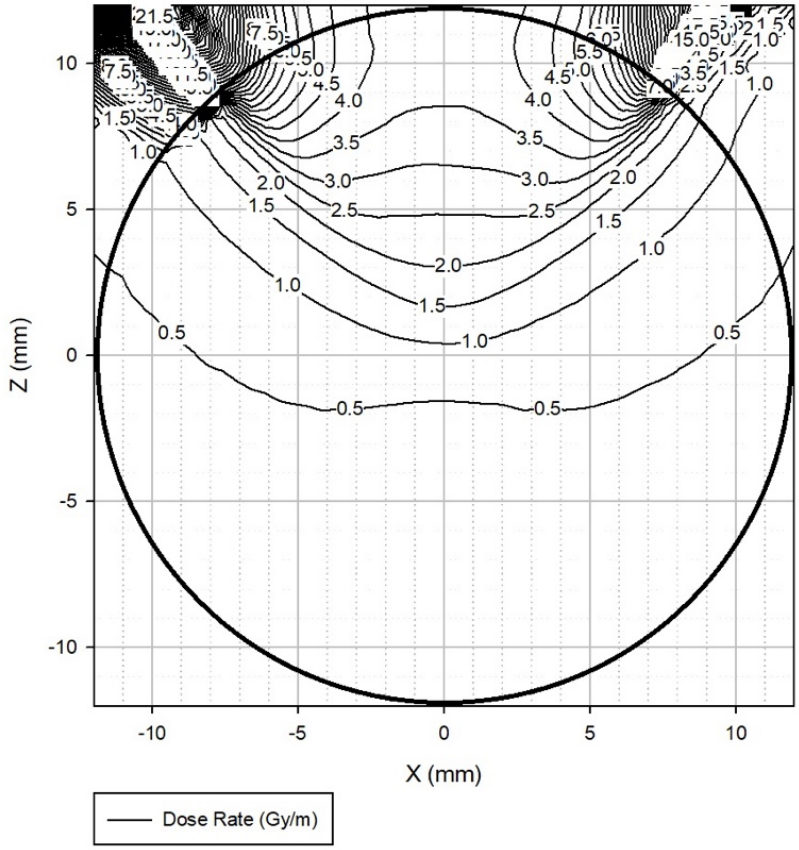

Figure 26D: Isodose curve of an 18 mm applicator containing Yb-169. The prescription dose of 3 Gy/min was delivered to a 5.5 mm depth in the eye.

Figure 26E is an isodose curve of Yb-169 used with an 18 mm diameter applicator with a collimator apex at 1.5 mm, collimator angle at 44.8°, target diameter at 14.5 mm, and target depth at 6.0 mm. The maximum percent dose was 26.3% to cornea, 33.4% to the posterior lens, 29.0% to the iris, 18.5% to the optic nerve, 17.3% to the bone, 276.9% to the sclera, and 262.2% to the tumor. The absorbed dose to each structure was 0.79 Gy, 1.00 Gy, 0.87 Gy, 0.56 Gy, 0.52 Gy, 8.31 Gy, and 7.87 Gy respectively.

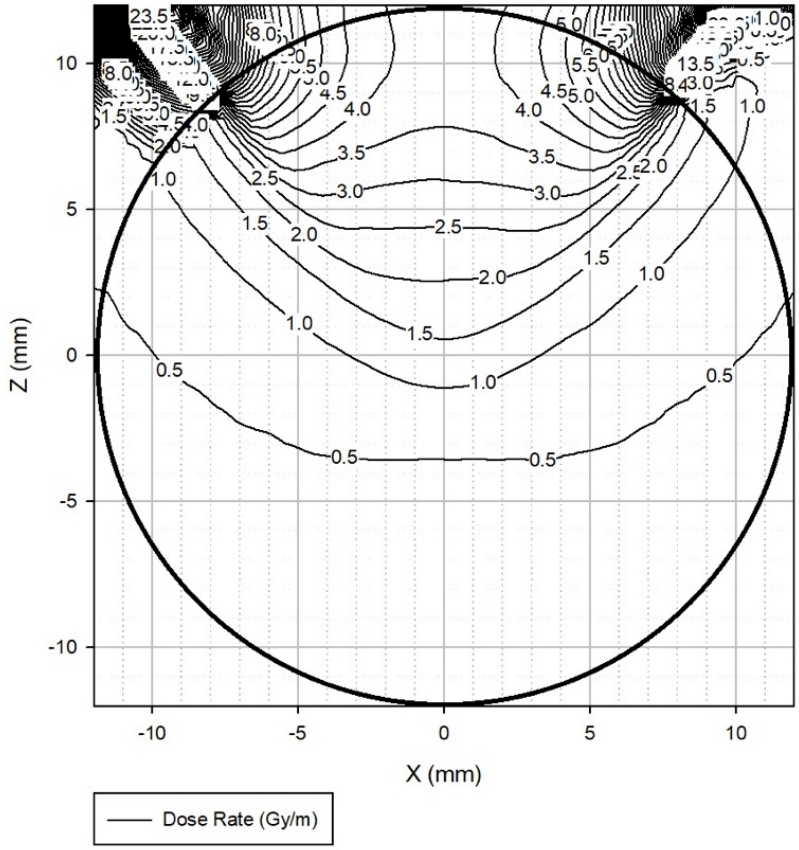

Figure 26E: Isodose curve of an 18 mm applicator containing Yb-169. The prescription dose of 3 Gy/min was delivered to a 6.0 mm depth in the eye.

Figure 26F is an isodose curve of Yb-169 used with an 18 mm diameter applicator with a collimator apex at -0.1 mm, collimator angle at 40.1°, target diameter at 14.8 mm, and target depth at 6.5 mm. The maximum percent dose was 28.2% to cornea, 38.1% to the posterior lens, 31.6% to the iris, 20.5% to the optic nerve, 18.4% to the bone, 290.1% to the sclera, and 273.6% to the tumor. The absorbed dose to each structure was 0.85 Gy, 1.14 Gy, 0.95 Gy, 0.61 Gy, 0.55 Gy, 8.70 Gy, and 8.21 Gy respectively.

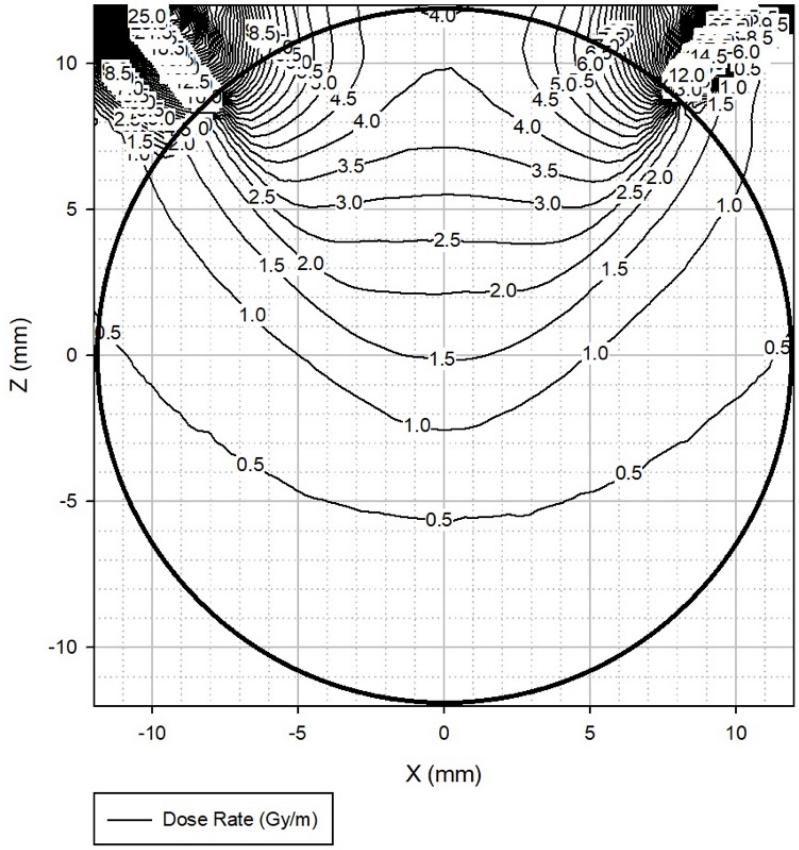

Figure 26F: Isodose curve of an 18 mm applicator containing Yb-169. The prescription dose of 3 Gy/min was delivered to a 6.5 mm depth in the eye.

Figure 26G is an isodose curve of Yb-169 used with an 18 mm diameter applicator with a collimator apex at -1.9 mm, collimator angle at 35.7°, target diameter at 15.0 mm, and target depth at 7.0 mm. The maximum percent dose was 31.1% to cornea, 43.9% to the posterior lens, 35.0% to the iris, 23.2% to the optic nerve, 19.9% to the bone, 307.5% to the sclera, and 288.0% to the tumor. The absorbed dose to each structure was 0.93 Gy, 1.32 Gy, 1.05 Gy, 0.70 Gy, 0.60 Gy, 9.23 Gy, and 8.64 Gy respectively.

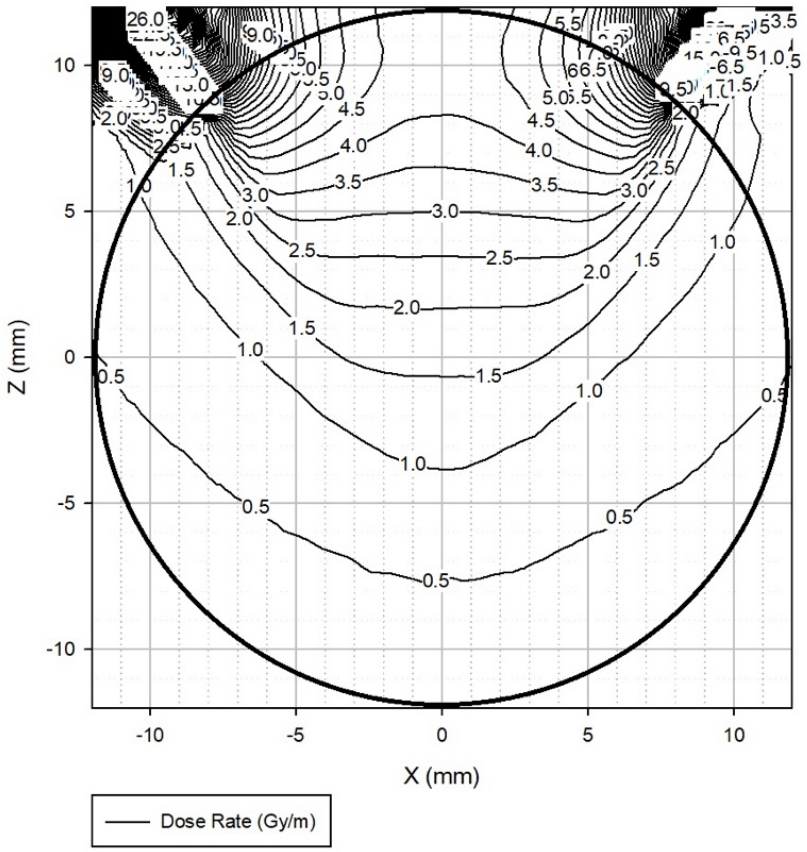

Figure 26G: Isodose curve of an 18 mm applicator containing Yb-169. The prescription dose of 3 Gy/min was delivered to a 7.0 mm depth in the eye.

Figure 26H is an isodose curve of Yb-169 used with an 18 mm diameter applicator with a collimator apex at -4.1 mm, collimator angle at 31.5°, target diameter at 15.2 mm, and target depth at 7.5 mm. The maximum percent dose was 33.9% to cornea, 51.0% to the posterior lens, 38.2% to the iris, 26.1% to the optic nerve, 21.5% to the bone, 326.4% to the sclera, and 305.1% to the tumor. The absorbed dose to each structure was 1.02 Gy, 1.53 Gy, 1.15 Gy, 0.78 Gy, 0.64 Gy, 9.79 Gy, and 9.15 Gy respectively.

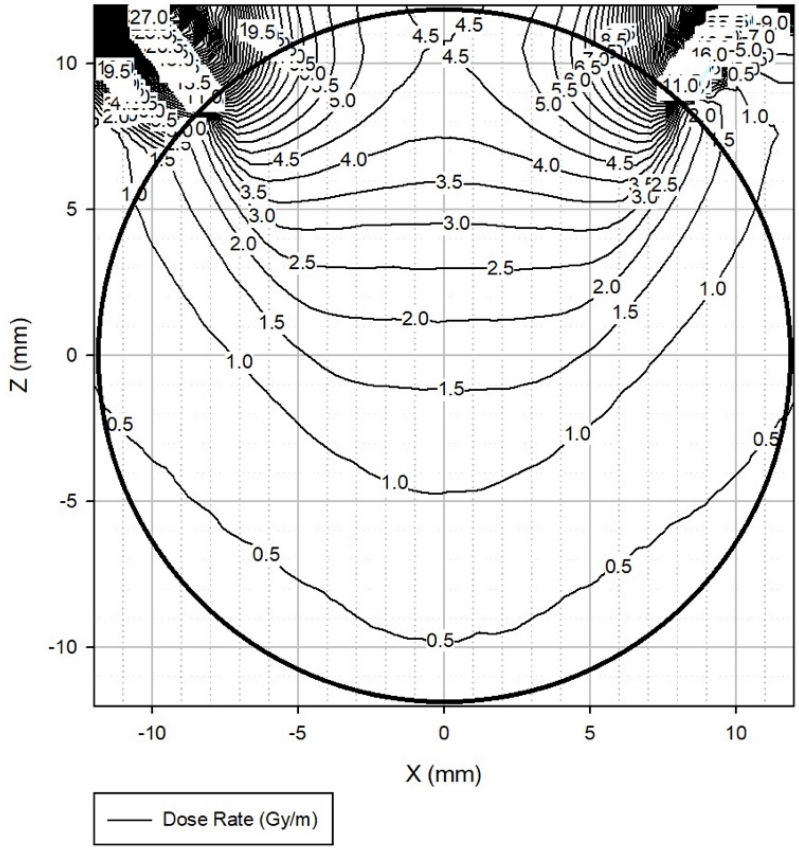

Figure 26H: Isodose curve of an 18 mm applicator containing Yb-169. The prescription dose of 3 Gy/min was delivered to a 7.5 mm depth in the eye.

Figure 26I is an isodose curve of Yb-169 used with an 18 mm diameter applicator with a collimator apex at -6.6 mm, collimator angle at 27.4°, target diameter at 15.5 mm, and target depth at 8.0 mm. The maximum percent dose was 36.8% to cornea, 59.7% to the posterior lens, 42.0% to the iris, 28.9% to the optic nerve, 23.1% to the bone, 344.5% to the sclera, and 322.1% to the tumor. The absorbed dose to each structure was 1.11 Gy, 1.79 Gy, 1.26 Gy, 0.87 Gy, 0.69 Gy, 10.34 Gy, and 9.66 Gy respectively.

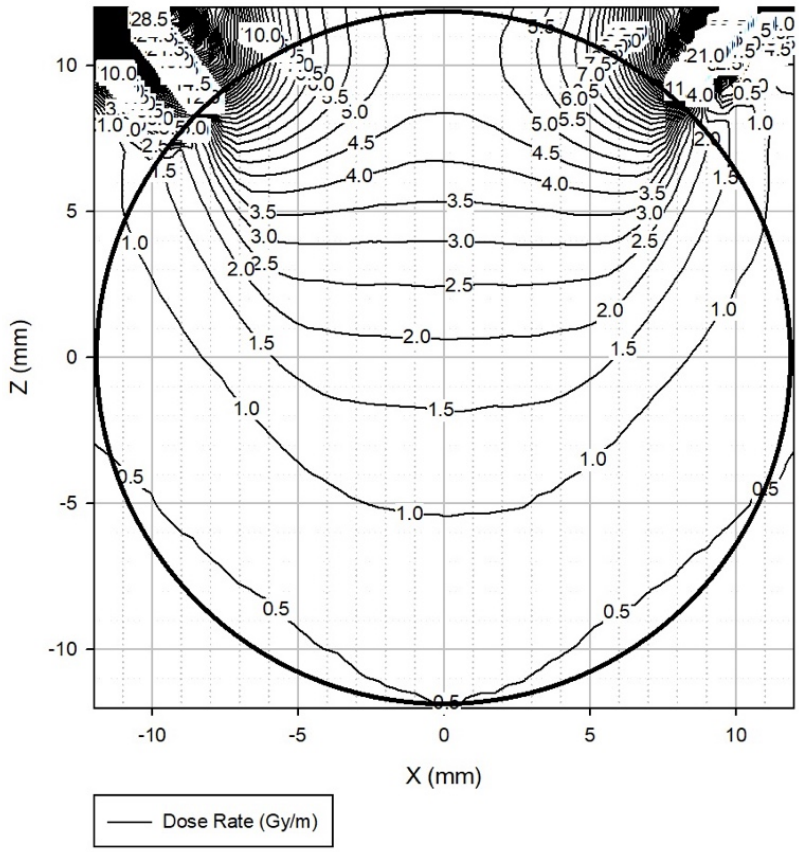

Figure 26I: Isodose curve of an 18 mm applicator containing Yb-169. The prescription dose of 3 Gy/min was delivered to an 8.0 mm depth in the eye.

Table 10: Dose rates to ocular structures from a Yb-169 18 mm applicator

Target Depth		4.0		4.5		5.0		5.5		6.0		6.5		7.0		7.5		8.0	
Simulation	Geometry	D	D (%)	D	D (%)	D	D (%)	D	D (%)	D	D (%)	D	D (%)	D	D (%)	D	D (%)	D	D (%)
Cornea	Max	0.53	17.7%	0.59	19.7%	0.65	21.8%	0.72	24.0%	0.79	26.3%	0.85	28.2%	0.93	31.1%	1.02	33.9%	1.11	36.8%
	Avg	0.23	7.6%	0.28	9.2%	0.32	10.7%	0.36	12.1%	0.41	13.5%	0.45	14.9%	0.50	16.5%	0.55	18.3%	0.60	20.1%
	Min	0.11	3.6%	0.13	4.3%	0.17	5.7%	0.22	7.3%	0.25	8.5%	0.29	9.8%	0.33	11.1%	0.38	12.5%	0.42	14.1%
Posterior Lens	Max	0.59	19.7%	0.69	22.9%	0.78	26.0%	0.88	29.3%	1.00	33.4%	1.14	38.1%	1.32	43.9%	1.53	51.0%	1.79	59.7%
	Avg	0.27	9.0%	0.35	11.6%	0.43	14.3%	0.50	16.8%	0.58	19.3%	0.66	21.9%	0.75	25.1%	0.86	28.6%	0.98	32.6%
	Min	0.14	4.5%	0.16	5.2%	0.21	7.0%	0.27	9.1%	0.33	10.9%	0.38	12.6%	0.44	14.6%	0.50	16.8%	0.57	19.1%
Iris	Max	0.58	19.3%	0.65	21.6%	0.72	24.0%	0.79	26.5%	0.87	29.0%	0.95	31.6%	1.05	35.0%	1.15	38.2%	1.26	42.0%
	Avg	0.26	8.8%	0.32	10.7%	0.38	12.6%	0.43	14.5%	0.49	16.3%	0.54	18.1%	0.61	20.3%	0.68	22.6%	0.75	25.1%
	Min	0.11	3.7%	0.13	4.3%	0.18	5.9%	0.23	7.6%	0.27	9.0%	0.31	10.4%	0.36	11.9%	0.41	13.5%	0.46	15.3%
Optic Nerve	Max	0.29	9.6%	0.37	12.2%	0.43	14.4%	0.49	16.5%	0.56	18.5%	0.61	20.5%	0.70	23.2%	0.78	26.1%	0.87	28.9%
	Avg	0.21	7.1%	0.27	8.9%	0.31	10.4%	0.36	11.9%	0.40	13.3%	0.44	14.7%	0.49	16.4%	0.54	18.2%	0.60	20.0%
	Min	0.16	5.3%	0.20	6.6%	0.23	7.5%	0.26	8.6%	0.29	9.6%	0.32	10.6%	0.35	11.7%	0.39	12.9%	0.42	14.1%
Bone	Max	0.37	12.5%	0.41	13.7%	0.45	14.9%	0.48	16.1%	0.52	17.3%	0.55	18.4%	0.60	19.9%	0.64	21.5%	0.69	23.1%
	Avg	0.14	4.7%	0.17	5.5%	0.19	6.4%	0.22	7.3%	0.25	8.3%	0.28	9.3%	0.31	10.4%	0.35	11.6%	0.38	12.8%
	Min	0.06	1.9%	0.07	2.2%	0.07	2.5%	0.09	2.9%	0.10	3.4%	0.12	4.0%	0.13	4.4%	0.14	4.8%	0.15	5.0%
Sclera	Max	6.37	212.5%	6.98	232.7%	7.53	250.9%	7.95	264.9%	8.31	276.9%	8.70	290.1%	9.23	307.5%	9.79	326.4%	10.34	344.5%
	Avg	0.66	22.0%	0.74	24.8%	0.84	27.9%	0.93	31.0%	1.03	34.4%	1.14	38.1%	1.26	42.0%	1.39	46.2%	1.53	50.9%
	Min	0.09	2.8%	0.09	3.0%	0.10	3.3%	0.11	3.8%	0.13	4.4%	0.17	5.5%	0.24	8.2%	0.34	11.3%	0.40	13.5%
Tumor	Max	6.68	222.8%	6.93	231.0%	7.21	240.3%	7.53	250.9%	7.87	262.2%	8.21	273.6%	8.64	288.0%	9.15	305.1%	9.66	322.1%
	Avg	3.99	133.1%	4.10	136.6%	4.21	140.3%	4.34	144.7%	4.46	148.7%	4.58	152.6%	4.70	156.7%	4.85	161.8%	5.00	166.6%
	Min	3.00	100.0%	3.00	100.0%	3.00	100.0%	3.00	100.0%	3.00	100.0%	3.00	100.0%	3.00	100.0%	3.00	100.0%	3.00	100.0%

DVH curves were made to demonstrate how the dose can be delivered to the tumor while shielding the critical structures in the eye for various applicator sizes and collimators using Yb-169. Figure 27 shows these DVH curves for applicators 12 and 16 mm in diameter. The 12 mm diameter applicator delivers the prescription dose to a 5 mm depth in the eye. The 16 mm diameter applicator delivers the prescription dose to a 7 mm depth in the eye. These curves are useful for showing a comparison of the volume of each structure that is receiving a certain dose rate.

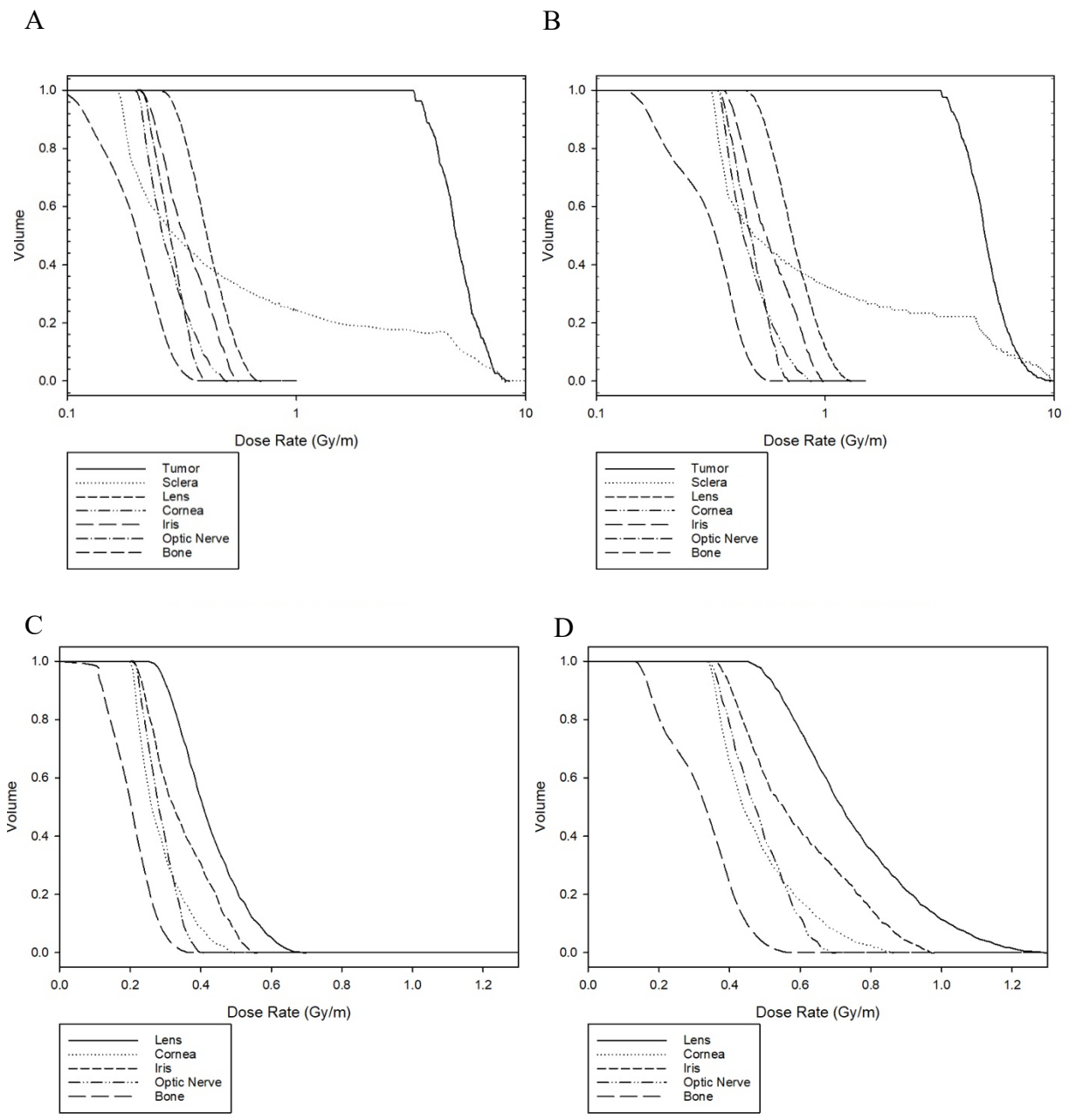

Figure 27: A) and C) represent DVH curves for the 12 mm applicator that delivers 3 Gy/min to a 5 mm depth in the eye. B) and D) represent DVH curves for the 16 mm applicator that delivers 3 Gy/min to a 7 mm depth in the eye. A) and B) in log scale display the dose rates to the tumor compared to the critical structures. C) and D) are the dose rates in Gy/min vs volume of ocular structures of interest.

Due to the use of the HDR source, Yb-169, there is some lateral dose behind the applicator. Therefore, the lateral dose rate at a distance of 5 mm behind a 12 and 16 mm diameter applicator was measured. This is presented in Figure 28. The 12 mm diameter applicator delivers the prescription dose to a 5 mm depth in the eye. The maximum, average, and minimum dose rates for the 12 mm diameter applicator were 0.26 Gy/min, 0.18 Gy/min, and 0.08 Gy/min respectively. The 16 mm diameter applicator delivers the prescription dose to a 7 mm depth in the eye. The maximum, average, and minimum dose rates for the 16 mm diameter applicator were 0.25 Gy/min, 0.17 Gy/min, and 0.10 Gy/min respectively.

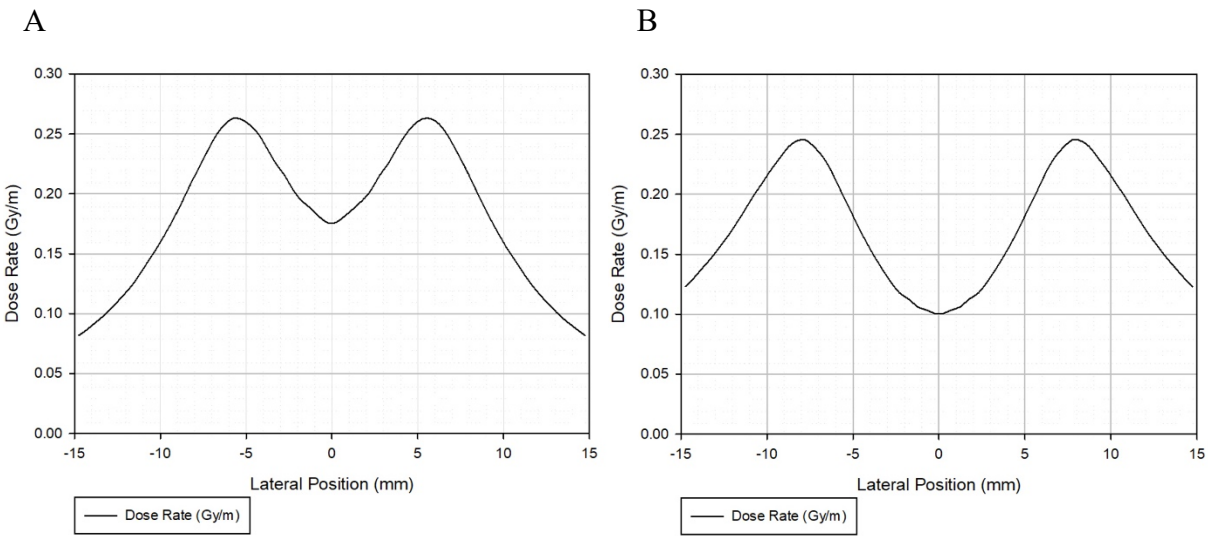

Figure 28: A) The lateral dose rate at a distance of 5 mm behind a 12 mm applicator that delivers the prescription dose to a depth of 5 mm in the eye. B) is the lateral dose rate at a distance of 5 mm behind a 16 mm applicator that delivers the prescription dose to a depth of 7 mm in the eye.

4.2.2 Se-75

Applicators ranging from 12-18 mm in diameter containing Se-75 were simulated. Isodose curves of these simulations are presented in Figures 29-32 for the 12-18 mm diameter applicators respectively that delivers the prescription dose to a target depth of 3.5-8 mm in the eye. Their corresponding dose rates to ocular structures of interest are presented in Tables 11-14, which gives the maximum, average, and minimum dose rates in Gy/min for structures of interest in the eye for a 12 mm applicator containing Se-75. The dose rate, D, was normalized to a tumor minimum dose rate of 3 Gy/min. D (%) is the normalized dose rate in percentage. Several dose volume histograms are shown for different diameter applicators that deliver the prescription dose to varying depths in the eye, in Figure 33. An example of the lateral dose rate behind the applicator is also shown, in Figure 34.

Figure 29A is an isodose curve of Se-75 used with a 12 mm diameter applicator with a collimator apex at 5.3 mm, collimator angle at 44.6°, target diameter at 10.0 mm, and target depth at 3.5 mm. The maximum percent dose was 17.4% to cornea, 20.5% to the posterior lens, 18.8% to the iris, 12.1% to the optic nerve, 14.7% to the bone, 227.5% to the sclera, and 225.0% to the tumor. The absorbed dose to each structure was 0.52 Gy, 0.62 Gy, 0.57 Gy, 0.36 Gy, 0.44 Gy, 6.82 Gy, and 6.75 Gy respectively.

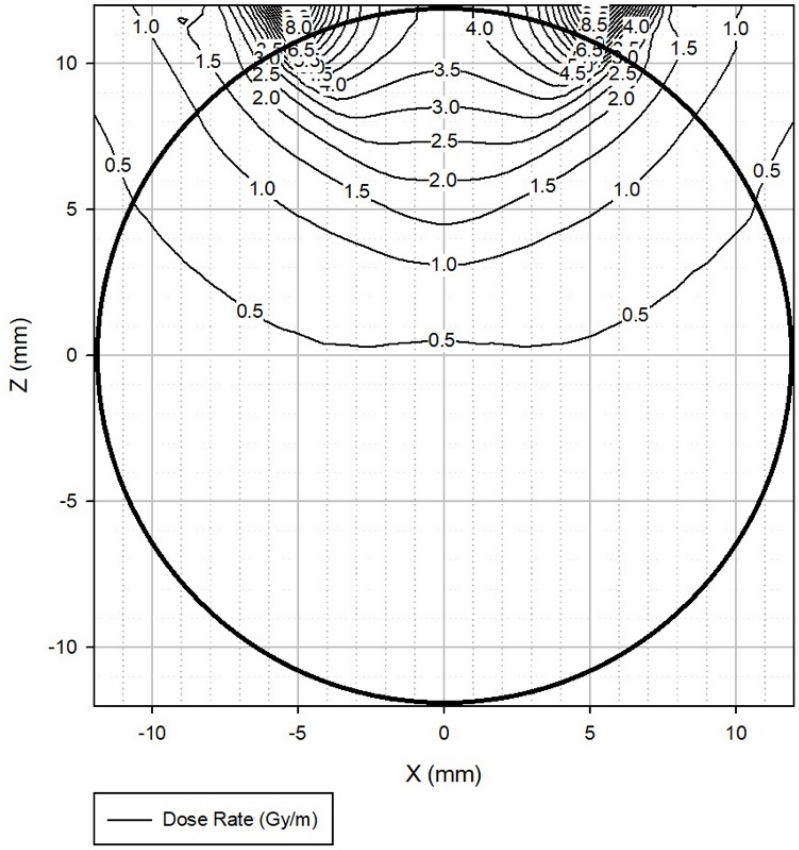

Figure 29A: Isodose curve of a 12 mm applicator containing Se-75. The prescription dose of 3 Gy/min was delivered to a 3.5 mm depth in the eye.

Figure 29B is an isodose curve of Se-75 used with a 12 mm diameter applicator with a collimator apex at 3.7 mm, collimator angle at 38.5°, target diameter at 10.4 mm, and target depth at 4.0 mm. The maximum percent dose was 19.5% to cornea, 23.3% to the posterior lens, 21.2% to the iris, 13.7% to the optic nerve, 15.8% to the bone, 247.1% to the sclera, and 243.2% to the tumor. The absorbed dose to each structure was 0.58 Gy, 0.70 Gy, 0.63 Gy, 0.41 Gy, 0.47 Gy, 7.41 Gy, and 7.30 Gy respectively.

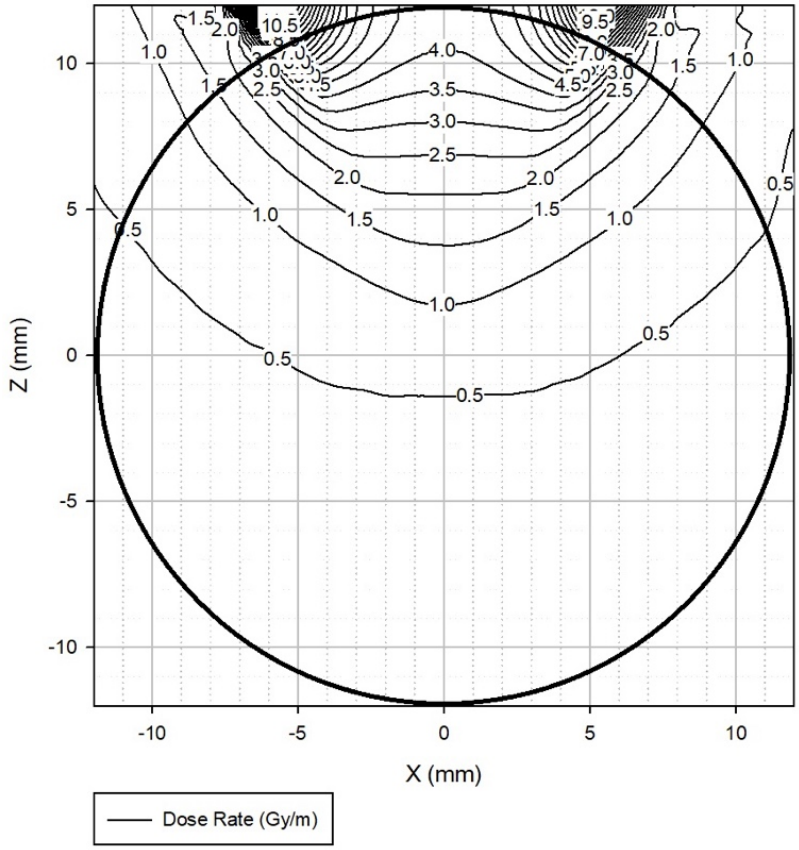

Figure 29B: Isodose curve of a 12 mm applicator containing Se-75. The prescription dose of 3 Gy/min was delivered to a 4.0 mm depth in the eye.

Figure 29C is an isodose curve of Se-75 used with a 12 mm diameter applicator with a collimator apex at 1.8 mm, collimator angle at 32.7°, target diameter at 10.8 mm, and target depth at 4.5 mm. The maximum percent dose was 21.6% to cornea, 26.5% to the posterior lens, 23.4% to the iris, 15.5% to the optic nerve, 17.1% to the bone, 267.1% to the sclera, and 262.7% to the tumor. The absorbed dose to each structure was 0.65 Gy, 0.79 Gy, 0.70 Gy, 0.46 Gy, 0.51 Gy, 8.01 Gy, and 7.88 Gy respectively.

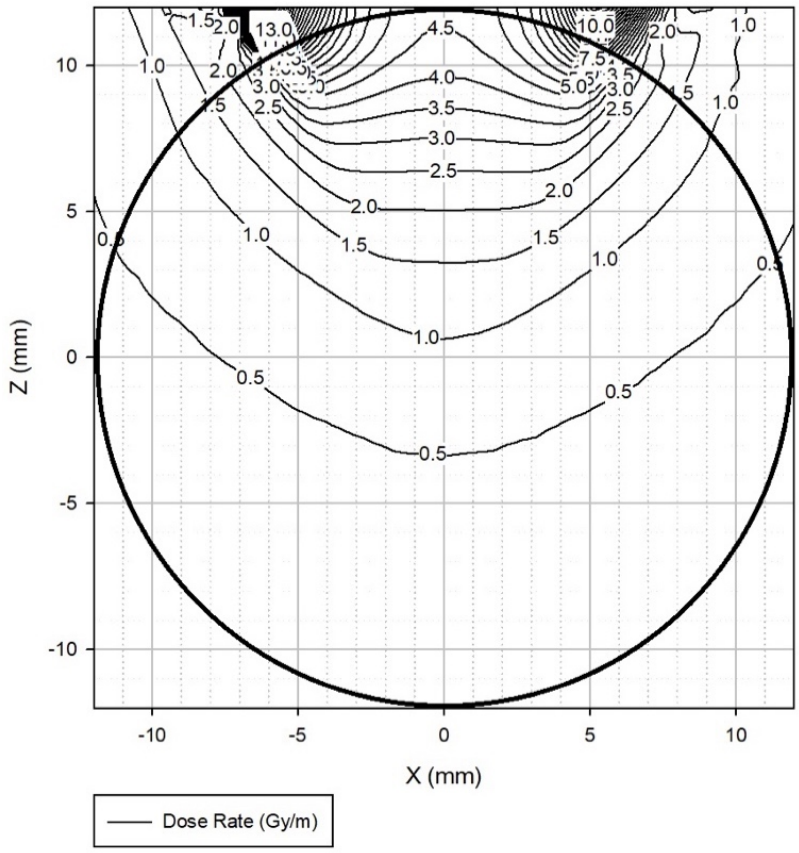

Figure 29C: Isodose curve of a 12 mm applicator containing Se-75. The prescription dose of 3 Gy/min was delivered to a 4.5 mm depth in the eye.

Figure 29D is an isodose curve of Se-75 used with a 12 mm diameter applicator with a collimator apex at -0.7 mm, collimator angle at 27.2°, target diameter at 11.1 mm, and target depth at 5.0 mm. The maximum percent dose was 23.6% to cornea, 30.0% to the posterior lens, 26.1% to the iris, 17.4% to the optic nerve, 18.5% to the bone, 289.7% to the sclera, and 284.5% to the tumor. The absorbed dose to each structure was 0.72 Gy, 0.90 Gy, 0.78 Gy, 0.52 Gy, 0.55 Gy, 8.69 Gy, and 8.53 Gy respectively.

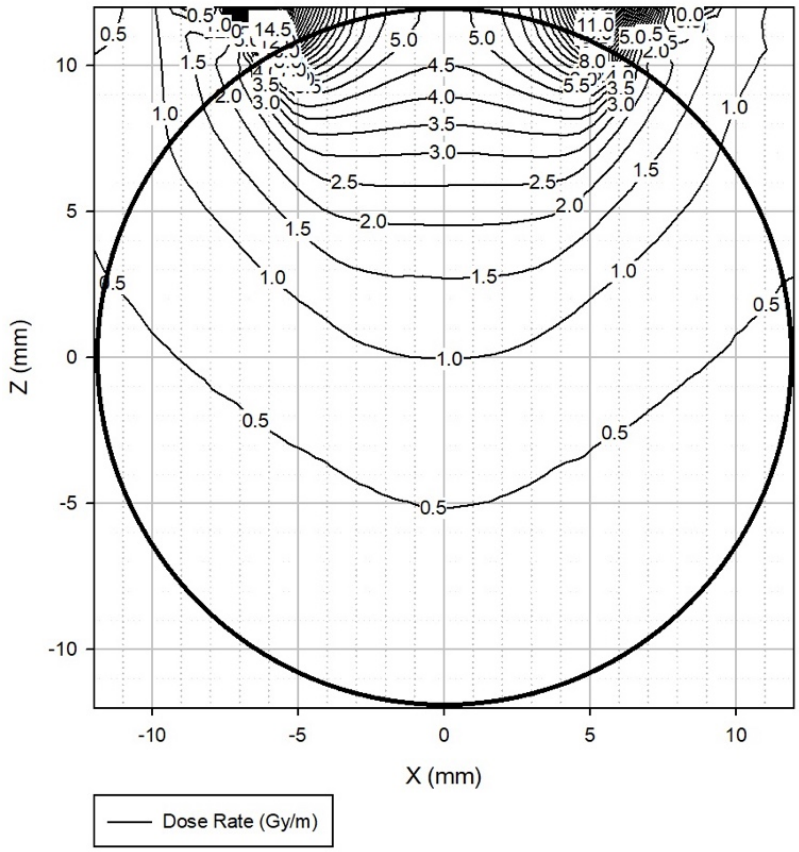

Figure 29D: Isodose curve of a 12 mm applicator containing Se-75. The prescription dose of 3 Gy/min was delivered to a 5.0 mm depth in the eye.

Figure 29E is an isodose curve of Se-75 used with a 12 mm diameter applicator with a collimator apex at -4.0 mm, collimator angle at 22.1°, target diameter at 11.4 mm, and target depth at 5.5 mm. The maximum percent dose was 26.5% to cornea, 34.1% to the posterior lens, 29.1% to the iris, 19.6% to the optic nerve, 20.0% to the bone, 314.1% to the sclera, and 308.0% to the tumor. The absorbed dose to each structure was 0.79 Gy, 1.02 Gy, 0.87 Gy, 0.59 Gy, 0.60 Gy, 9.42 Gy, and 9.24 Gy respectively.

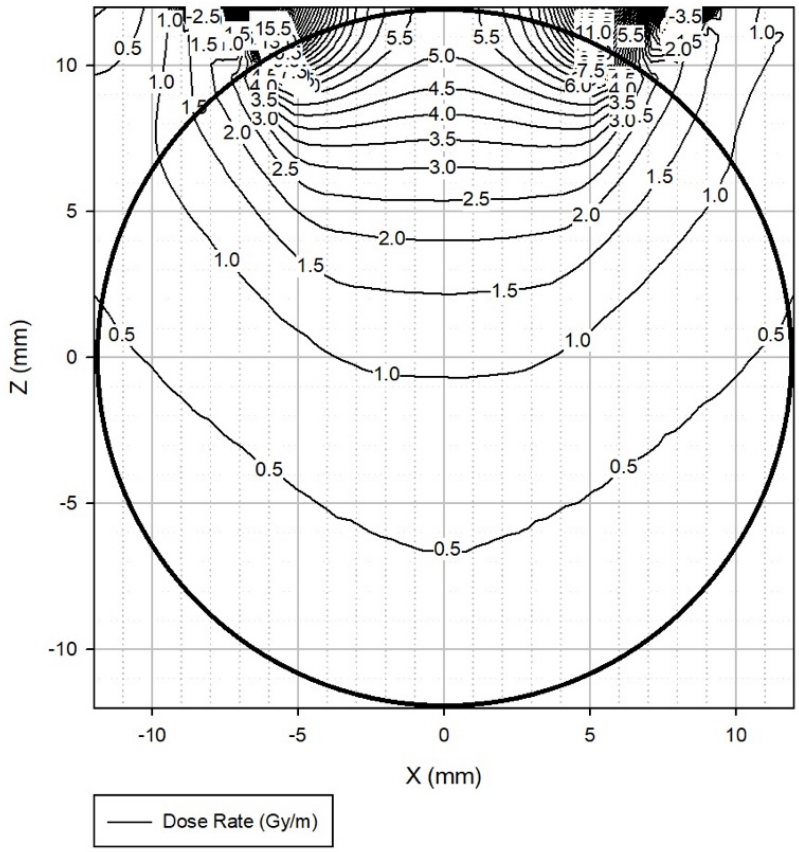

Figure 29E: Isodose curve of a 12 mm applicator containing Se-75. The prescription dose of 3 Gy/min was delivered to a 5.5 mm depth in the eye.

Figure 29F is an isodose curve of Se-75 used with a 12 mm diameter applicator with a collimator apex at -8.7 mm, collimator angle at 17.4°, target diameter at 11.6 mm, and target depth at 6.0 mm. The maximum percent dose was 29.4% to cornea, 38.6% to the posterior lens, 32.3% to the iris, 22.0% to the optic nerve, 21.6% to the bone, 339.5% to the sclera, and 332.6% to the tumor. The absorbed dose to each structure was 0.88 Gy, 1.16 Gy, 0.97 Gy, 0.66 Gy, 0.65 Gy, 10.19 Gy, and 9.98 Gy respectively.

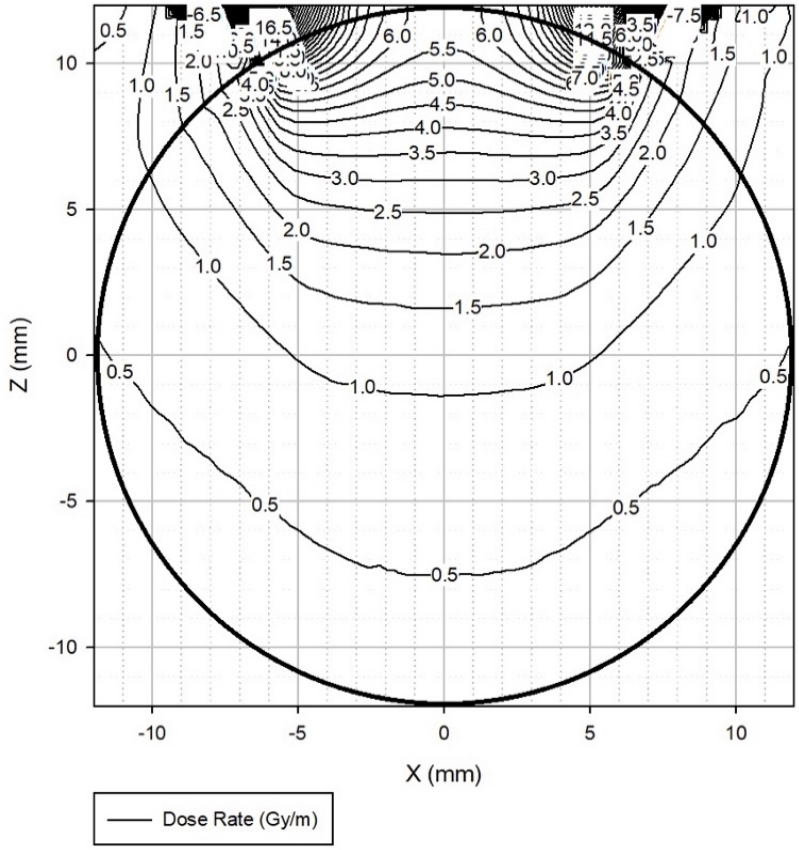

Figure 29F: Isodose curve of a 12 mm applicator containing Se-75. The prescription dose of 3 Gy/min was delivered to a 6.0 mm depth in the eye.

Table 11: Dose rates to ocular structures from a Se-75 12 mm applicator

Target Depth		3.5		4.0		4.5		5.0		5.5		6.0	
Simulation	Geometry	D	D (%)	D	D (%)	D	D (%)	D	D (%)	D	D (%)	D	D (%)
Cornea	Max	0.52	17.4%	0.58	19.5%	0.65	21.6%	0.72	23.6%	0.79	26.5%	0.88	29.4%
	Avg	0.28	9.3%	0.32	10.5%	0.35	11.8%	0.40	13.1%	0.44	14.8%	0.49	16.4%
	Min	0.17	5.8%	0.20	6.8%	0.23	7.7%	0.27	8.8%	0.30	10.0%	0.34	11.4%
Posterior	Max	0.62	20.5%	0.70	23.3%	0.79	26.5%	0.90	30.0%	1.02	34.1%	1.16	38.6%
Lens	Avg	0.37	12.3%	0.42	14.2%	0.48	16.2%	0.55	18.4%	0.63	20.9%	0.71	23.7%
	Min	0.21	7.0%	0.25	8.3%	0.29	9.6%	0.33	11.0%	0.38	12.6%	0.43	14.3%
Iris	Max	0.57	18.8%	0.63	21.2%	0.70	23.4%	0.78	26.1%	0.87	29.1%	0.97	32.3%
	Avg	0.32	10.7%	0.37	12.2%	0.41	13.7%	0.46	15.5%	0.52	17.3%	0.58	19.4%
	Min	0.18	5.9%	0.21	7.0%	0.24	8.0%	0.27	9.2%	0.31	10.4%	0.36	11.9%
Optic	Max	0.36	12.1%	0.41	13.7%	0.46	15.5%	0.52	17.4%	0.59	19.6%	0.66	22.0%
Nerve	Avg	0.27	8.9%	0.30	10.1%	0.34	11.4%	0.38	12.8%	0.43	14.3%	0.48	15.9%
	Min	0.20	6.7%	0.23	7.6%	0.25	8.4%	0.28	9.5%	0.32	10.6%	0.35	11.7%
Bone	Max	0.44	14.7%	0.47	15.8%	0.51	17.1%	0.55	18.5%	0.60	20.0%	0.65	21.6%
	Avg	0.14	4.1%	0.15	5.1%	0.17	5.7%	0.19	6.4%	0.21	7.1%	0.23	7.8%
	Min	0.06	1.9%	0.07	2.2%	0.08	2.6%	0.10	3.2%	0.12	4.1%	0.15	4.9%
Sclera	Max	6.82	227.5%	7.41	247.1%	8.01	267.1%	8.69	289.7%	9.42	314.1%	10.19	339.5%
	Avg	0.60	20.1%	0.68	22.8%	0.77	25.6%	0.86	28.8%	0.97	32.2%	1.08	36.0%
	Min	0.11	3.8%	0.13	4.4%	0.16	5.5%	0.22	7.4%	0.27	9.0%	0.32	10.5%
Tumor	Max	6.75	225.0%	7.30	243.2%	7.88	262.7%	8.53	284.5%	9.24	308.0%	9.98	332.6%
	Avg	4.43	147.8%	4.68	155.9%	4.97	165.8%	5.25	175.0%	5.51	183.6%	5.75	191.6%
	Min	3.00	100.0%	3.00	100.0%	3.00	100.0%	3.00	100.0%	3.00	100.0%	3.00	100.0%

Figure 30A is an isodose curve of Se-75 used with a 14 mm diameter applicator with a collimator apex at 6.1 mm, collimator angle at 53.6°, target diameter at 11.0 mm, and target depth at 3.5 mm. The maximum percent dose was 20.6% to cornea, 23.5% to the posterior lens, 22.1% to the iris, 13.4% to the optic nerve, 13.4% to the bone, 224.1% to the sclera, and 203.0% to the tumor. The absorbed dose to each structure was 0.62 Gy, 0.70 Gy, 0.66 Gy, 0.40 Gy, 0.40 Gy, 6.72 Gy, and 6.09 Gy respectively.

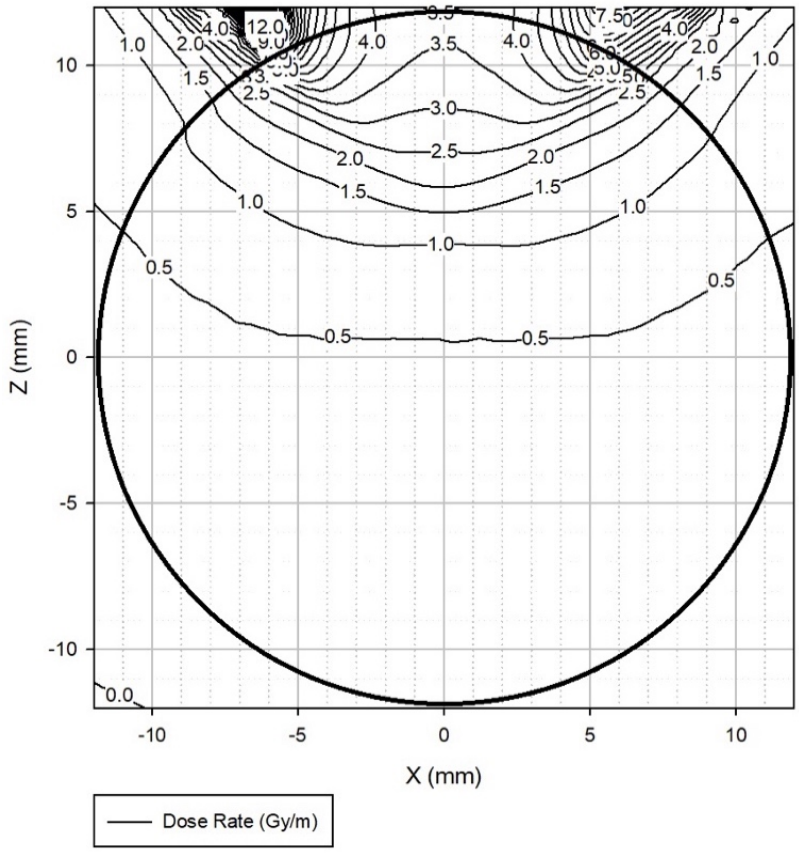

Figure 30A: Isodose curve of a 14 mm applicator containing Se-75. The prescription dose of 3 Gy/min was delivered to a 3.5 mm depth in the eye.

Figure 30B is an isodose curve of Se-75 used with a 14 mm diameter applicator with a collimator apex at 4.8 mm, collimator angle at 47.6°, target diameter at 11.4 mm, and target depth at 4.0 mm. The maximum percent dose was 22.4% to cornea, 25.9% to the posterior lens, 24.3% to the iris, 15.0% to the optic nerve, 14.1% to the bone, 243.8% to the sclera, and 231.4% to the tumor. The absorbed dose to each structure was 0.67 Gy, 0.78 Gy, 0.73 Gy, 0.45 Gy, 0.42 Gy, 7.31 Gy, and 6.94 Gy respectively.

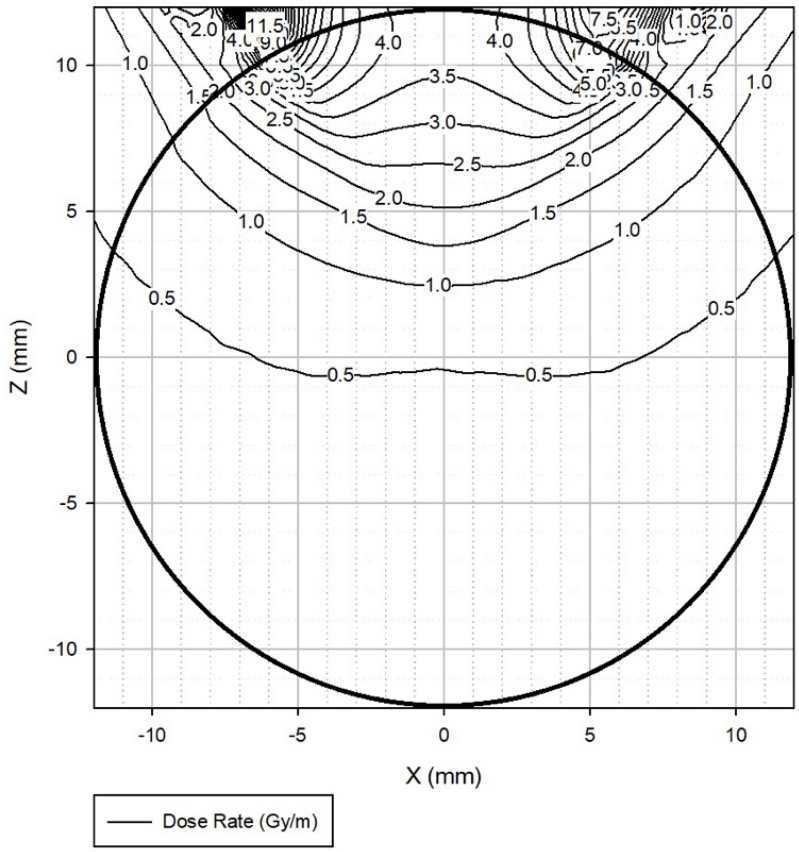

Figure 30B: Isodose curve of a 14 mm applicator containing Se-75. The prescription dose of 3 Gy/min was delivered to a 4.0 mm depth in the eye.

Figure 30C is an isodose curve of Se-75 used with a 14 mm diameter applicator with a collimator apex at 3.4 mm, collimator angle at 41.9°, target diameter at 11.7 mm, and target depth at 4.5 mm. The maximum percent dose was 24.7% to cornea, 28.9% to the posterior lens, 26.7% to the iris, 16.8% to the optic nerve, 15.0% to the bone, 263.3% to the sclera, and 260.6% to the tumor. The absorbed dose to each structure was 0.74 Gy, 0.87 Gy, 0.80 Gy, 0.50 Gy, 0.45 Gy, 7.90 Gy, and 7.82 Gy respectively.

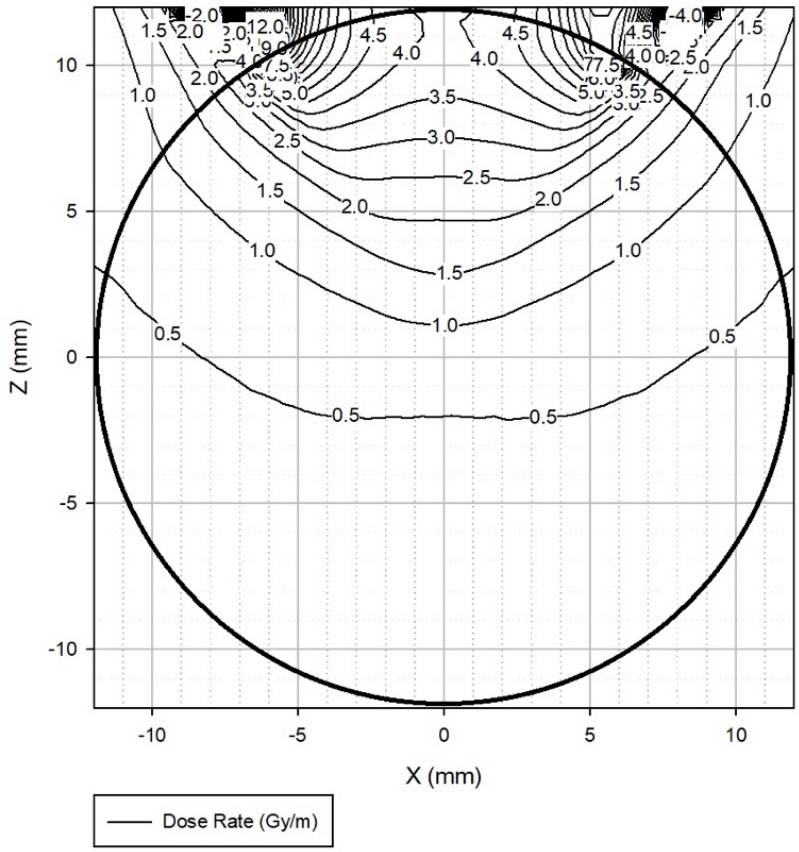

Figure 30C: Isodose curve of a 14 mm applicator containing Se-75. The prescription dose of 3 Gy/min was delivered to a 4.5 mm depth in the eye.

Figure 30D is an isodose curve of Se-75 used with a 14 mm diameter applicator with a collimator apex at 1.6 mm, collimator angle at 36.5°, target diameter at 12.0 mm, and target depth at 5.0 mm. The maximum percent dose was 27.1% to cornea, 32.1% to the posterior lens, 29.3% to the iris, 18.8% to the optic nerve, 16.0% to the bone, 280.5% to the sclera, and 279.0% to the tumor. The absorbed dose to each structure was 0.81 Gy, 0.96 Gy, 0.88 Gy, 0.56 Gy, 0.48 Gy, 8.41 Gy, and 8.37 Gy respectively.

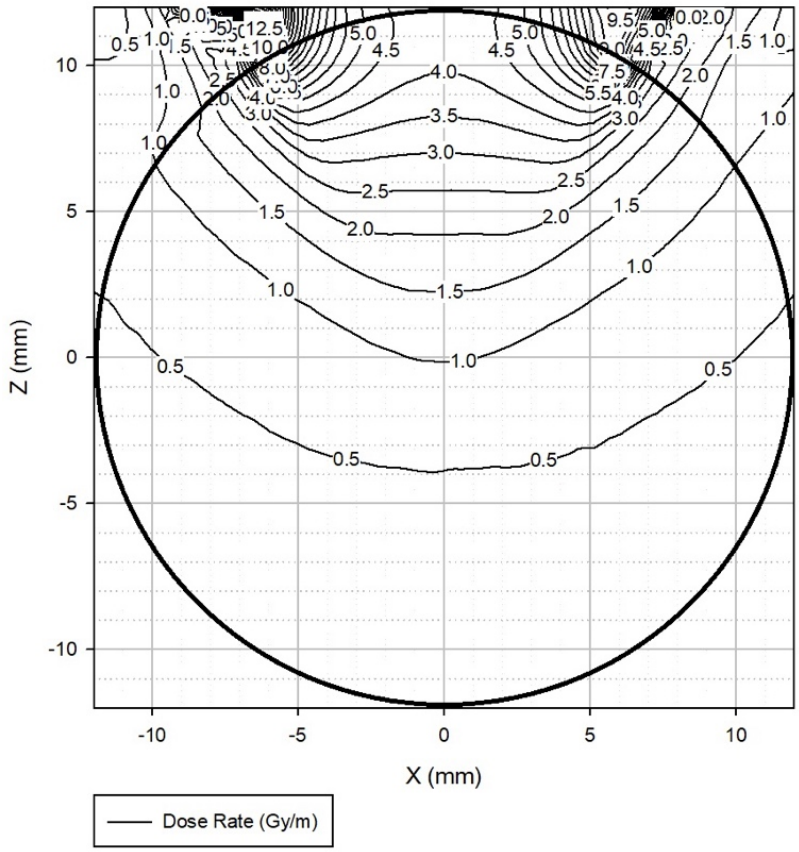

Figure 30D: Isodose curve of a 14 mm applicator containing Se-75. The prescription dose of 3 Gy/min was delivered to a 5.0 mm depth in the eye.

Figure 30E is an isodose curve of Se-75 used with a 14 mm diameter applicator with a collimator apex at -0.5 mm, collimator angle at 31.4°, target diameter at 12.3 mm, and target depth at 5.5 mm. The maximum percent dose was 29.7% to cornea, 35.8% to the posterior lens, 32.3% to the iris, 21.0% to the optic nerve, 17.1% to the bone, 302.2% to the sclera, and 299.3% to the tumor. The absorbed dose to each structure was 0.89 Gy, 1.07 Gy, 0.97 Gy, 0.63 Gy, 0.51 Gy, 9.06 Gy, and 8.98 Gy respectively.

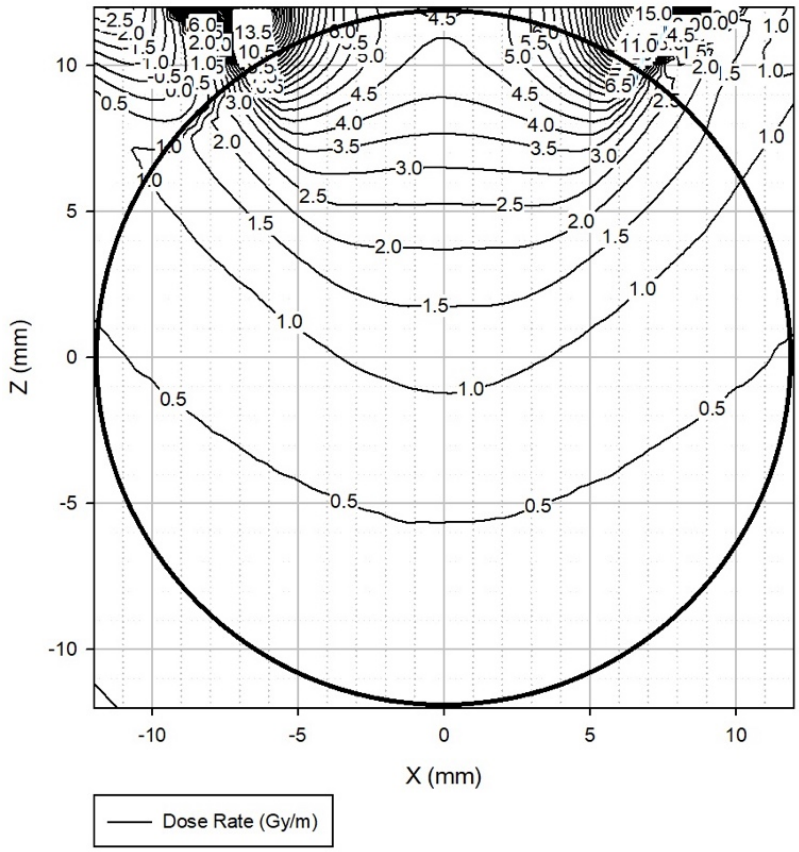

Figure 30E: Isodose curve of a 14 mm applicator containing Se-75. The prescription dose of 3 Gy/min was delivered to a 5.5 mm depth in the eye.

Figure 30F is an isodose curve of Se-75 used with a 14 mm diameter applicator with a collimator apex at -3.1 mm, collimator angle at 26.5°, target diameter at 12.5 mm, and target depth at 6.0 mm. The maximum percent dose was 32.4% to cornea, 40.4% to the posterior lens, 35.4% to the iris, 23.2% to the optic nerve, 18.3% to the bone, 324.0% to the sclera, and 320.6% to the tumor. The absorbed dose to each structure was 0.97 Gy, 1.21 Gy, 1.06 Gy, 0.70 Gy, 0.55 Gy, 9.72 Gy, and 9.62 Gy respectively.

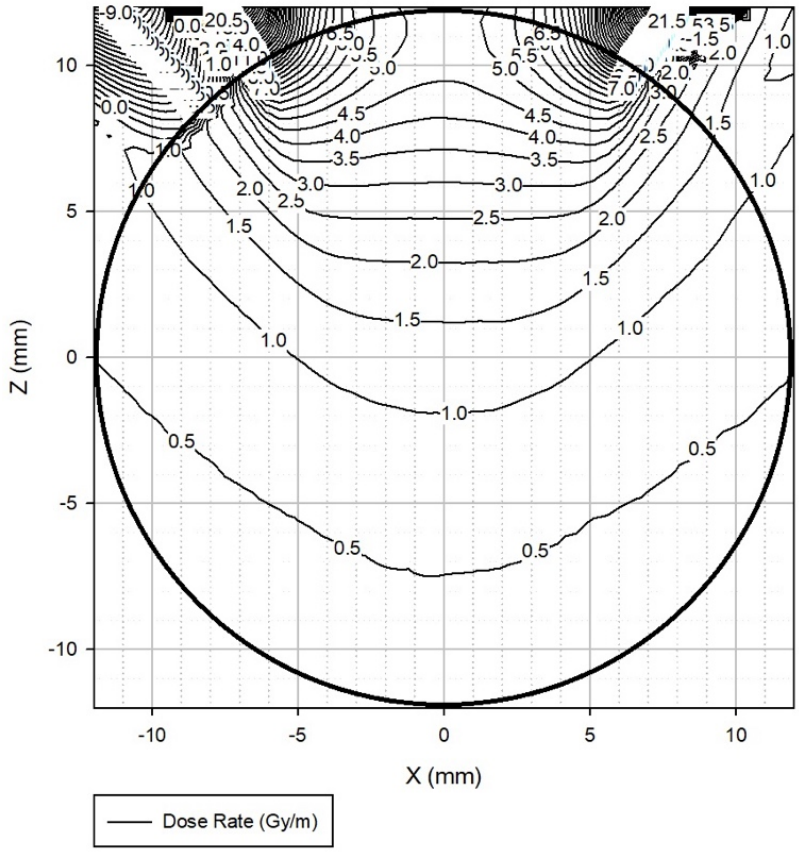

Figure 30F: Isodose curve of a 14 mm applicator containing Se-75. The prescription dose of 3 Gy/min was delivered to a 6.0 mm depth in the eye.

Figure 30G is an isodose curve of Se-75 used with a 14 mm diameter applicator with a collimator apex at -6.5 mm, collimator angle at 22.0°, target diameter at 12.9 mm, and target depth at 6.5 mm. The maximum percent dose was 35.4% to cornea, 45.8% to the posterior lens, 39.1% to the iris, 25.8% to the optic nerve, 19.7% to the bone, 348.7% to the sclera, and 344.9% to the tumor. The absorbed dose to each structure was 1.06 Gy, 1.37 Gy, 1.17 Gy, 0.77 Gy, 0.59 Gy, 10.46 Gy, and 10.35 Gy respectively.

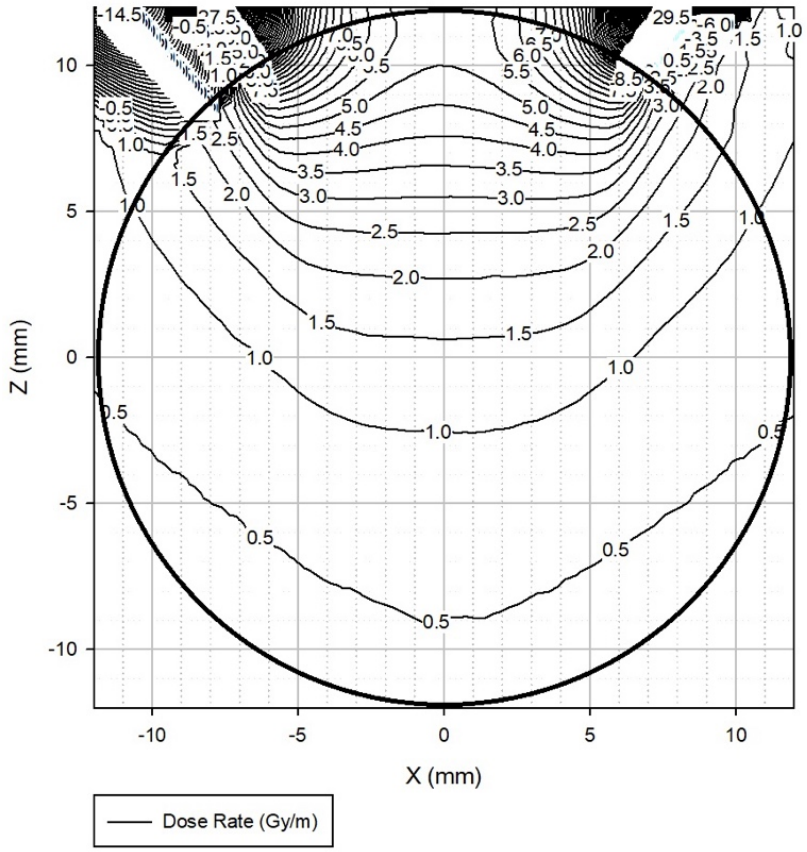

Figure 30G: Isodose curve of a 14 mm applicator containing Se-75. The prescription dose of 3 Gy/min was delivered to a 6.5 mm depth in the eye.

Table 12: Dose rates to ocular structures from a Se-75 14 mm applicator

Target Depth		3.5		4.0		4.5		5.0		5.5		6.0		6.5	
Simulation	Geometry	D	D (%)	D	D (%)	D	D (%)	D	D (%)	D	D (%)	D	D (%)	D	D (%)
Cornea	Max	0.62	20.6%	0.67	22.4%	0.74	24.7%	0.81	27.1%	0.89	29.7%	0.97	32.4%	1.06	35.4%
	Avg	0.31	10.4%	0.35	11.6%	0.39	12.9%	0.43	14.3%	0.47	15.8%	0.52	17.4%	0.58	19.3%
	Min	0.17	5.8%	0.21	6.9%	0.24	8.0%	0.27	9.1%	0.31	10.3%	0.34	11.5%	0.39	13.0%
Posterior Lens	Max	0.70	23.5%	0.78	25.9%	0.87	28.9%	0.96	32.1%	1.07	35.8%	1.21	40.4%	1.37	45.8%
	Avg	0.40	13.2%	0.45	15.1%	0.52	17.2%	0.58	19.3%	0.65	21.7%	0.73	24.4%	0.82	27.5%
	Min	0.21	6.9%	0.25	8.3%	0.29	9.8%	0.34	11.2%	0.38	12.8%	0.43	14.5%	0.49	16.4%
Iris	Max	0.66	22.1%	0.73	24.3%	0.80	26.7%	0.88	29.3%	0.97	32.3%	1.06	35.4%	1.17	39.1%
	Avg	0.36	11.8%	0.40	13.3%	0.45	14.9%	0.50	16.6%	0.55	18.4%	0.61	20.4%	0.68	22.7%
	Min	0.18	6.0%	0.21	7.1%	0.25	8.3%	0.28	9.5%	0.32	10.7%	0.36	12.0%	0.41	13.5%
Optic Nerve	Max	0.40	13.4%	0.45	15.0%	0.50	16.8%	0.56	18.8%	0.63	21.0%	0.70	23.2%	0.77	25.8%
	Avg	0.30	9.9%	0.33	11.0%	0.37	12.3%	0.41	13.7%	0.45	15.1%	0.50	16.8%	0.56	18.6%
	Min	0.22	7.4%	0.25	8.2%	0.27	9.1%	0.30	10.1%	0.33	11.2%	0.37	12.3%	0.41	13.5%
Bone	Max	0.40	13.4%	0.42	14.1%	0.45	15.0%	0.48	16.0%	0.51	17.1%	0.55	18.3%	0.59	19.7%
	Avg	0.15	5.0%	0.16	5.4%	0.18	6.0%	0.20	6.6%	0.22	7.2%	0.24	7.9%	0.26	8.7%
	Min	0.06	2.2%	0.07	2.3%	0.08	2.6%	0.09	3.0%	0.11	3.5%	0.13	4.3%	0.16	5.3%
Sclera	Max	6.72	224.1%	7.31	243.8%	7.90	263.3%	8.41	280.5%	9.06	302.2%	9.72	324.0%	10.46	348.7%
	Avg	0.68	22.7%	0.76	25.3%	0.84	28.1%	0.94	31.2%	1.04	34.6%	1.15	38.3%	1.28	42.5%
	Min	0.13	4.3%	0.14	4.6%	0.15	5.2%	0.18	6.0%	0.23	7.7%	0.30	10.0%	0.35	11.6%
Tumor	Max	6.09	203.0%	6.94	231.4%	7.82	260.6%	8.37	279.0%	8.98	299.3%	9.62	320.6%	10.35	344.9%
	Avg	4.25	141.7%	4.43	147.4%	4.67	155.8%	4.86	162.1%	5.08	169.5%	5.30	176.6%	5.44	181.2%
	Min	3.00	100.0%	3.00	100.0%	3.00	100.0%	3.00	100.0%	3.00	100.0%	3.00	100.0%	3.00	100.0%

Figure 31A is an isodose curve of Se-75 used with a 16 mm diameter applicator with a collimator apex at 5.6 mm, collimator angle at 56.4°, target diameter at 12.3 mm, and target depth at 4.0 mm. The maximum percent dose was 26.0% to cornea, 29.4% to the posterior lens, 28.2% to the iris, 16.5% to the optic nerve, 14.0% to the bone, 240.1% to the sclera, and 228.1% to the tumor. The absorbed dose to each structure was 0.78 Gy, 0.88 Gy, 0.85 Gy, 0.49 Gy, 0.42 Gy, 7.20 Gy, and 6.84 Gy respectively.

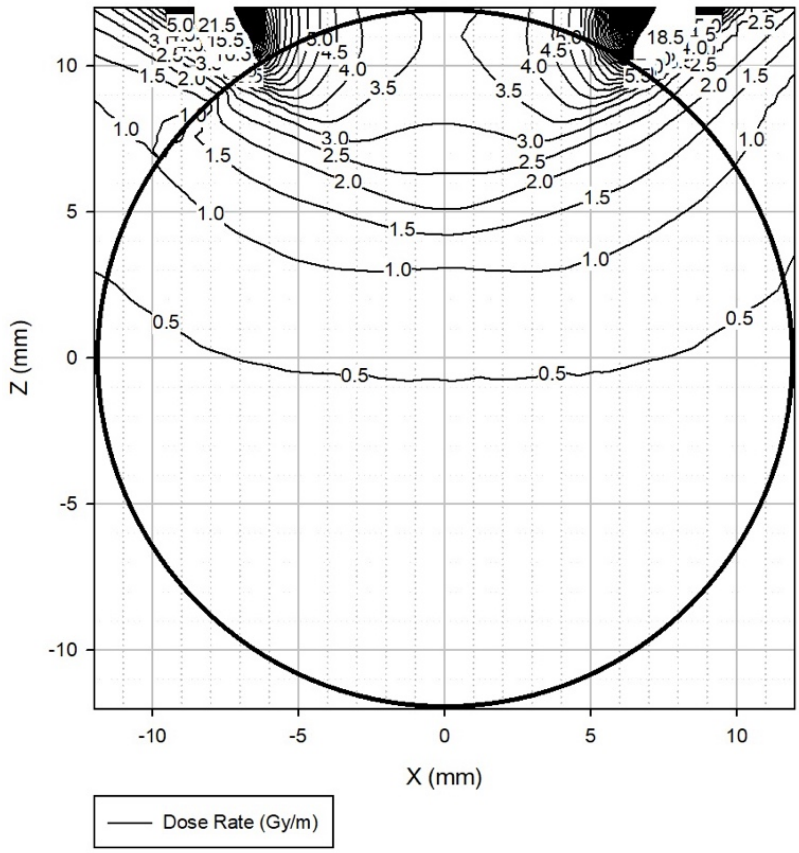

Figure 31A: Isodose curve of a 16 mm applicator containing Se-75. The prescription dose of 3 Gy/min was delivered to a 4.0 mm depth in the eye.

Figure 31B is an isodose curve of Se-75 used with a 16 mm diameter applicator with a collimator apex at 4.4 mm, collimator angle at 50.9°, target diameter at 12.7 mm, and target depth at 4.5 mm. The maximum percent dose was 28.1% to cornea, 32.2% to the posterior lens, 30.4% to the iris, 18.3% to the optic nerve, 14.6% to the bone, 260.1% to the sclera, and 237.9% to the tumor. The absorbed dose to each structure was 0.84 Gy, 0.97 Gy, 0.91 Gy, 0.55 Gy, 0.44 Gy, 7.80 Gy, and 7.14 Gy respectively.

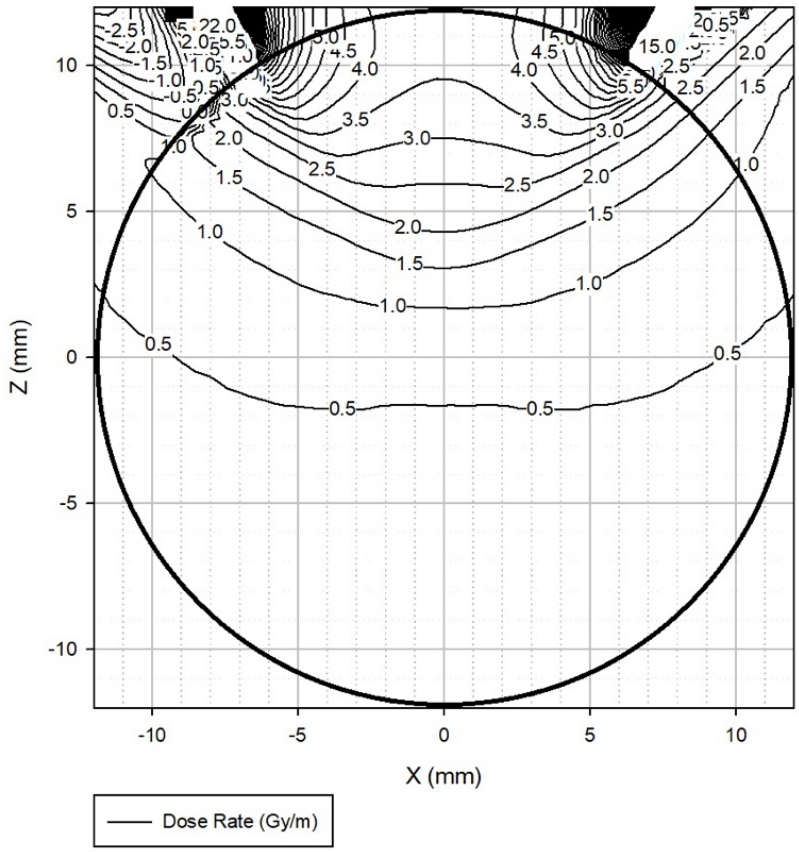

Figure 31B: Isodose curve of a 16 mm applicator containing Se-75. The prescription dose of 3 Gy/min was delivered to a 4.5 mm depth in the eye.

Figure 31C is an isodose curve of Se-75 used with a 16 mm diameter applicator with a collimator apex at 3.1 mm, collimator angle at 45.6°, target diameter at 13.0 mm, and target depth at 5.0 mm. The maximum percent dose was 30.5% to cornea, 35.7% to the posterior lens, 33.3% to the iris, 20.1% to the optic nerve, 15.4% to the bone, 278.0% to the sclera, and 267.3% to the tumor. The absorbed dose to each structure was 0.92 Gy, 1.07 Gy, 1.00 Gy, 0.60 Gy, 0.46 Gy, 8.34 Gy, and 8.02 Gy respectively.

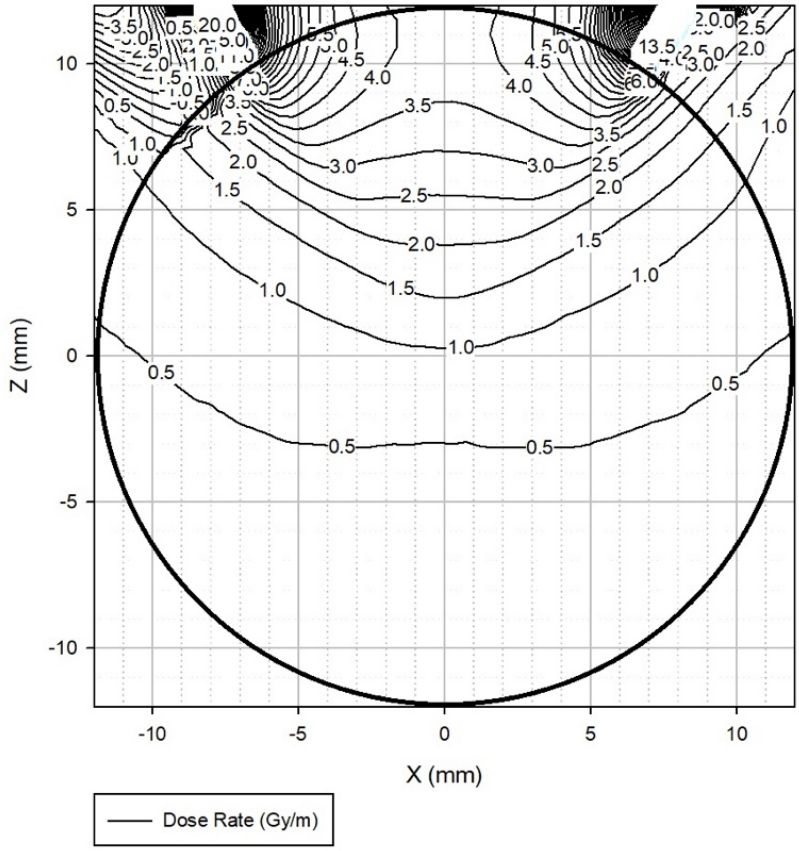

Figure 31C: Isodose curve of a 16 mm applicator containing Se-75. The prescription dose of 3 Gy/min was delivered to a 5.0 mm depth in the eye.

Figure 31D is an isodose curve of Se-75 used with a 16 mm diameter applicator with a collimator apex at 1.5 mm, collimator angle at 40.5°, target diameter at 13.3 mm, and target depth at 5.5 mm. The maximum percent dose was 33.3% to cornea, 39.3% to the posterior lens, 36.3% to the iris, 22.3% to the optic nerve, 16.3% to the bone, 294.0% to the sclera, and 285.9% to the tumor. The absorbed dose to each structure was 1.00 Gy, 1.18 Gy, 1.09 Gy, 0.67 Gy, 0.49 Gy, 8.82 Gy, and 8.58 Gy respectively.

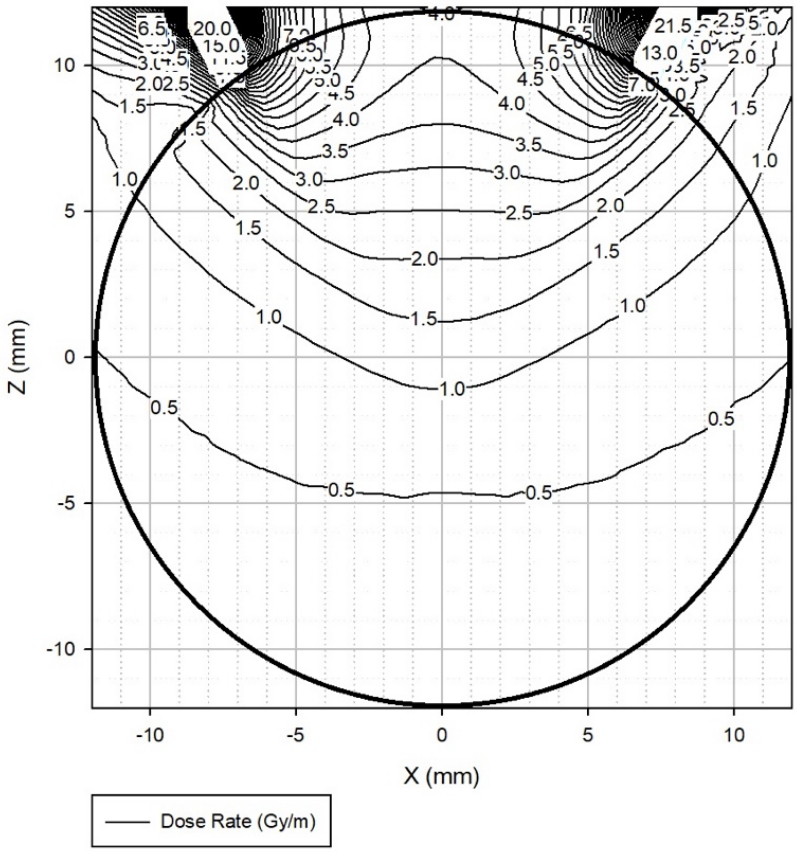

Figure 31D: Isodose curve of a 16 mm applicator containing Se-75. The prescription dose of 3 Gy/min was delivered to a 5.5 mm depth in the eye.

Figure 31E is an isodose curve of Se-75 used with a 16 mm diameter applicator with a collimator apex at -0.3 mm, collimator angle at 35.6°, target diameter at 13.6 mm, and target depth at 6.0 mm. The maximum percent dose was 36.1% to cornea, 43.2% to the posterior lens, 39.6% to the iris, 24.4% to the optic nerve, 17.3% to the bone, 312.7% to the sclera, and 303.1% to the tumor. The absorbed dose to each structure was 1.08 Gy, 1.30 Gy, 1.19 Gy, 0.73 Gy, 0.52 Gy, 9.38 Gy, and 9.09 Gy respectively.

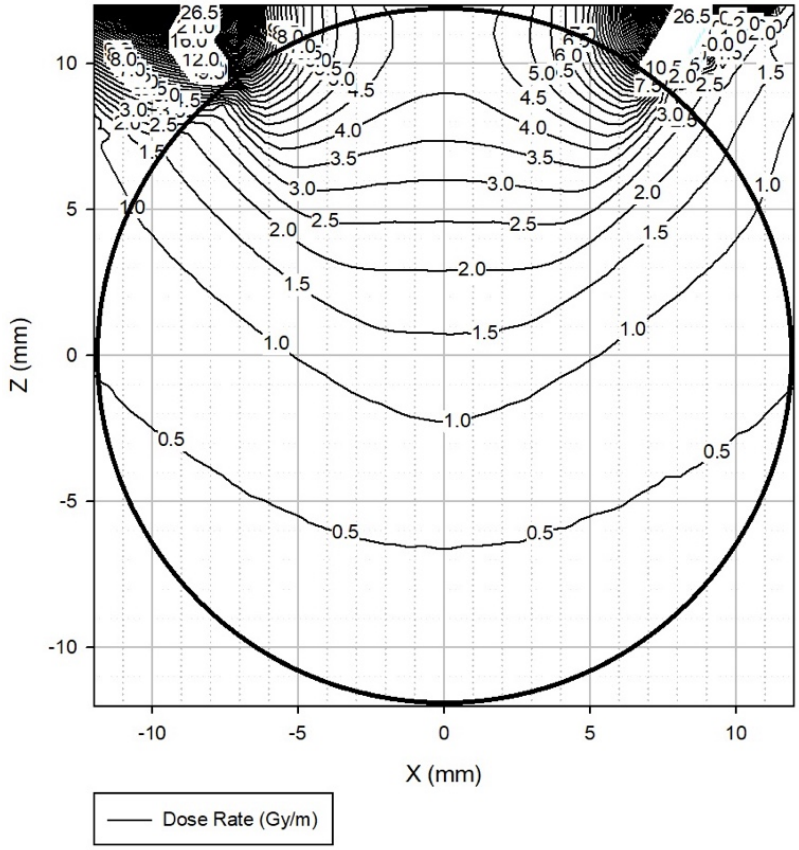

Figure 31E: Isodose curve of a 16 mm applicator containing Se-75. The prescription dose of 3 Gy/min was delivered to a 6.0 mm depth in the eye.

Figure 31F is an isodose curve of Se-75 used with a 16 mm diameter applicator with a collimator apex at -2.4 mm, collimator angle at 31.0°, target diameter at 13.8 mm, and target depth at 6.5 mm. The maximum percent dose was 39.4% to cornea, 48.3% to the posterior lens, 43.1% to the iris, 27.0% to the optic nerve, 18.4% to the bone, 333.6% to the sclera, and 323.1% to the tumor. The absorbed dose to each structure was 1.18 Gy, 1.45 Gy, 1.29 Gy, 0.81 Gy, 0.55 Gy, 10.01 Gy, and 9.69 Gy respectively.

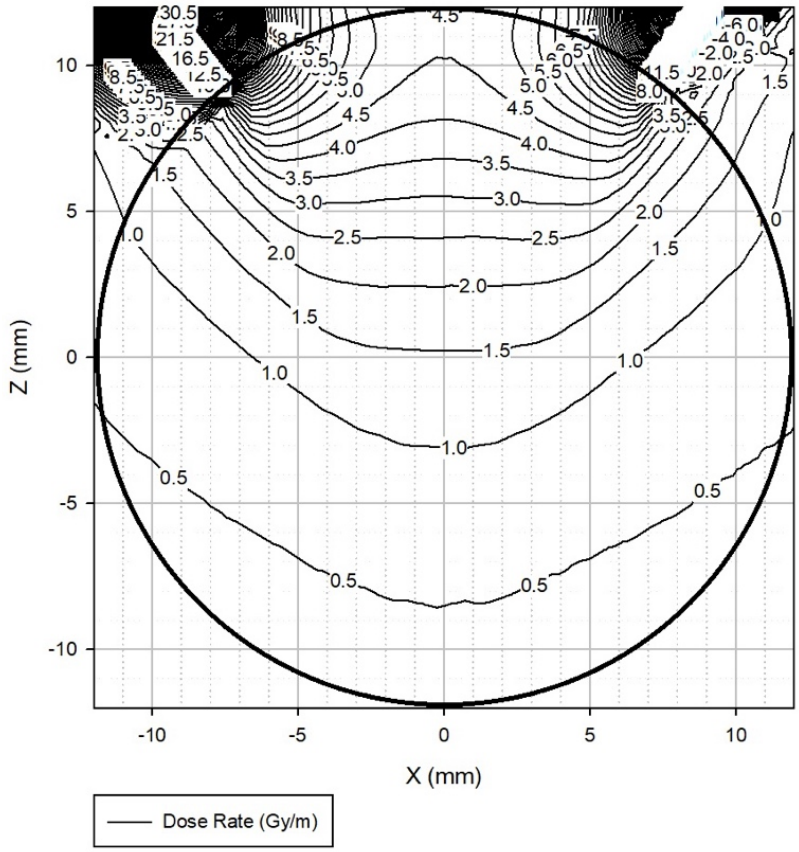

Figure 31F: Isodose curve of a 16 mm applicator containing Se-75. The prescription dose of 3 Gy/min was delivered to a 6.5 mm depth in the eye.

Figure 31G is an isodose curve of Se-75 used with a 16 mm diameter applicator with a collimator apex at -5.1 mm, collimator angle at 26.6°, target diameter at 14.1 mm, and target depth at 7.0 mm. The maximum percent dose was 42.7% to cornea, 54.2% to the posterior lens, 47.0% to the iris, 29.6% to the optic nerve, 19.6% to the bone, 354.7% to the sclera, and 343.2% to the tumor. The absorbed dose to each structure was 1.28 Gy, 1.63 Gy, 1.41 Gy, 0.89 Gy, 0.59 Gy, 10.64 Gy, and 10.30 Gy respectively.

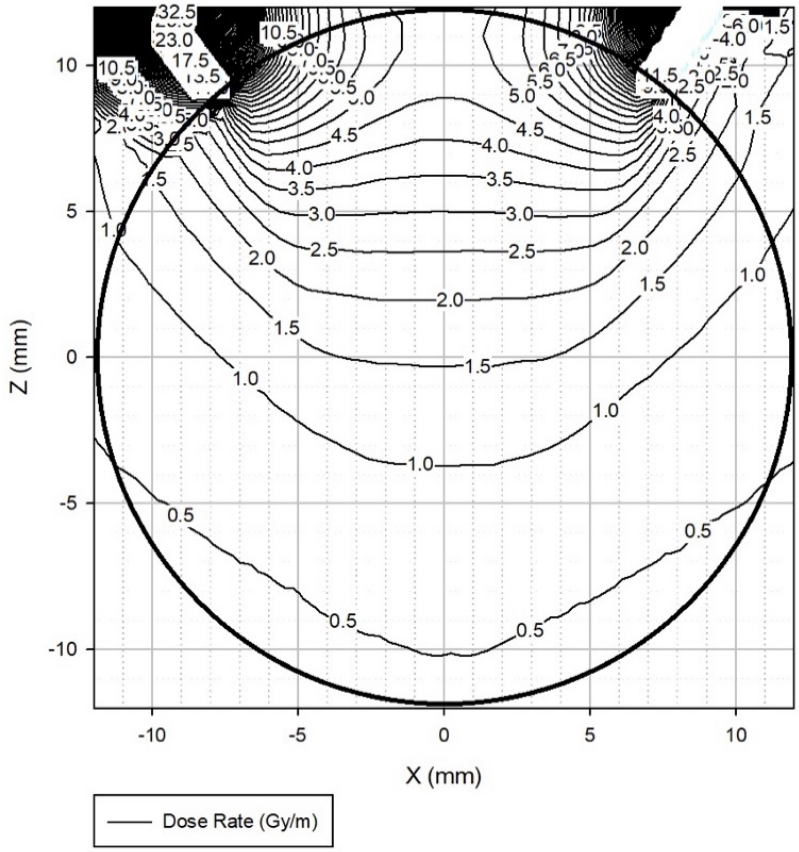

Figure 31G: Isodose curve of a 16 mm applicator containing Se-75. The prescription dose of 3 Gy/min was delivered to a 7.0 mm depth in the eye.

Figure 31H is an isodose curve of Se-75 used with a 16 mm diameter applicator with a collimator apex at -8.5 mm, collimator angle at 22.5°, target diameter at 14.3 mm, and target depth at 7.5 mm. The maximum percent dose was 46.3% to cornea, 61.2% to the posterior lens, 51.3% to the iris, 32.6% to the optic nerve, 20.8% to the bone, 377.3% to the sclera, and 365.1% to the tumor. The absorbed dose to each structure was 1.39 Gy, 1.83 Gy, 1.54 Gy, 0.98 Gy, 0.62 Gy, 11.32 Gy, and 10.95 Gy respectively.

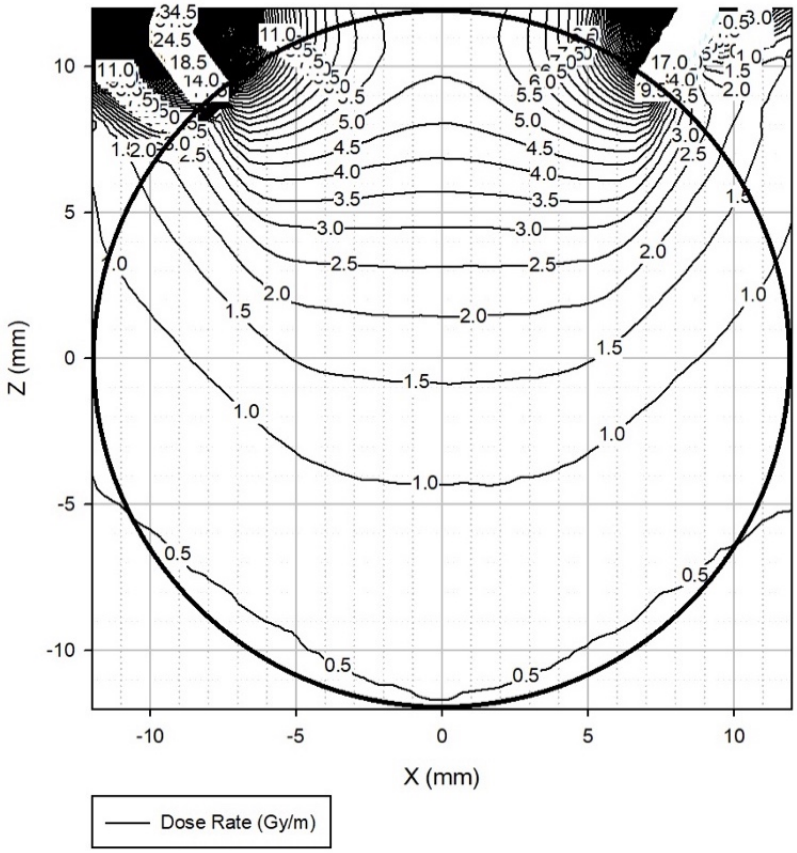

Figure 31H: Isodose curve of a 16 mm applicator containing Se-75. The prescription dose of 3 Gy/min was delivered to a 7.5 mm depth in the eye.

Table 13: Dose rates to ocular structures from a Se-75 16 mm applicator

Target Depth		4.0		4.5		5.0		5.5		6.0		6.5		7.0		7.5	
Simulation	Geometry	D	D (%)	D	D (%)	D	D (%)	D	D (%)	D	D (%)	D	D (%)	D	D (%)	D	D (%)
Cornea	Max	0.78	26.0%	0.84	28.1%	0.92	30.5%	1.00	33.3%	1.08	36.1%	1.18	39.4%	1.28	42.7%	1.39	46.3%
	Avg	0.38	12.8%	0.42	14.1%	0.47	15.6%	0.51	17.1%	0.56	18.7%	0.62	20.5%	0.67	22.4%	0.73	24.5%
	Min	0.21	7.0%	0.25	8.3%	0.29	9.5%	0.32	10.7%	0.36	12.0%	0.40	13.3%	0.44	14.7%	0.49	16.3%
Posterior Lens	Max	0.88	29.4%	0.97	32.2%	1.07	35.7%	1.18	39.3%	1.30	43.2%	1.45	48.3%	1.63	54.2%	1.83	61.2%
	Avg	0.49	16.2%	0.55	18.3%	0.62	20.7%	0.69	23.0%	0.77	25.6%	0.86	28.6%	0.96	31.9%	1.07	35.6%
	Min	0.26	8.5%	0.30	10.0%	0.35	11.7%	0.40	13.4%	0.45	15.0%	0.50	16.7%	0.56	18.8%	0.63	20.9%
Iris	Max	0.85	28.2%	0.91	30.4%	1.00	33.3%	1.09	36.3%	1.19	39.6%	1.29	43.1%	1.41	47.0%	1.54	51.3%
	Avg	0.44	14.6%	0.49	16.3%	0.54	18.1%	0.60	19.9%	0.65	21.8%	0.72	24.1%	0.79	26.4%	0.87	29.0%
	Min	0.21	7.1%	0.25	8.9%	0.30	9.9%	0.33	11.1%	0.37	12.4%	0.41	13.8%	0.46	15.2%	0.51	16.9%
Optic Nerve	Max	0.49	16.5%	0.55	18.3%	0.60	20.1%	0.67	22.3%	0.73	24.4%	0.81	27.0%	0.89	29.6%	0.98	32.6%
	Avg	0.36	12.1%	0.40	13.3%	0.44	14.8%	0.49	16.2%	0.53	17.8%	0.58	19.5%	0.64	21.3%	0.70	23.3%
	Min	0.27	9.1%	0.30	10.0%	0.33	11.0%	0.36	12.0%	0.39	13.1%	0.43	14.3%	0.47	15.5%	0.51	16.9%
Bone	Max	0.42	14.0%	0.44	14.6%	0.46	15.4%	0.49	16.3%	0.52	17.3%	0.55	18.4%	0.59	19.6%	0.62	20.8%
	Avg	0.18	5.9%	0.19	6.4%	0.21	7.0%	0.23	7.6%	0.25	8.3%	0.27	9.0%	0.29	9.8%	0.32	10.6%
	Min	0.08	2.6%	0.08	2.8%	0.09	3.1%	0.10	3.4%	0.12	3.9%	0.14	4.6%	0.17	5.7%	0.20	6.7%
Sclera	Max	7.20	240.1%	7.80	260.1%	8.34	278.0%	8.82	294.0%	9.38	312.7%	10.01	333.6%	10.64	354.7%	11.32	377.3%
	Avg	0.85	28.4%	0.94	31.2%	1.03	34.4%	1.13	37.7%	1.24	41.4%	1.36	45.4%	1.49	49.8%	1.64	54.5%
	Min	0.16	5.3%	0.17	5.6%	0.19	6.2%	0.21	7.0%	0.25	8.5%	0.34	11.2%	0.39	13.1%	0.45	15.1%
Tumor	Max	6.84	228.1%	7.14	237.9%	8.02	267.3%	8.58	285.9%	9.09	303.1%	9.69	323.1%	10.30	343.2%	10.95	365.1%
	Avg	4.22	140.6%	4.36	145.3%	4.55	151.7%	4.72	157.4%	4.89	163.1%	5.10	169.9%	5.27	175.8%	5.46	182.1%
	Min	3.00	100.0%	3.00	100.0%	3.00	100.0%	3.00	100.0%	3.00	100.0%	3.00	100.0%	3.00	100.0%	3.00	100.0%

Figure 32A is an isodose curve of Se-75 used with an 18 mm diameter applicator with a collimator apex at 6.2 mm, collimator angle at 65.1°, target diameter at 13.3 mm, and target depth at 4.0 mm. The maximum percent dose was 31.0% to cornea, 33.5% to the posterior lens, 33.4% to the iris, 17.5% to the optic nerve, 15.8% to the bone, 237.0% to the sclera, and 230.6% to the tumor. The absorbed dose to each structure was 0.93 Gy, 1.01 Gy, 1.00 Gy, 0.53 Gy, 0.47 Gy, 7.11 Gy, and 6.92 Gy respectively.

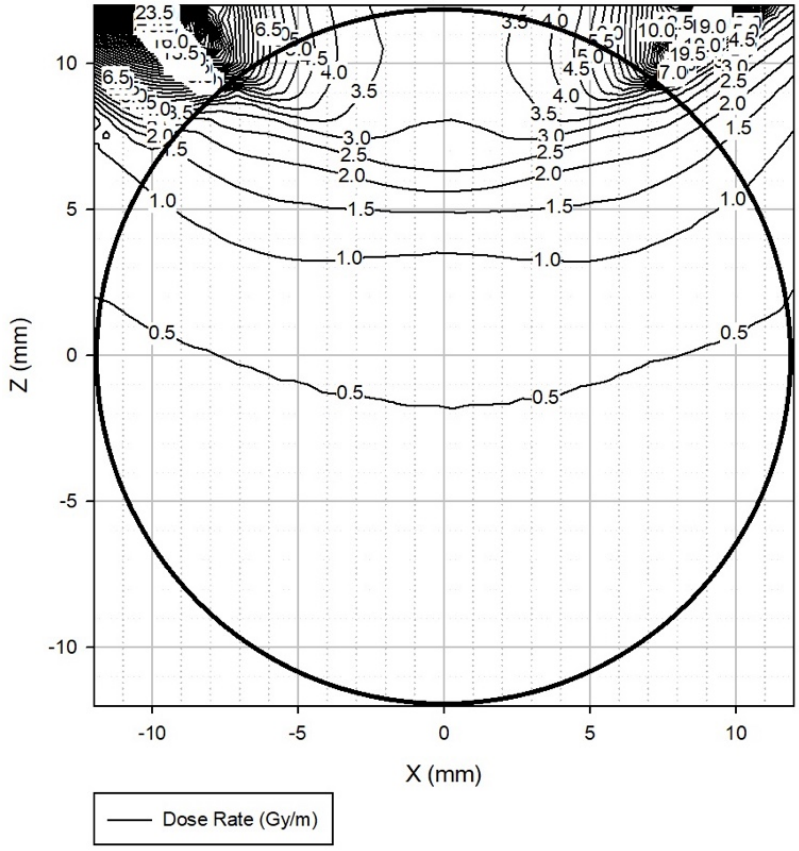

Figure 32A: Isodose curve of an 18 mm applicator containing Se-75. The prescription dose of 3 Gy/min was delivered to a 4.0 mm depth in the eye.

Figure 32B is an isodose curve of Se-75 used with an 18 mm diameter applicator with a collimator apex at 5.2 mm, collimator angle at 59.8°, target diameter at 13.6 mm, and target depth at 4.5 mm. The maximum percent dose was 33.3% to cornea, 36.5% to the posterior lens, 35.9% to the iris, 19.8% to the optic nerve, 16.2% to the bone, 253.5% to the sclera, and 238.3% to the tumor. The absorbed dose to each structure was 1.00 Gy, 1.10 Gy, 1.08 Gy, 0.59 Gy, 0.48 Gy, 7.61 Gy, and 7.15 Gy respectively.

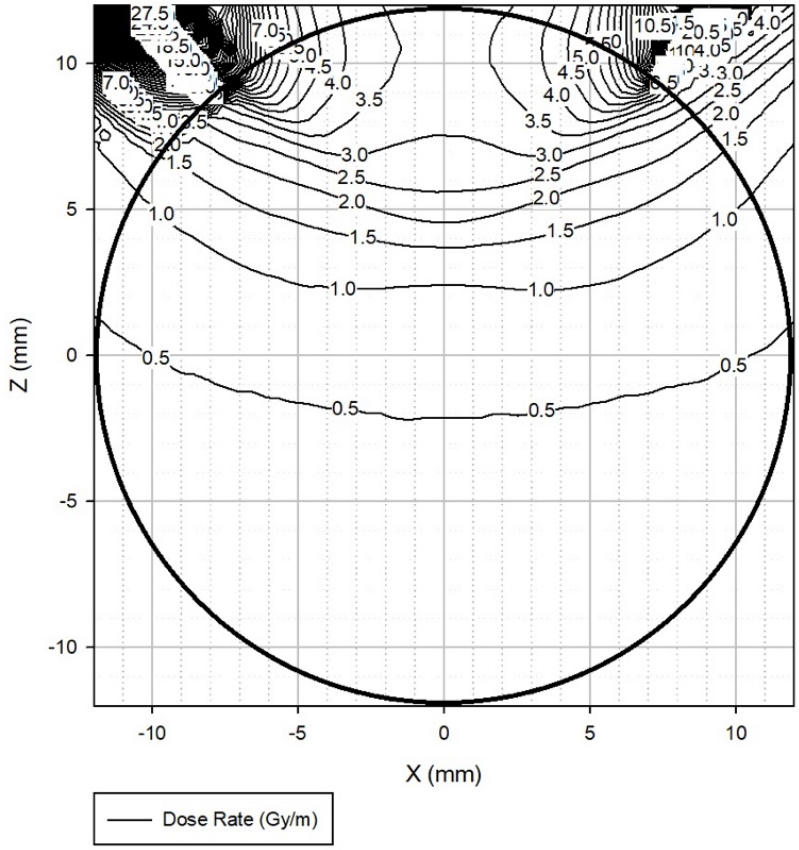

Figure 32B: Isodose curve of an 18 mm applicator containing Se-75. The prescription dose of 3 Gy/min was delivered to a 4.5 mm depth in the eye.

Figure 32C is an isodose curve of Se-75 used with an 18 mm diameter applicator with a collimator apex at 4.1 mm, collimator angle at 54.6°, target diameter at 14.0 mm, and target depth at 5.0 mm. The maximum percent dose was 35.8% to cornea, 40.1% to the posterior lens, 38.7% to the iris, 21.9% to the optic nerve, 16.8% to the bone, 277.6% to the sclera, and 248.1% to the tumor. The absorbed dose to each structure was 1.07 Gy, 1.20 Gy, 1.16 Gy, 0.66 Gy, 0.50 Gy, 8.33 Gy, and 7.44 Gy respectively.

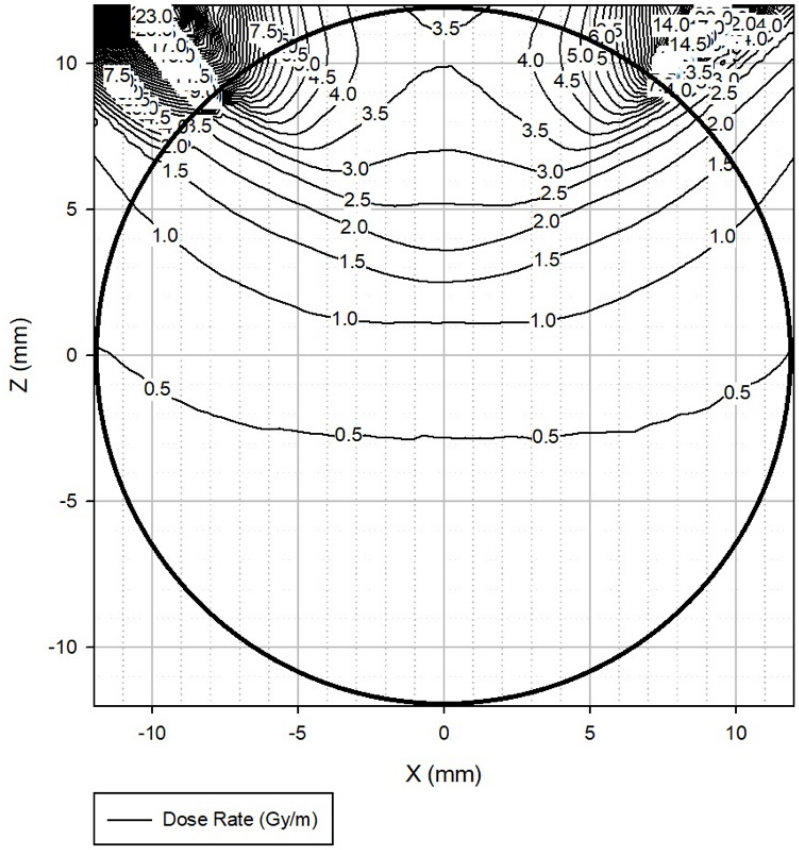

Figure 32C: Isodose curve of an 18 mm applicator containing Se-75. The prescription dose of 3 Gy/min was delivered to a 5.0 mm depth in the eye.

Figure 32D is an isodose curve of Se-75 used with an 18 mm diameter applicator with a collimator apex at 2.8 mm, collimator angle at 49.6°, target diameter at 14.3 mm, and target depth at 5.5 mm. The maximum percent dose was 38.5% to cornea, 43.7% to the posterior lens, 41.7% to the iris, 24.0% to the optic nerve, 17.6% to the bone, 292.0% to the sclera, and 259.6% to the tumor. The absorbed dose to each structure was 1.16 Gy, 1.31 Gy, 1.25 Gy, 0.72 Gy, 0.53 Gy, 8.76 Gy, and 7.79 Gy respectively.

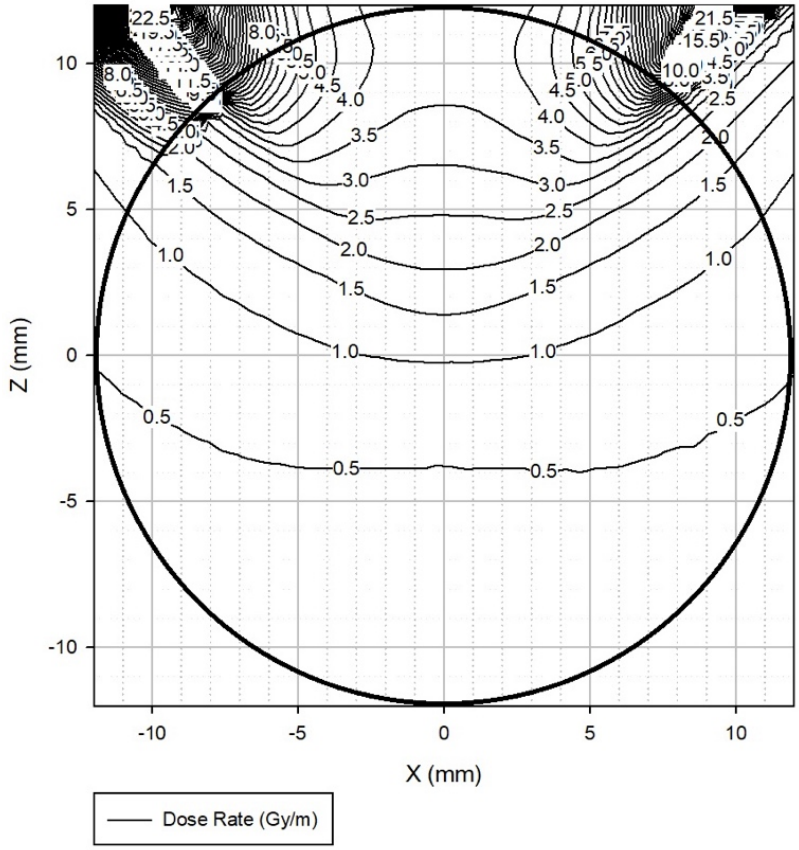

Figure 32D: Isodose curve of an 18 mm applicator containing Se-75. The prescription dose of 3 Gy/min was delivered to a 5.5 mm depth in the eye.

Figure 32E is an isodose curve of Se-75 used with an 18 mm diameter applicator with a collimator apex at 1.5 mm, collimator angle at 44.8°, target diameter at 14.5 mm, and target depth at 6.0 mm. The maximum percent dose was 41.3% to cornea, 47.5% to the posterior lens, 44.8% to the iris, 26.0% to the optic nerve, 18.3% to the bone, 306.4% to the sclera, and 270.8% to the tumor. The absorbed dose to each structure was 1.24 Gy, 1.43 Gy, 1.34 Gy, 0.78 Gy, 0.55 Gy, 9.19 Gy, and 8.12 Gy respectively.

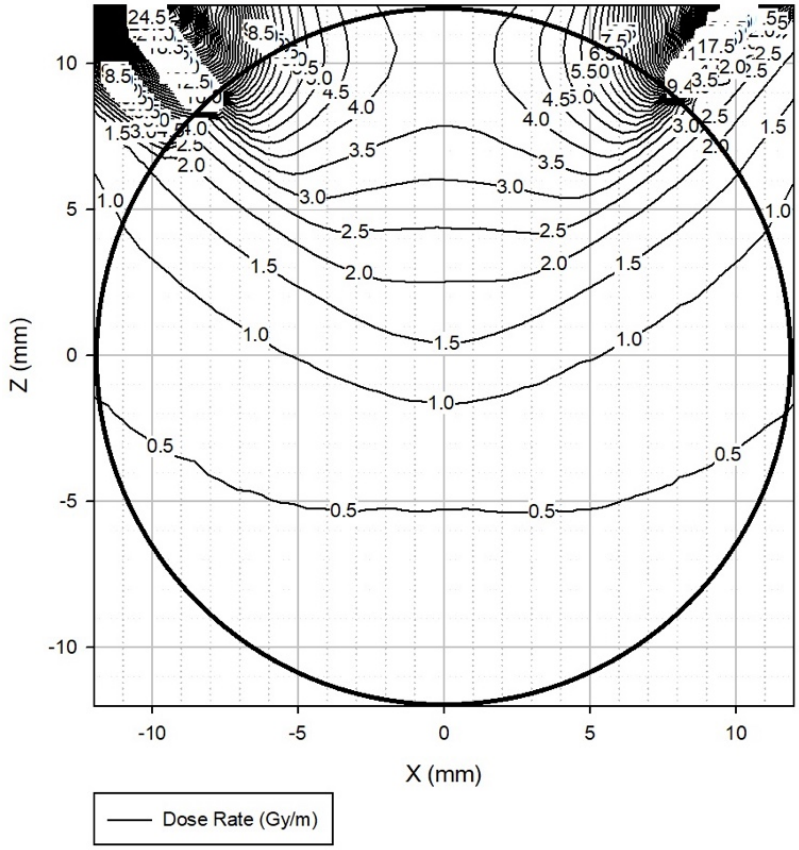

Figure 32E: Isodose curve of an 18 mm applicator containing Se-75. The prescription dose of 3 Gy/min was delivered to a 6.0 mm depth in the eye.

Figure 32F is an isodose curve of Se-75 used with an 18 mm diameter applicator with a collimator apex at -0.1 mm, collimator angle at 40.1°, target diameter at 14.8 mm, and target depth at 6.5 mm. The maximum percent dose was 44.3% to cornea, 51.9% to the posterior lens, 48.4% to the iris, 28.4% to the optic nerve, 19.3% to the bone, 323.2% to the sclera, and 283.9% to the tumor. The absorbed dose to each structure was 1.33 Gy, 1.56 Gy, 1.45 Gy, 0.85 Gy, 0.58 Gy, 9.70 Gy, and 8.52 Gy respectively.

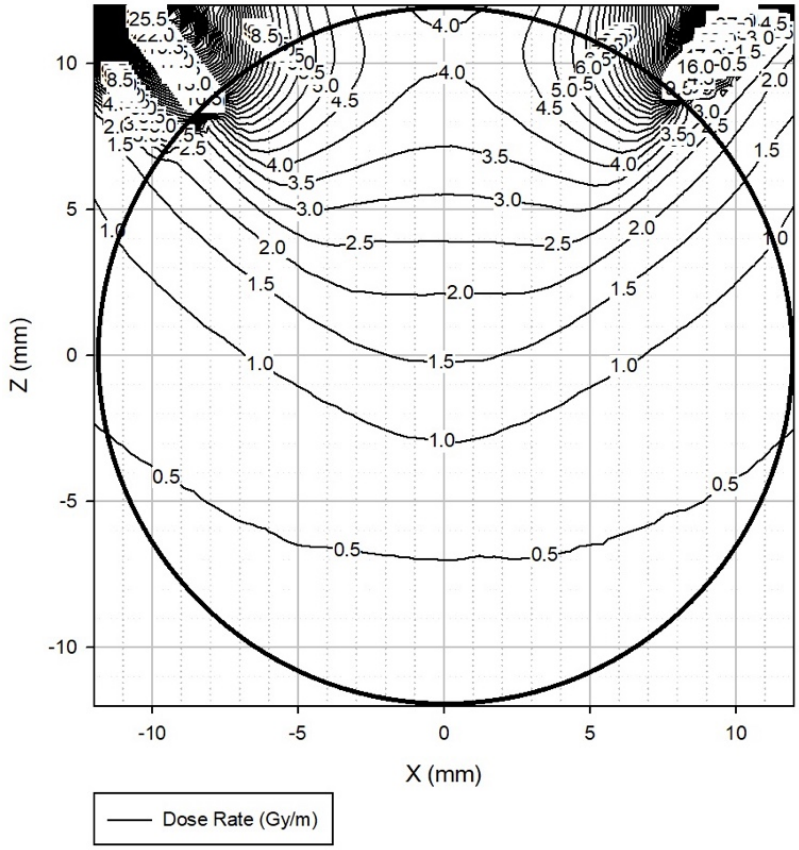

Figure 32F: Isodose curve of an 18 mm applicator containing Se-75. The prescription dose of 3 Gy/min was delivered to a 6.5 mm depth in the eye.

Figure 32G is an isodose curve of Se-75 used with an 18 mm diameter applicator with a collimator apex at -1.9 mm, collimator angle at 35.7°, target diameter at 15.0 mm, and target depth at 7.0 mm. The maximum percent dose was 48.2% to cornea, 57.4% to the posterior lens, 52.6% to the iris, 31.1% to the optic nerve, 20.4% to the bone, 342.6% to the sclera, and 300.4% to the tumor. The absorbed dose to each structure was 1.44 Gy, 1.72 Gy, 1.58 Gy, 0.93 Gy, 0.61 Gy, 10.28 Gy, and 9.01 Gy respectively.

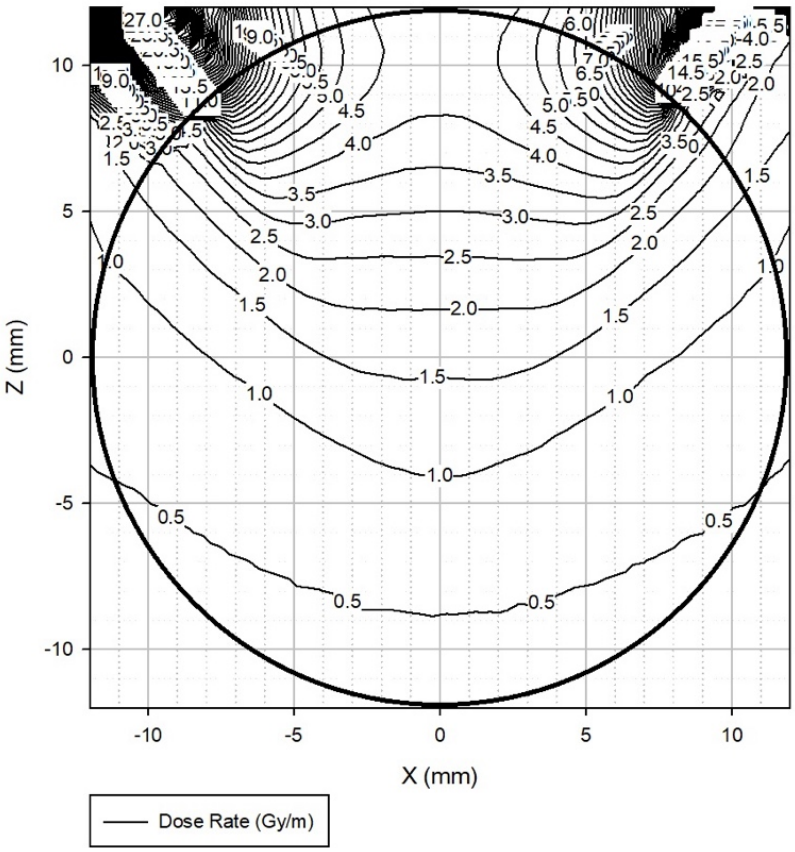

Figure 32G: Isodose curve of an 18 mm applicator containing Se-75. The prescription dose of 3 Gy/min was delivered to a 7.0 mm depth in the eye.

Figure 32H is an isodose curve of Se-75 used with an 18 mm diameter applicator with a collimator apex at -4.1 mm, collimator angle at 31.5°, target diameter at 15.2 mm, and target depth at 7.5 mm. The maximum percent dose was 51.9% to cornea, 64.1% to the posterior lens, 56.8% to the iris, 34.1% to the optic nerve, 21.6% to the bone, 362.1% to the sclera, and 317.2% to the tumor. The absorbed dose to each structure was 1.56 Gy, 1.92 Gy, 1.70 Gy, 1.02 Gy, 0.65 Gy, 10.86 Gy, and 9.52 Gy respectively.

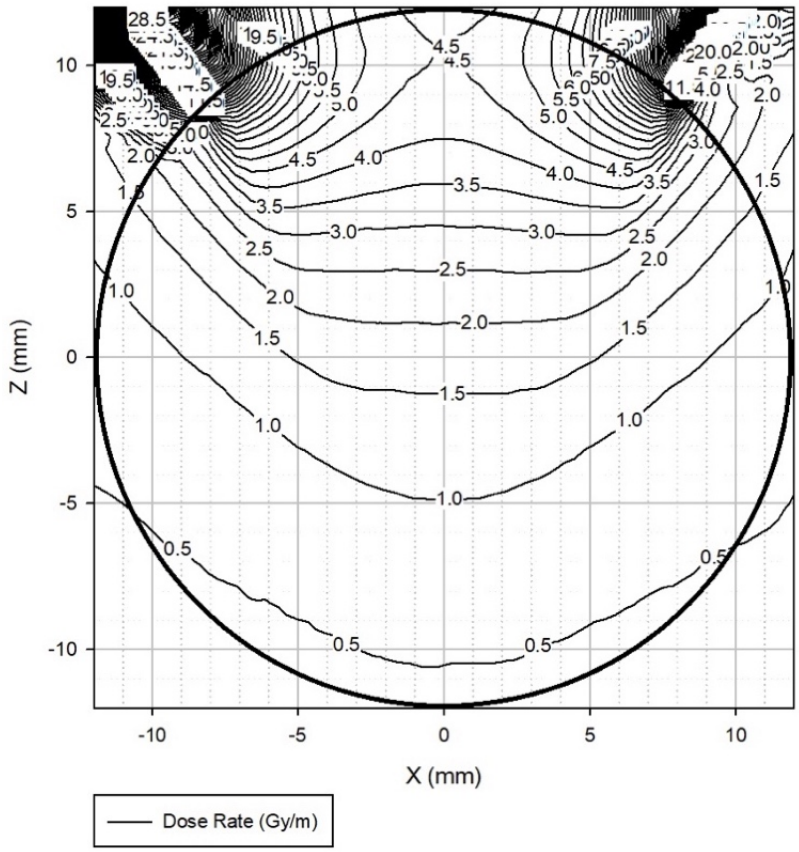

Figure 32H: Isodose curve of an 18 mm applicator containing Se-75. The prescription dose of 3 Gy/min was delivered to a 7.5 mm depth in the eye.

Figure 32I is an isodose curve of Se-75 used with an 18 mm diameter applicator with a collimator apex at -6.6 mm, collimator angle at 27.4°, target diameter at 15.5 mm, and target depth at 8.0 mm. The maximum percent dose was 56.1% to cornea, 72.5% to the posterior lens, 61.5% to the iris, 37.4% to the optic nerve, 22.8% to the bone, 382.3% to the sclera, and 334.9% to the tumor. The absorbed dose to each structure was 1.68 Gy, 2.17 Gy, 1.84 Gy, 1.12 Gy, 0.68 Gy, 11.47 Gy, and 10.05 Gy respectively.

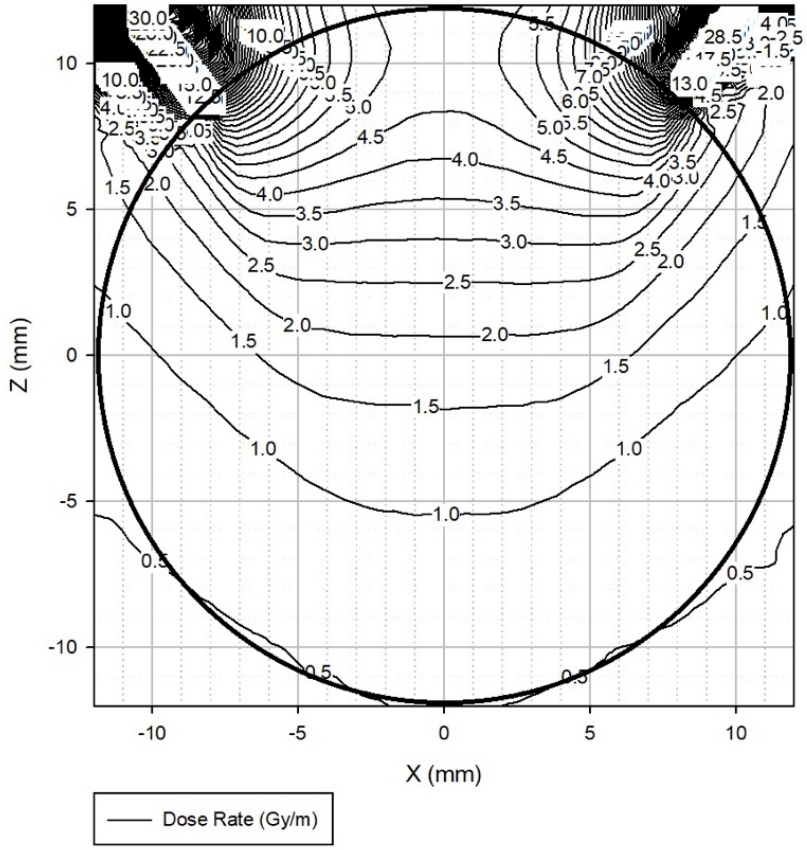

Figure 32I: Isodose curve of an 18 mm applicator containing Se-75. The prescription dose of 3 Gy/min was delivered to an 8.0 mm depth in the eye.

Table 14: Dose rates to ocular structures from a Se-75 18 mm applicator

Target Depth		4.0		4.5		5.0		5.5		6.0		6.5		7.0		7.5		8.0	
Simulation	Geometry	D	D (%)	D	D (%)	D	D (%)	D	D (%)	D	D (%)	D	D (%)	D	D (%)	D	D (%)	D	D (%)
Cornea	Max	0.93	31.0%	1.00	33.3%	1.07	35.8%	1.16	38.5%	1.24	41.3%	1.33	44.3%	1.44	48.2%	1.56	51.9%	1.68	56.1%
	Avg	0.42	14.1%	0.47	15.6%	0.51	17.2%	0.56	18.7%	0.61	20.3%	0.66	212.0%	0.72	23.9%	0.78	26.0%	0.85	28.2%
	Min	0.23	7.8%	0.25	8.4%	0.29	9.8%	0.34	11.2%	0.37	12.4%	0.41	13.7%	0.45	15.1%	0.50	16.5%	0.55	18.3%
Posterior Lens	Max	1.01	33.5%	1.10	36.5%	1.20	40.1%	1.31	43.7%	1.43	47.5%	1.56	51.9%	1.72	57.4%	1.92	64.1%	2.17	72.5%
	Avg	0.52	17.2%	0.58	19.5%	0.66	22.0%	0.73	24.5%	0.81	267.0%	0.89	29.7%	0.99	33.0%	1.10	36.6%	1.22	40.7%
	Min	0.28	9.4%	0.30	10.2%	0.35	11.7%	0.41	13.7%	0.46	15.2%	0.51	17.0%	0.57	18.9%	0.63	21.1%	0.70	23.4%
Iris	Max	1.00	33.4%	1.08	35.9%	1.16	38.7%	1.25	41.7%	1.34	44.8%	1.45	48.4%	1.58	52.6%	1.70	56.8%	1.84	61.5%
	Avg	0.48	16.1%	0.54	17.9%	0.59	19.8%	0.65	21.7%	0.71	23.6%	0.77	25.7%	0.84	28.1%	0.92	30.7%	1.00	33.4%
	Min	0.24	7.9%	0.26	8.6%	0.30	9.9%	0.34	11.5%	0.38	12.7%	0.43	14.2%	0.47	15.7%	0.52	17.4%	0.57	19.1%
Optic Nerve	Max	0.53	17.5%	0.59	19.8%	0.66	21.9%	0.72	24.0%	0.78	26.0%	0.85	28.4%	0.93	31.1%	1.02	34.1%	1.12	37.4%
	Avg	0.39	12.9%	0.44	14.5%	0.48	16.0%	0.53	17.5%	0.57	19.0%	0.62	20.6%	0.68	22.5%	0.73	24.5%	0.80	26.6%
	Min	0.29	9.7%	0.33	10.9%	0.36	11.9%	0.39	12.9%	0.42	14.0%	0.45	15.1%	0.49	16.4%	0.53	17.8%	0.58	19.3%
Bone	Max	0.47	15.8%	0.48	16.2%	0.50	16.8%	0.53	17.6%	0.55	18.3%	0.58	19.3%	0.61	20.4%	0.65	21.6%	0.68	22.8%
	Avg	0.20	6.6%	0.21	7.1%	0.23	7.6%	0.24	8.2%	0.26	8.7%	0.28	9.4%	0.31	10.2%	0.33	11.0%	0.35	11.8%
	Min	0.09	3.0%	0.09	3.2%	0.10	3.4%	0.11	3.7%	0.12	3.9%	0.13	4.4%	0.15	5.0%	0.18	5.9%	0.21	7.0%
Sclera	Max	7.11	237.0%	7.61	253.5%	8.33	277.6%	8.76	292.0%	9.19	306.4%	9.70	323.2%	10.28	342.6%	10.86	362.1%	11.47	382.3%
	Avg	0.96	31.9%	1.04	34.7%	1.14	37.9%	1.24	41.2%	1.34	44.8%	1.46	48.8%	1.59	53.1%	1.73	57.7%	1.89	62.9%
	Min	0.18	6.0%	0.19	6.3%	0.20	6.6%	0.21	7.1%	0.24	7.8%	0.27	9.2%	0.35	11.5%	0.43	14.4%	0.49	16.4%
Tumor	Max	6.92	230.6%	7.15	238.3%	7.44	248.1%	7.79	259.6%	8.12	270.8%	8.52	283.9%	9.01	300.4%	9.52	317.2%	10.05	334.9%
	Avg	4.02	134.0%	4.12	137.4%	4.25	141.5%	4.38	146.1%	4.50	150.1%	4.64	154.8%	4.82	160.6%	4.99	166.2%	5.15	171.6%
	Min	3.00	100.0%	3.00	100.0%	3.00	100.0%	3.00	100.0%	3.00	100.0%	3.00	100.0%	3.00	100.0%	3.00	100.0%	3.00	100.0%

DVH curves were made to demonstrate how the dose can be delivered to the tumor while shielding the critical structures in the eye for various applicator sizes and collimators using Se-75. Figure 33 shows these DVH curves for applicators 12 and 16 mm in diameter. The 12 mm diameter applicator delivers the prescription dose to a 5 mm depth in the eye. The 16 mm diameter applicator delivers the prescription dose to a 7 mm depth in the eye.

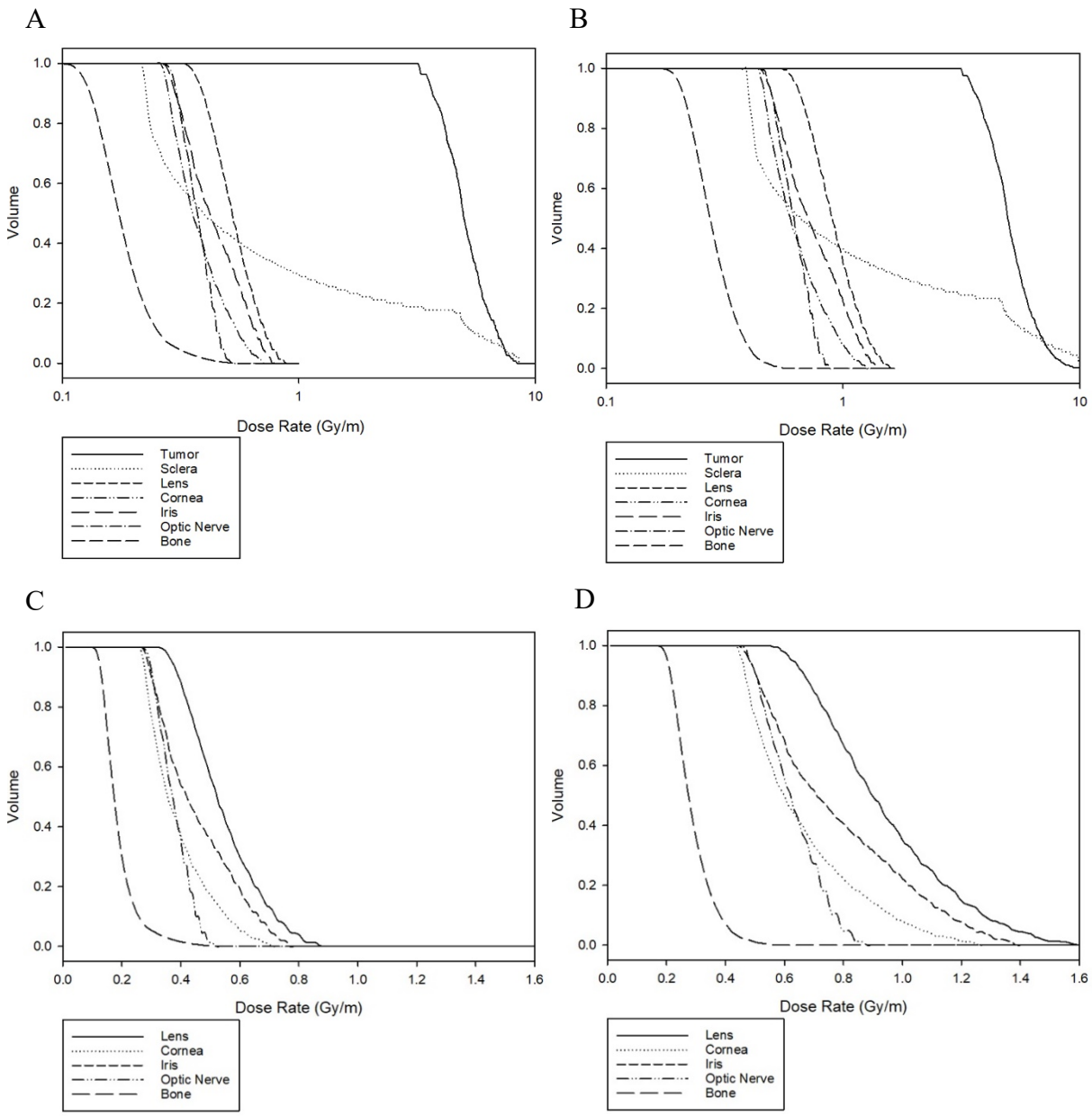

Figure 33: A) and C) are DVH curves of a 12 mm applicator with a target apex at a 5 mm depth in the eye. B) and D) are of a 16 mm applicator with a target apex at a 7 mm depth in the eye. Both applicators deliver a dose rate of 3 Gy/min. A) and B) are in log scale and display the tumor versus critical structures of interest. C) and D) are the dose rates in Gy/min comparing the ocular structures.

Due to the higher energy of Se-75, there is some lateral dose behind the applicator. Therefore, the lateral dose rate at a distance of 5 mm behind a 12 and 16 mm diameter applicator was measured. This is presented in Figure 34. The 12 mm diameter applicator delivers the prescription dose to a 5 mm depth in the eye. The maximum dose rate for this is 0.74 Gy/min, the average is 0.52 Gy/min, and the minimum is 0.20 Gy/min. The 16 mm diameter applicator delivers the prescription dose to a 7 mm depth in the eye. The maximum dose rate is 0.68 Gy/min, the average is 0.50 Gy/min, and the minimum is 0.31 Gy/min.

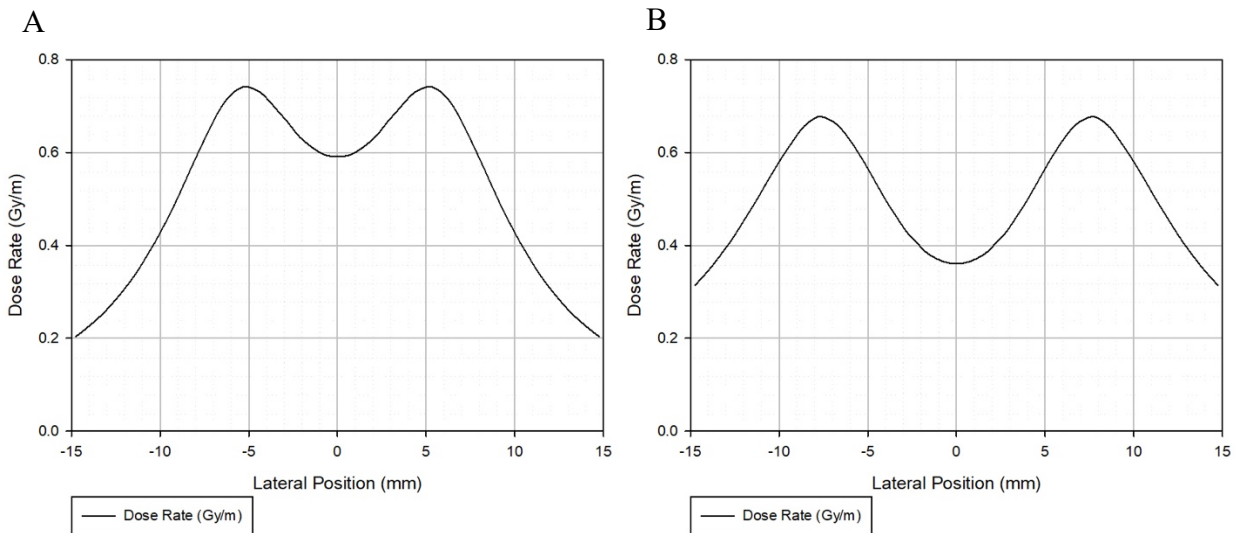

Figure 34: A) is the dose rate 5 mm from the eye behind a 12 mm applicator that delivers the prescription dose to a 5 mm depth in the eye. B) is the dose rate 5 mm from the eye behind a 16 mm applicator that delivers the prescription dose to a 7 mm depth in the eye.

4.3 Comparison of LDR vs HDR

Previous MCNP6 calculations were performed for a COMS plaque containing I-125 and a ring applicator containing Yb-169 and Se-75, all 16 mm in diameter with the prescription dose delivered to a depth of 5 mm in the eye. A comparison of the calculated percent dose rates for each radionuclide was made in Table 15. Their isodose curves are presented in Figure 35 and their DVH curves in Figure 36.

Table 15: Comparison of percent dose rates to ocular structures

		I-125	Yb-169	Se-75
Simulation	Geometry	D (%)	D (%)	D (%)
Cornea	Max	17.6%	19.3%	30.5%
	Avg	9.9%	10.3%	15.6%
	Min	6.3%	6.3%	9.5%
Posterior Lens	Max	25.8%	24.5%	35.7%
	Avg	15.2%	14.4%	20.7%
	Min	8.5%	7.9%	11.7%
Iris	Max	23.7%	21.6%	33.3%
	Avg	14.0%	12.3%	18.1%
	Min	7.4%	6.7%	9.9%
Optic Nerve	Max	16.3%	14.2%	20.1%
	Avg	10.5%	10.2%	14.8%
	Min	6.0%	7.6%	11.0%
Sclera	Max	255.4%	252.2%	278.0%
	Avg	23.7%	25.8%	34.4%
	Min	4.6%	3.3%	6.2%
Tumor	Max	369.0%	250.3%	267.3%
	Avg	175.0%	149.5%	151.7%
	Min	100.0%	100.0%	100.0%

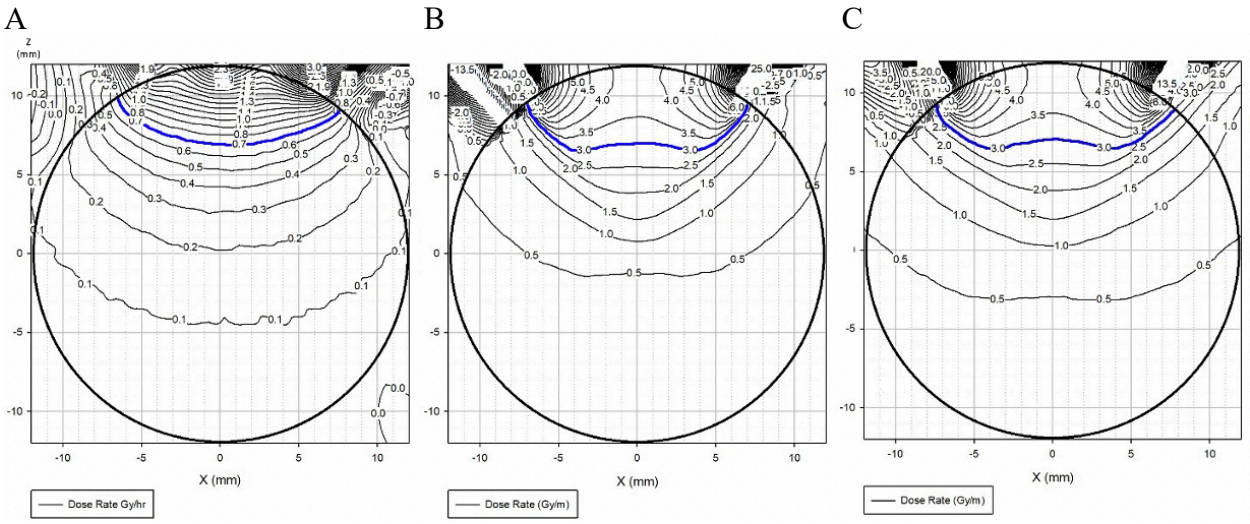

Figure 35: Isodose curves of A) an I-125 COMS plaque compared to the ring applicator containing B) Yb-169 and C) Se-75.

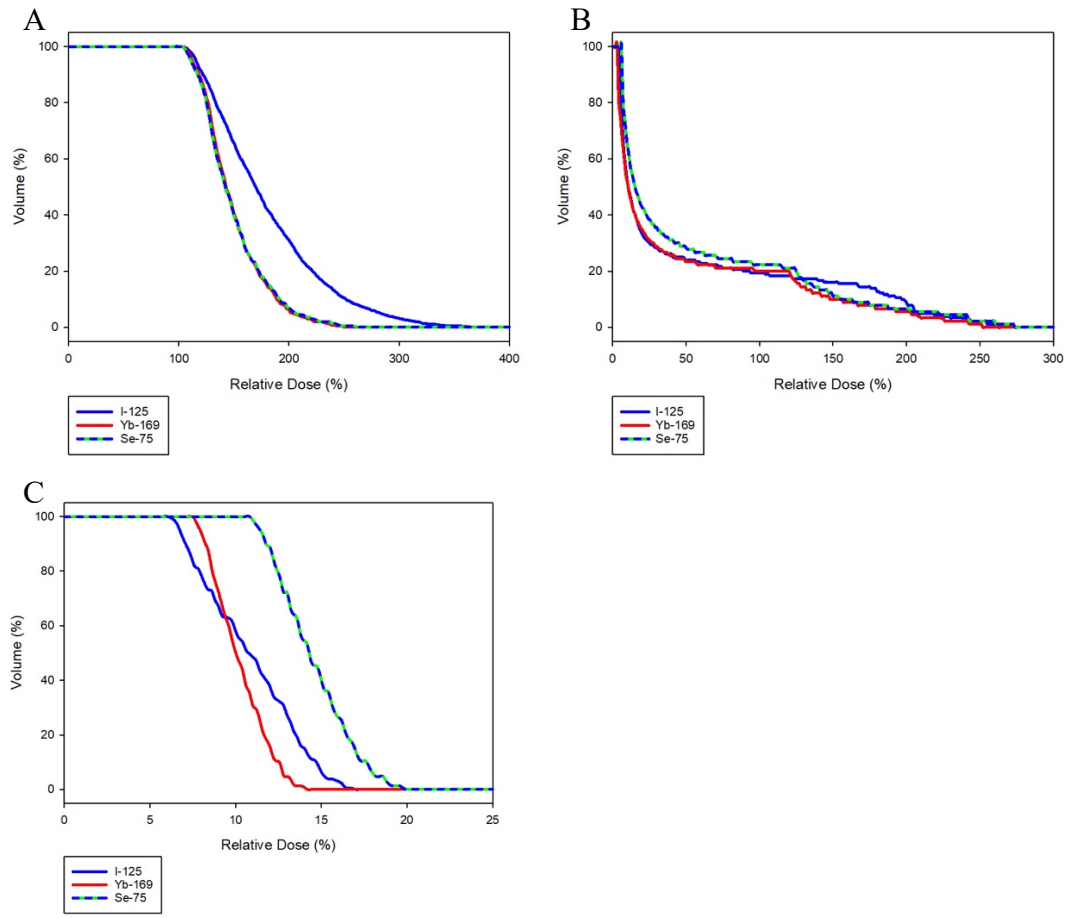

Figure 36: DVH curves of the relative percent dose from I-125, Yb-169, and Se-75 to the A) tumor, B) sclera, and C) optic nerve.

4.4 Experimental Validation

4.4.1 Film Calibration

A batch of Gafchromic EBT3 film was calibrated using Cs-137 at Massachusetts General Hospital. The film was exposed to 0-100 cGy in 25 cGy increments and 100-600 cGy in 50 cGy increments. The film was scanned to determine the corresponding grayscale value for the dose, which was then converted to net optical density (OD). The Net OD vs Dose was then plotted, as seen in Figure 37. The equation of this curve can be used to convert grayscale to dose.

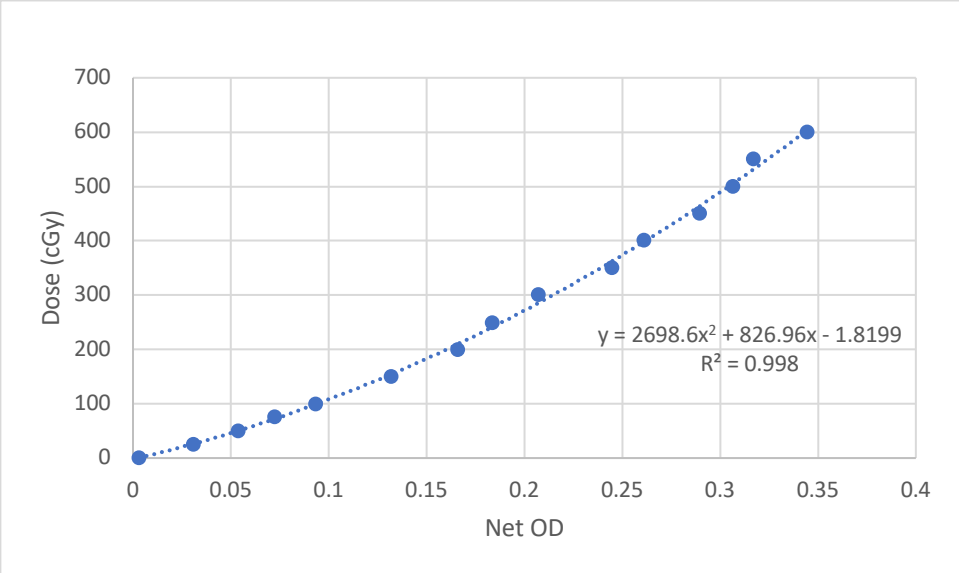

Figure 37: Optical density of the film calibration used for the shielding experiments. A second order polynomial was fitted to the curve.

4.4.2 Measurements

Measurements were taken using Gafchromic EBT3 film of Yb-169 with various thicknesses of gold shielding, Table 16. These measurements were taken at multiple distances away from the source in a tank of water therefore, the increased amount of water at further distances contributes to attenuation of the dose in addition to dose falloff. A graphical representation of the shielded to unshielded dose was plotted over various angles of the shielding in Figure 38. Significant reductions in dose were observed for both the 0.1 and 0.3 mm thick gold shielding.

Table 16: Shielding results of Yb-169 using Gafchromic EBT3 film in cGy

Thickness of gold	Distance from source	Unshielded dose at center	Shielded dose at center	% Difference
0.1 mm	1cm	119.47	55.36	53.7%
	2cm	169.58	89.74	47.1%
	3cm	110.35	63.46	42.5%
0.3mm	1cm	127.35	23.15	81.8%

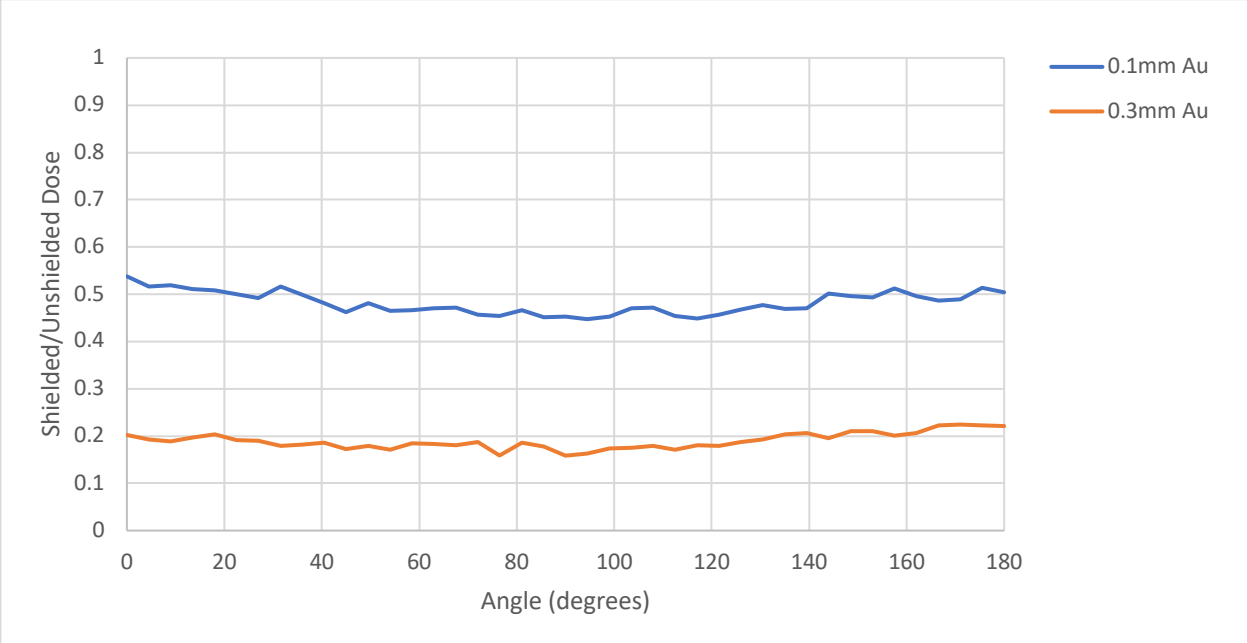

Figure 38: Ratio of shielded to unshielded dose over various angles using 0.1 and 0.3 mm thick gold foil.

5 Discussion

5.1 Computational Validation

A standard 16 mm COMS plaque was simulated in MCNP6. The average percent dose to critical structures was 9.9% to the cornea, 15.2% to the posterior lens, 14.0% to the iris, 10.5% to the optic nerve, 28.0% to the vitreous, 23.7% to the sclera, and 175.0% to the tumor. The maximum relative error for each structure from the MCNP6 simulations was 5.9% for the cornea, 4.11% for the lens, 5.0% for the iris, 4.1% for the optic nerve, 2.1% for the vitreous, 3.3% for the sclera, and 1.2% for the tumor. In addition, there is about a 2% uncertainty from the MCPLIB04 cross-section library.

It is important to note, the method of calculation impacts the results, especially for the average sclera value. By simply taking the average of the mesh tally, this would overestimate the dose. The mesh tally is represented by a cylindrical ring 1 mm thick around the circumference of the eye. Due to symmetry, this would accurately represent the maximum and minimum dose. However, this would not accurately represent the average dose. This would weigh all of the volume elements equally however the volume of the sclera is not uniformly thick. It is an ellipsoid, thinner at the poles and larger at the equator. Therefore, a weighted average needed to be taken over the volume of the sclera. This was accomplished using an F6 tally for each cell comprising the sclera, which calculates the energy deposition. The product of the sum of each cell's dose by its volume was taken over the average volume to calculate the weighted average.

It is also interesting to note that due to the sources being located at the top of the eye near the thinnest section of the sclera, the lowest average dose is actually located there. This is because the volume exposed to the highest dose rate would be the thinnest, therefore not having

much volume. A simulation was performed with the sclera rotated so that the tumor and sources were on the thickest end of the sclera, which has a much greater volume exposed to the highest dose rate. This increased the dose to the sclera considerably with a 55% difference compared to the thinner side of the sclera.

The Lesperance report did not specify what tallies they used or if they took a weighted average of their values. Also, due to the sources being located so close to the sclera and other ocular structures, any differences between the models would be amplified. Their maximum doses were 18.2% for the posterior lens, 9.8% for the optic nerve, 28.8% for the vitreous, 30.2% for the sclera, and 183.1% for the tumor, when delivering the full prescription dose to the tumor apex. Therefore, the percent differences between my calculations were 18.0% for the posterior lens, 6.9% for the optic nerve, 2.8% for the vitreous, 24.1% for the sclera, and 4.5% for the tumor. Without knowing Lesperance's exact calculation methods, it is difficult to minimize these differences. However, the results are comparable therefore, I have confidence in MCNP6 and using this method for my work.

5.2 HDR Applicator

In this study, a novel eye plaque design was proposed for HDR ocular brachytherapy using Yb-169 and Se-75 with gold shielding. This concept was examined for applicators 12-18 mm in diameter to treat targets 10.0-15.5 mm in diameter and 3.5-8.0 mm depths.

For a 16 mm applicator that delivers the prescription dose to a depth of 5 mm in the eye, average percent differences in dose of Yb-169 compared to Se-75 were 40.9% for the cornea, 35.9% for the posterior lens, 38.2% for the iris, 36.8% for the optic nerve, 28.6% for the sclera,

and 1.5% for the tumor. This is due to the more energetic photons of Se-75, which are not as easily shielded as Yb-169.

Maximum statistical uncertainties from the simulations with Yb-169 were 2.2% for the cornea, 1.5% for the lens, 1.8% for the iris, 1.6% for the optic nerve, 6.6% for the bone, 1.7% for the sclera, and 0.4% for the tumor. For Se-75 this was 1.1% for the cornea, 1.0% for the lens, 1.1% for the iris, 1.0% for the optic nerve, 1.8% for the bone, 1.0% for the sclera, and 0.3% for the tumor. In addition there is a 2% uncertainty from the MCPLIB04 cross-section library.

Dose volume histograms were used to compare the dose to the volume of the critical structures in and around the eye. This illustrates how much dose per volume a structure will receive. The entire volume of the structure is equal to 1.0. The curves start at this point where the entire volume of each structure is receiving 0 dose. Then the curves drop according to what fraction of the volume receives an increasing dose. For example, in Figure 27, the critical structures such as the lens, cornea, iris, optic nerve, and bone receive minimal dose because they are further from the plaque and the dose is collimated away from these structures. Therefore, these curves drop to 0 volume after only receiving a small dose. Since the sclera is the closest critical structure to the plaque, it receives the most dose. As a result, this curve extends further. These curves are helpful when comparing dose to critical structures in different plans. In C) and D) of Figure 27, it's clear that the larger applicator delivers a higher dose. This is because the larger applicator contains more sources. In C), the critical structures aren't receiving more than 0.7 Gy/m whereas in D), this maximum is just over 1.2 Gy/m.

The activity of the sources was adjusted in each simulation in order to normalize the dose rate at the treatment depth to 3 Gy/min. For example, when using Yb-169 and treating a depth of 5 mm, a 12 mm applicator requires a total activity of 8.34 Ci or 0.521 Ci/source to deliver

exactly 3 Gy/min. For applicators 14-18 mm, this is 9.11 Ci or 0.506 Ci/source, 10.22 Ci or 0.511 Ci/source, and 11.23 Ci or 0.510 Ci/source respectively. For a 12 mm applicator with a treatment depth at 3.5 mm, this requires 6.71 Ci or 0.419 Ci/source and for a 6 mm depth this is 9.74 Ci or 0.609 Ci/source. Therefore, when using the source array clinically, the dose rate would have to be adjusted slightly based on the source's activity.

When using HDR sources for plaque brachytherapy, there is some dose behind the applicator due to the higher photon energy compared to I-125. For Yb-169, the average lateral dose rate behind the applicator at a distance of 5 mm is about 0.18 Gy/min. The dose rate behind the back of the applicator using Se-75 is about 0.5 Gy/min. However, the treatment time for these plaques are only 10 minutes and the surgeon would be suturing and unsuturing an empty plaque as the sources would be remotely afterloaded, therefore this should not be an issue. The sources could also be shielded locally during treatment if needed. A lead shielded box, 1 cm thick, could be placed around the patient's head if the surgeon or staff wanted to remain in the treatment room during the delivery of the dose. The patient would be anesthetized during this time so the shielding would not be uncomfortable for the patient.

5.3 LDR vs HDR

A comparison was then made between the ring applicator and COMS plaque, both of which I simulated in MCNP6. The average percent differences between Yb-169 and I-125 for a 16 mm applicator that delivers that prescription dose to a depth of 5 mm in the eye was 4.0% for the cornea and 8.5% for the sclera, which had an increase in dose for Yb-169. However, the maximum sclera dose was lower for Yb-169. The remainder of the structures had a reduced dose for Yb-169 with an average percent difference of 5.4% for the posterior lens, 12.9% for the iris,

2.9% for the optic nerve, and 15.7% for the tumor. My I-125 results were slightly lower than Lesperance's. Therefore, when comparing average percent differences for the Yb-169 applicator to Lesperance's published results, the Yb-169 had a decrease of 23.3% for the posterior lens, 15.7% for the sclera, and 20.2% for the tumor. The optic nerve increased 4.0% however the maximum dose reduced by a percent difference of 36.3%.

For the same applicator, when comparing Se-75 with the I-125 MCNP6 results, dose was increased to the critical structures, except to the tumor, which decreased from 175.0% to 151.7%. The average percent difference in dose was 44.7% for the cornea, 30.6% for the posterior lens, 25.5% for the iris, 34.0% for the optic nerve, and 36.8% for the sclera. When comparing the Se-75 results to Lesperance's, the dose was still increased: 12.9% for the posterior lens, 40.7% for the optic nerve, and 13.0% for the sclera.

Although the dose is higher when using Se-75, the advantages of the collimator would be more apparent for deeper depths. For a COMS plaque to treat a larger tumor, a larger applicator would need to be used, which would greatly increase dose to the critical structures. However, with the ring applicator, it may be possible to only have to select a different collimator (depending on tumor size) to deliver the prescription dose to the apex, rather than using a larger applicator. This would help reduce dose to the critical structures. In addition, the other benefits of HDR brachytherapy include reduced costs and no hand dose to the surgeon.

5.4 Experimental Validation

Gafchromic EBT3 film dosimetry techniques were employed to experimentally measure the absorbed dose from Yb-169 using gold shielding. First, a calibration curve was calculated using known exposures to determine the net optical density. Fitting the curve with a second order polynomial made it possible to then use a known optical density to calculate the dose. Therefore, measurements were then taken of Yb-169 shielded with 0.1 mm thick gold from 1-3 cm from the source. This resulted in a percent decrease of 53.7%, 48.6%, and 42.4% respectively, which shows the more efficient shielding is located closer to the source. When using 0.3 mm thick gold 1 cm from the source, the percent decrease in dose was 81.0%. The positional accuracy of the source was about ±2 mm and the uncertainty from the Gafchromic film was < 2%. These results verify the significant dose reductions that can be achieved when coupling a middle-energy brachytherapy source such as Yb-169 with gold shielding.

6 Conclusions

In this work, a dosimetric analysis of a new intensity modulated brachytherapy high dose rate source design was performed and found the dose distributions with Yb-169 and Se-75 suitable for the treatment of ocular melanoma. Intensity modulated HDR ocular brachytherapy has great potential because it drastically minimizes treatment time and cost, eliminates hand dose to the surgeon, and optimizes dose to the target. The static modulation from the collimator allows for the dose to more easily be delivered to the target apex without overexposing the surrounding tissue therefore, introducing shielding to modulate the intensity results in a reduction of dose to the critical structures. Yb-169 is an excellent isotope for this ring applicator design because its lower photon spectrum can easily be modulated by thin amounts of gold. Se-75 although slightly higher in energy, can still be modulated to acceptable levels. Therefore, the longer half-life of Se-75 may make this radionuclide the more practical option to use for this treatment method.

7 Future Work

7.1 Simulations

In the future, it would be beneficial to perform additional simulations. My study only investigated circular shaped applicators and spherical tumors. It would be interesting to compare the dose distributions to an elliptical shaped applicator. Different shaped tumors should also be simulated, which may give a more accurate dose distribution for individual patients as not all tumor shapes are the same. If various applicator shapes were available, dose could even more accurately be delivered to patients. Then, the applicator shape, size, and collimator could be selected to match patient specific measurements as closely as possible. In this way, dose could be greatly maximized to the tumor while protecting healthy tissue.

7.2 Experimental Testing

I would also like to experimentally verify my calculations using Gafchromic EBT3 film dosimetry. Trichter's method for obtaining dose measurements of an eye plaque can be employed for the ring applicator.[78] In this way, it would be possible to experimentally verify the dose distributions that were computationally obtained from MCNP6.

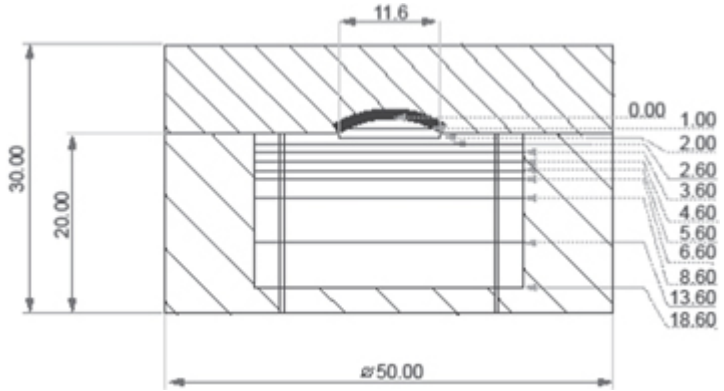

Figure 39: Trichter et al solid water eye phantom cross section with dimensions in mm.[78]

7.3 Clinical Application

The work on the source array and ring applicator was only performed as a physics study. I would like to work on developing this device and implementing it into the clinic. A unique afterloader device would also have to be made for this applicator. It would be a simple design with only one delivery channel, and it could be remote or automatic. It would only require minimal shielding as Yb-169 and Se-75 are much lower in energy compared to Ir-192.

8 Publications and Presentations

This work has been submitted as an article paper to the Physics in Medicine and Biology Journal entitled “Shielded high dose rate ocular brachytherapy using Yb-169” as well as to the Brachytherapy Journal entitled “Intensity modulated high dose rate ocular brachytherapy using Se-75.”

This work has also been presented at the World Congress of Brachytherapy 2021 conference as an oral presentation entitled Intensity modulated HDR ocular brachytherapy using Yb-169 and Se-75, the New England American Association of Physics in Medicine 2020 conference as an oral presentation entitled Eye HDR brachytherapy using Yb-169, and the American Brachytherapy Society 2018 conference as a poster entitled Evaluation of intensity modulated brachytherapy using Yb-169.

9 References

1 Nag S, Quivey JM, Earle JD, Followill D, Fontanesi J, Finger PT; American Brachytherapy Society. The American Brachytherapy Society recommendations for brachytherapy of uveal melanomas. *Int J Radiat Oncol Biol Phys*. 2003; 56(2): 544-55. https://doi.org/10.1016/s0360-3016(03)00006-3

2 Chiu-Tsao ST, Astrahan MA, Finger PT, et al. Dosimetry of 125I and 103Pd COMS eye plaques for intraocular tumors: Report of Task Group 129 by the AAPM and ABS. *Med Phys*. 2012; 39: 6161-6184. https://doi.org/10.1118/1.4749933

3 Classic KL, Furutani KM, Stafford SL, Pulido JS. Radiation dose to the surgeon during plaque brachytherapy. *Retina.* 2012; 32(9): 1900-1905. https://doi.org/10.1097/IAE.0b013e3182509827

4 New York Eye Cancer Center. Available at: https://eyecancer.com/eye-cancer/image-galleries/radiation-images/attachment/5-coms-gold-eye-plaque-with-coms-type-silicone-insert-filled-with-iodine-125-seeds/. Accessed March 3, 2021.

5 Wen JC, Oliver SC, McCannel TA. Ocular complications following I-125 brachytherapy for choroidal melanoma. *Eye* 2009; 23: 1254–1268. https://doi.org/10.1038/eye.2009.43

6 Peddada KV, Sangani R, Menon H, Verma V. Complications and adverse events of plaque brachytherapy for ocular melanoma. *Journal of contemporary brachytherapy.* 2019; 11(4): 392-397. https://doi.org/10.5114%2Fjcb.2019.87407

7 Thomson RM, Furutani KM, Kaulich TW, et al. AAPM recommendations on medical physics practices for ocular plaque brachytherapy: Report of task group 221.*Med. Phys.* 2020; 47:92-124. https://doi.org/10.1002/mp.13996

8 Laube T, Flühs D, Kessler C, Bornfeld N. Determination of surgeon's absorbed dose in iodine 125 and ruthenium 106 ophthalmic plaque surgery. *Ophthalmology.* 2000; 107(2): 366-369. https://doi.org/10.1016/s0161-6420(99)00050-0

9 Hong TS, Ritter MA, Tomé WA, Harari PM. Intensity-modulated radiation therapy: emerging cancer treatment technology. *British journal of cancer*. 2005; *92*(10): 1819–1824. https://doi.org/10.1038/sj.bjc.6602577

10 Callaghan CM, Adams Q, Flynn RT, Wu X, Xu W, Kim Y. Systematic review of intensity-modulated brachytherapy (IMBT): static and dynamic techniques. *Int J Radiat Oncol Biol Phys*. 2019; 105(1): 206-221. https://doi.org/10.1016/j.ijrobp.2019.04.009

11 Belousov AV, Belianov AA, Krusanov GA, *et al.* Simulation of ^{75}Se encapsulated sources for their potential use in brachytherapy. *Moscow Univ. Phys.* 2018; 73: 339–34. https://doi.org/10.3103/S0027134918030049

12 Medich DC, Munro JJ 3rd. Dependence of Yb-169 absorbed dose energy correction factors on self-attenuation in source material and photon buildup in water. *Med Phys*. 2010; 37(5): 2135-2144. https://doi.org/10.1118/1.3372291

13 Lesperance M, Inglis-Whalen M, Thomson RM. Model-based dose calculations for COMS eye plaque brachytherapy using an anatomically realistic eye phantom. *Med Phys.* 2014; 41(2): 021717. https://doi.org/10.1118/1.4861715

14 Martini FH, Bartholomew EF, Nath JL. Chapter 17: The Special Senses. *Fundamentals of Anatomy and Physiology*. Pearson; 2012. p. 556–565.

15 Science Photo Library. Available at: https://www.sciencephoto.com/media/995563/view/eye-anatomy-labelled-illustration. Accessed December 16, 2020.

16 Chang AE, Karnell LH, Menck HR. The National Cancer Data Base report on cutaneous and noncutaneous melanoma: a summary of 84,836 cases from the past decade. The American College of Surgeons Commission on Cancer and the American Cancer Society. *Cancer* 1998; 83(8): 1664–1678. https://doi.org/10.1002/(sici)1097-0142(19981015)83:8<1664::aid-cncr23>3.0.co;2-g

17 Shields CL, Furuta M, Thangappan A, *et al*. Metastasis of uveal melanoma millimeter-by-millimeter in 8033 consecutive eyes. *Arch Ophthalmol.* 2009; 127(8): 989–998. https://doi.org/10.1001/archophthalmol.2009.208

18 Singh AD, Turell ME, Topham AK. Uveal melanoma: trends in incidence, treatment, and survival. *Ophthalmology.* 2011; 118(9): 1881–1885. https://doi.org/10.1016/j.ophtha.2011.01.040

19 Andreoli MT, Mieler WF, Leiderman YI. Epidemiological trends in uveal melanoma. *Br J Ophthalmol* 2015; 99(11): 1550–1553. https://doi.org/10.1136/bjophthalmol-2015-306810

20 Siegel RL, Miller KD, Jemal A. Cancer Statistics, 2019. *CA: A Cancer Journal for Clinicians.* 2019; 69: 7-34. https://doi.org/10.3322/caac.21551

21 Vajdic CM, Kricker A, Giblin M, McKenzie J, Aitken J, Giles GG, et al. Incidence of ocular melanoma in Australia from 1990 to 1998. *Int J Cancer.* 2003; 105(1): 117–122. http://doi.org/10.1002/ijc.11057

22 Shields CL, Kaliki S, Cohen MN, Shields PW, Furuta M, Shields JA. Prognosis of uveal melanoma based on race in 8100 patients: The 2015 Doyne Lecture. *Eye (Lond).* 2015; 29(8): 1027–1035. https://doi.org/10.1038/eye.2015.51

23 Weis E, Shah CP, Lajous M, Shields JA, Shields CL. The association between host susceptibility factors and uveal melanoma: a meta-analysis. *Arch Ophthalmol.* 2006; 124(1): 54–60. https://doi.org/10.1001/archopht.124.1.54

24 Singh M, Durairaj P, Yeung J. Uveal Melanoma: A Review of the Literature. *Oncol Ther.* 2018; 6: 87-104. https://doi.org/10.1007/s40487-018-0056-8

25 Diener-West M, Reynolds SM, Agugliaro DJ. Screening for metastasis from choroidal melanoma: the collaborative ocular melanoma study group report 23. *Journal of Clinical Oncology*. 2004; 22(12): 2438–2444. https://doi.org/10.1200/JCO.2004.08.194

26 Shields JA, Shields CL. Intraocular Tumors. An Atlas and Textbook, 2nd ed. Philadelphia, PA: Lippincott Williams and Wilkins; 2008.

27 Henderson E, Margo CE. Iris melanoma. *Arch Pathol Lab Med.* 2008; 132(2): 268–272. https://doi.org/10.1043/1543-2165(2008)132[268:IM]2.0.CO;2

28 Shields CL, Manquez ME, Ehya H, Mashayekhi A, Danzig CJ, Shields JA. Fine-needle aspiration biopsy of iris tumors in 100 consecutive cases: technique and complications. *Ophthalmology.* 2006; 113(11): 2080–2086. https://doi.org/10.1016/j.ophtha.2006.05.042

29 Demirci H, Shields CL, Shields JA, Eagle Jr RC, Honavar SG. Diffuse iris melanoma: a report of 25 cases. *Ophthalmology.* 2002; 109(8): 1553–1560. https://doi.org/10.1016/s0161-6420(02)01104-1

30 Kaliki S, Shields CL, Mashayekhi A, Ganesh A, Furuta M, Shields JA. Influence of age on prognosis of young patients with uveal melanoma: a matched retrospective cohort study. *Eur J Ophthalmol.* 2013; 23(2): 208–216. https://doi.org/10.5301/ejo.5000200

31 Oittinen HA, O'Shaughnessy M, Cullinane AB, Keohane C. Malignant melanoma of the ciliary body presenting as extraocular metastasis in the temporalis muscle. *J Clin Pathol*. 2007; 60(7): 834-835. https://doi.org/10.1136/jcp.2005.033613

32 Damato EM, Damato BE. Detection and time to treatment of uveal melanoma in the United Kingdom: an evaluation of 2,384 patients. *Ophthalmology.* 2012; 119(8): 1582–1589. https://doi.org/10.1016/j.ophtha.2012.01.048

33 Bianciotto CG, Shields CL, Romanelli M, Romanelli-Gobbi M, Mazzuca Jr D, Green WR, *et al*. Assessment of anterior segment tumors with ultrasound biomicroscopy versus anterior segment optical coherence tomography in 200 cases. *Ophthalmology.* 2011; 118(7): 1297–1302. https://doi.org/10.1016/j.ophtha.2010.11.011

34 Costache M, Patrascu OM, Adrian D, et al. Ciliary body melanoma - a particularly rare type of ocular tumor. Case report and general considerations. *Maedica (Buchar)*. 2013; 8(4): 360-364. PMID: 24790669

35 McLaughlin CC, Wu XC, Jemal A, Martin HJ, Roche LM, Chen VW. Incidence of noncutaneous melanomas in the U.S. *Cancer*. 2005;103(5): 1000-1007. https://doi.org/10.1002/cncr.20866

36 Shields CL, Kaliki S, Rojanaporn D, Ferenczy SR, Shields JA. Enhanced depth imaging optical coherence tomography of small choroidal melanoma: comparison with choroidal nevus. *Arch Ophthalmol.* 2012; 130(7): 850–856. https://doi.org/10.1001/archophthalmol.2012.1135

37 Houle V, Bélair M, Allaire GS. AIRP best cases in radiologic-pathologic correlation: choroidal melanoma. *Radiographics*. 2011; 31(5): 1231-1236. https://doi.org/10.1148/rg.315105211

38 Mayo Clinic. Available at: https://www.mayoclinic.org/diseases-conditions/eye-melanoma/symptoms-causes/syc-20372371. Accessed March 3, 2021.

39 Jaffray DA, Gospodarowicz MK. Radiation Therapy for Cancer. *Cancer: Disease Control Priorities*. 2015; 3. https://doi.org/10.1596/978-1-4648-0349-9_ch14

40 Szumiel I. Ionizing radiation-induced cell death. *Int J Radiat Biol*. 1994; 66:329-341. https://doi.org/10.1080/09553009414551271

41 Little JB. Principal Cellular and Tissue Effects of Radiation. In: Kufe DW, Pollock RE, Weichselbaum RR, et al., editors. Holland-Frei Cancer Medicine. 6th edition. Hamilton (ON): BC Decker; 2003.

42 Mishra KK, Daftari IK. Proton therapy for the management of uveal melanoma and other ocular tumors. *Chin Clin Oncol*. 2016; 5:50. https://doi.org/10.21037/cco.2016.07.06

43 Akbaba S, Foerster R, Nicolay NH, *et al.* Linear accelerator-based stereotactic fractionated photon radiotherapy as an eye-conserving treatment for uveal melanoma. *Radiat Oncol.* 2018; 13:140. https://doi.org/10.1186/s13014-018-1088-9

44 New York Eye Cancer Center. Available at: https://eyecancer.com/eye-cancer/treatments/proton-beam-versus-plaque. Accessed March 3, 2021.

45 Kemikler G. History of brachytherapy. *Turkish Journal of Oncology*. 2019. https://doi.org/10.5505/tjo.2019.1

46 Rivard MJ, Venselaar JL, Beaulieu L. The evolution of brachytherapy treatment planning. *Med Phys*. 2009; 36(6): 2136-2153. https://doi.org/10.1118/1.3125136

47 Chassagne D, Dutreix A, Almond P, Burgers JMV, Busch M, Joslin CA. Report 38. *Journal of the International Commission on Radiation Units and Measurements*. 1985; 20: 1. https://doi.org/10.1093/jicru/os20.1.Report38

48 Zimmerman LE, McLean IW, Foster WD. Does enucleation of the eye containing a malignant melanoma prevent or accelerate the dissemination of tumour cells. *Br J Ophthalmol*. 1978; 62(6): 420-425. https://doi.org/10.1136/bjo.62.6.420

49 Manschot WA, Van Strik R. Is irradiation a justifiable treatment of choroidal melanoma? Analysis of published results. *Br J Ophthalmol*. 1987; 71(5): 348-352. https://doi.org/10.1136/bjo.71.5.348

50 Gass JD. Comparison of prognosis after enucleation vs cobalt 60 irradiation of melanomas. *Arch Ophthalmol*. 1985; 103(7): 916-923. https://doi.org/10.1001/archopht.1985.01050070042027

51 Diener-West M, Hawkins BS, Markowitz JA, Schachat AP. Review of mortality from choroidal melanoma, part II, a meta-analysis of five-year mortality rates following enucleation, 1966 through 1988. *Arch Ophthalmol*. 1992; 110: 245–
50. https://doi.org/10.1001/archopht.1992.01080140101036

52 Margo CE. The Collaborative Ocular Melanoma Study: An overview. *Cancer Control*. 2004; 11: 304–9. https://doi.org/10.1177/107327480401100504

53 The Collaborative Ocular Melanoma Study (COMS) randomized trial of pre-enucleation radiation of large choroidal melanoma, II: Initial mortality findings. COMS report no.10. *Am J Ophthalmol*. 1998; 125: 779–96. https://doi.org/10.1016/s0002-9394(98)00039-7

54 Hawkins BS, Collaborative Ocular Melanoma Study Group. The Collaborative Ocular Melanoma Study (COMS) randomized trial of pre-enucleation radiation of large choroidal melanoma: IV. Ten-year mortality findings and prognostic factors. COMS report number 24. *Am J Ophthalmol*. 2004; 138: 936–51. https://doi.org/10.1016/j.ajo.2004.07.006

55 Diener-West M, Earle JD, Fine SL, Hawkins BS, Moy CS, Reynolds SM, Schachat AP, Straatsma BR, Collaborative Ocular Melanoma Study Group. The COMS randomized trial of iodine 125 brachytherapy for choroidal melanoma. III. Initial mortality findings. COMS Report No. 18. *Arch Ophthalmol*. 2001; 119: 969–82. https://doi.org/10.1001/archopht.119.7.969

56 Collaborative Ocular Melanoma Study Group. The COMS randomized trial of iodine125 brachytherapy for choroidal melanoma, V: Twelve-year mortality rates and prognostic factors. COMS Report No. 28. *Arch Ophthalmol*. 2006; 124: 1684–93. https://doi.org/10.1001/archopht.124.12.1684

57 Collaborative Ocular Melanoma Study Group: Mortality in patients with small choroidal melanoma. COMS Report No.4. *Arch Ophthalmol*. 1997; 115: 886–93. PMID: 9230829

58 Rivard MJ, Coursey BM, DeWerd LA, et al. Update of AAPM Task Group No. 43 Report: A revised AAPM protocol for brachytherapy dose calculations. *Med. Phys.* 2004; 31: 633-674. https://doi.org/10.1118/1.1646040

59 Thomson RM, Taylor REP, Rogers DWO. Monte Carlo dosimetry for 125I and 103Pd eye plaque brachytherapy. *Med. Phys*. 2008; 35:5530–5543. https://doi.org/10.1118/1.3002412

60 de la Zerda A, Chiu-Tsao ST, Lin J, et al. 125I eye plaque dose distribution including penumbra characteristics. *Med. Phys*. 1996; 23: 407–418. https://doi.org/10.1118/1.597803

61 Zhang H, Martin D, Chiu-Tsao ST, Meigooni A, Thomadsen BR. A comprehensive dosimetric comparison between 131Cs and125I brachytherapy sources for COMS eye plaque implant. *Brachytherapy.* 2010; 9:362–372. https://doi.org/10.1016/j.brachy.2009.07.007

62 Rivard MJ, Chiu-Tsao ST, Finger PT, et al. Comparison of dose calculation methods for brachytherapy of intraocular tumors. *Med. Phys*. 2011; 38: 306–316. https://doi.org/10.1118/1.3523614

63 Rivard MJ, Melhus CS, Granero D, Perez-Calatayud J, Ballester F. An approach to using conventional brachytherapy soft-ware for clinical treatment planning of complex, Monte Carlo-based brachytherapy dose distributions. *Med. Phys*. 2009; 36: 1968–1975. https://doi.org/10.1118/1.3121510

64 Rivard MJ, Beaulieu L, Mourtada F. Enhancements to commissioning techniques and quality assurance of brachytherapy treatment planning systems that use model-based dose calculation algorithms. *Med. Phys*. 2010; 37: 2645–2658. https://doi.org/10.1118/1.3429131

65 American Brachytherapy Society - Ophthalmic Oncology Task Force. The American Brachytherapy Society consensus guidelines for plaque brachytherapy of uveal melanoma and retinoblastoma. *Brachytherapy*. 2014; 13(1): 1-14. https://doi.org/10.1016/j.brachy.2013.11.008

66 Goorley T, James M, Booth T, et al. Features of MCNP6. *Elsevier Ltd.* 2016; 87(2):772-783. https://doi.org/10.1016/j.anucene.2015.02.020

67 ICRP. Basic anatomical and physiological data for use in radiological protection: Reference values. *ICRP Publication 89, Annals of the ICRP.* 2002; 32(3-4): 1-277.

68 ICRP. Adult reference computational phantoms. *ICRP Publication 110, Annals of the ICRP.* 2009; 39:1-166.

69 Yoriyaz H, Sanchez A, dos Santos A. A new human eye model for ophthalmic brachytherapy dosimetry. *Radiat Prot Dosimetry.* 2005; 115(1-4): 316-319. https://doi.org/10.1093/rpd/nci105

71 The Carleton Laboratory for Radiotherapy Physics TG-43 Parameter Database. Available at: http://www.physics. carleton.ca/clrp/seed_database. Accessed November 23, 2020.

72 National Nuclear Data Center Brookhaven National Laboratory Decay Radiation Search. Available at: https://www.nndc.bnl.gov/nudat2/indx_dec.jsp. Accessed November 23, 2020.

73 Munro III JJ. Radioactive therapeutic device able to turn small radii. U.S. Patent No. 10,576,299. *Washington, DC: U.S. Patent and Trademark Office* 2020.

74 Gagne NL, Leonard KL, Huber KE, Mignano JE, Duker JS, Laver NV, Rivard MJ. BEDVH-A method for evaluating biologically effective dose volume histograms: application to eye plaque brachytherapy implants. *Med Phys*. 2012; 39(2):976-83. https://doi.org/10.1118/1.3679010.

75 Turvey TA, Golden BA. Orbital anatomy for the surgeon. *Oral Maxillofa Surg Clin North Am.* 2012; *24*(4): 525–536. https://doi.org/10.1016%2Fj.coms.2012.08.003

76 Gafchromic Films. Available at: http://www.gafchromic.com/gafchromic-film/radiotherapy-films/EBT/index.asp. Accessed November 23, 2020.

77 Gafchromautomatic. Available at: https://github.com/WPIRadiationPhysics/Gafchromautomatic. Accessed November 23, 2020.

78 Trichter S, Soares CG, Zaider M, DeWyngaert JK, DeWerd LA, Kleiman N. 15 years of ^{106}Ru eye plaque dosimetry at Memorial Sloan-Kettering Cancer Center and Weill Cornell Medical Center using radiochromic film in a Solid Water phantom. *Biomed Phys Eng Express.* 2018; 4(4): 045017. https://doi.org/10.1088/2057-1976/aab674